UCID- 20063-Rev. 1
ESL-TR-87-14

EAGLE SERIES DATA REPORT:
1983 Nitrogen Tetroxide Spills

T.G. McRae, R.T. Cederwall, D.L. Ermak
H.C. Goldwire, Jr., D.L. Hipple, G.W. Johnson
R.P. Koopman, J.W. McClure, and L.K. Morris

March 1987

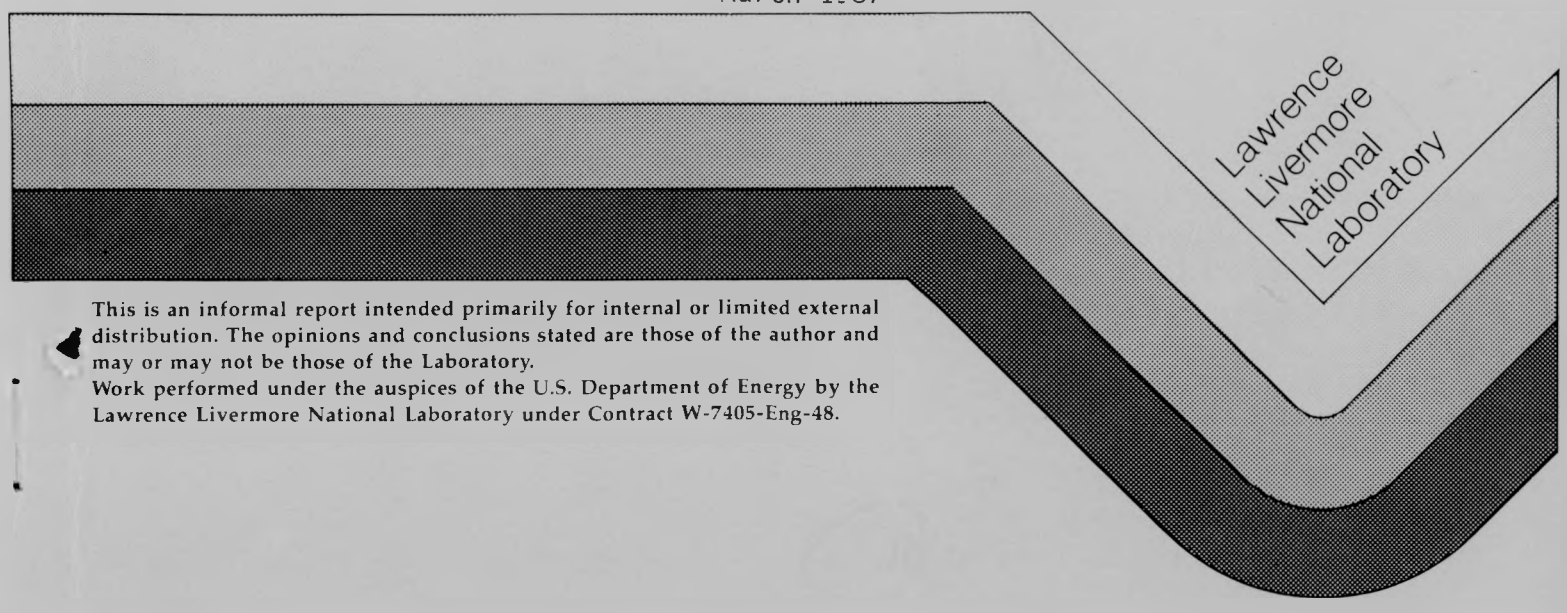

Printed in the United States of America
Available from
National Technical Information Service
U.S. Department of Commerce
5285 Port Royal Road
Springfield, VA 22161

Price Code	Page Range
A01	Microfiche
Papercopy Prices	
A02	001-050
A03	051-100
A04	101-200
A05	201-300
A06	301-400
A07	401-500
A08	501-600
A09	601

UCID--20063-Rev.1

DE87 009227

REVISIONS

This edition of the EAGLE SERIES DATA REPORT is a revision of the original report dated June 1984 and published under the Lawrence Livermore National Laboratory number of UCID-20063 and the USAF Engineering and Services Center number of ESL-TR-84-23. The part of the report that is revised is Section 4.1, The Atmospheric Boundary Layer Data, including Tables 3 - 8. The method of calculating the various meteorological parameters has been modified and is explained in Section 4.1. While these modifications result in minor changes in the values of the parameters listed in Tables 3 - 8, most of the difference is due to a change in the surface roughness length z_o. After re-evaluating the wind speed profiles taken during the tests under neutral meteorological conditions, a value of the surface friction length of z_o = .0003 m appears more appropriate than the original value of $z_o = 10^{-6}$ m obtained at a nearby location prior to the dispersion tests. This new value of z_o has been used to calculate the ambient meteorological parameters as described in Section 4.1. The remainder of the report is unchanged.

e14-87-UC

Contents

ACKNOWLEDGMENTS

The data reported here represent the work of many people from several different organizations. In particular, the authors wish to express their sincere thanks to Dr. Dan Stone and Major Gary Worley (AFESC), Mr. Bob McCall (TRW), and Mr. Terry Roy (LLNL/NTS) for their efforts in organizing and conducting the field experiments. In addition, we would also like to acknowledge the following individuals:

LLNL/Livermore

Rex Blocker
Denny Chakedis
Phil Coyle
Randy Flores
Mark Fowler
Cleo Fry
Bill Hogan
Rod Kiefer
Chris Martin
Joe Penland
Don Rock
Roberta Rodriques
Joe Shinn
Diane Soto
Myles Spann
Sam Spataro
Matt Traini

Aerospace Corp.

Sherman Lewis
Dr. H. Takimoto

TRW/Odgen

Steve Johnson
Steve Kato

DOE/NVO

Wendy Dixon
Ed Forness
Vince Iorii
Don Martin
John Stewart

LLNL/NTS

Vaughn Brugman
Bill Edwards
Ray Preston
Steve Stark
Hal Williams

ReeCo

Dennis Finney
Carlene Perkins

NOAA/WSNSO

Hal Mueller
Daryl Randerson
Doug Soule

Aerojet Tech. Systems Co.

Dick Belford
Don Brincka
Glen Jackson

OO-ALC/MMG

Jim Betschart
Ron Chapin
Ken Gomm
Bruce Scholer

Paul Henderson (T&E Int.)
Ralph Hiltz (MSAR)
Bette Hagan (AFSD)
Gilbert Noriega (Kelly AFB)
Jeff Wilson (SATAF)

1.0 INTRODUCTION

The Lawrence Livermore National Laboratory (LLNL) conducted a series of nitrogen tetroxide (N_2O_4) spill tests for the U.S. Air Force during the fall of 1983. The purpose of the test series was to determine the heavy gas dispersion aspects and source strength characteristics of large N_2O_4 spills, and to provide N_2O_4 spills for the evaluation of a Portable Foam Vapor Suppression System (PFVSS). The dispersion and source strength tests were under the sponsorship and direction of the Engineering and Services Center, Tyndall AFB. The PFVSS effort was under the direction of the Ogden Air Logistics Center, Hill AFB, with support from USAF Space Division and the Strategic Air Command. The tests were performed at the U.S. Department of Energy (DOE) Nevada Test Site (NTS) under the jurisdiction of the DOE Nevada Operations Office (NV).

The N_2O_4 tests were the fifth in a series of hazardous materials spill tests conducted by LLNL and were code-named the Eagle series. There were a total of six N_2O_4 spill tests. Four tests were for the purpose of dispersion and source strength studies (Eagles 1, 2, 3, and 6) and two tests for evaluation of the PFVSS (Eagles 4 and 5). The Eagle series was conducted in conjunction with a series of ammonia (NH_3) spill tests (Desert Tortoise series) at considerable savings to both sponsors. These back-to-back series were to have begun with the N_2O_4 tests in June of 1983, however, due to a timing problem with the availability of the N_2O_4 and additional environmental and safety requirements by DOE/NV, the NH_3 series led off on Aug. 12, 1983 after a three-week set-up period. The change-over to the N_2O_4 spill configuration began on Sept. 8, 1983 and the last test was performed on Nov. 30, 1983.

The purpose of this report is to make the data from the Eagle test series available in a format that will be most useful to the largest number of people. The data set itself is voluminous, consisting of over two million words of digital data stored in the LLNL data base. Because of the large amount of data, not all of it will be presented here. Only that data which is pertinent to the documentation of each spill test is presented. This report is intended to describe the experiment and to present the data only, and contains no analysis.

---

* Work performed for the United States Air Force Engineering and Services Center, Tyndall AFB (MIPR N84-18) under the auspices of the U.S. Department of Energy by the Lawrence Livermore National Laboratory (contract number W-7405-ENG-48).

2.0 THE EAGLE SERIES EXPERIMENT DESCRIPTION

The purpose of this section is to adequately describe the experiment and diagnostics in order that users of the data presented herein will be fully aware of the conditions and types of measurements used to produce the final results. The exact positions and operational status of the diagnostics for each individual test are given in the Experiment Summary section. The surveyed locations of each of the wind field and gas sensor towers are given in Table 1. The x and y coordinates are with respect to an origin at the spill point.

TABLE 1.
Surveyed Station Locations

Station	x position	y position	
G01	-50.00	0.00	- Met tower
*G02	25.00	-15.00	
G03	25.00	-10.00	
G04	25.00	-5.00	Mass
G05	25.00	0.00	
G06	25.00	5.00	Flux
G07	25.00	10.00	
G08	25.00	15.00	Array
W11	25.00	-7.50	
W12	25.00	+7.50	
*G20	785.00	-200.00	
G21	785.00	-100.00	Disperison
G22	785.00	0.00	
G23	785.00	100.00	Array
G24	785.00	200.00	
W01	-1015.00	0.00	
W02	-515.00	0.00	
W03	-315.00	-100.00	Wind
W04	-315.00	+100.00	
W05	585.00	-200.00	Field
W06	585.00	+200.00	
W07	985.00	0.00	Array
W08	1485.00	0.00	
W09	2785.00	0.00	

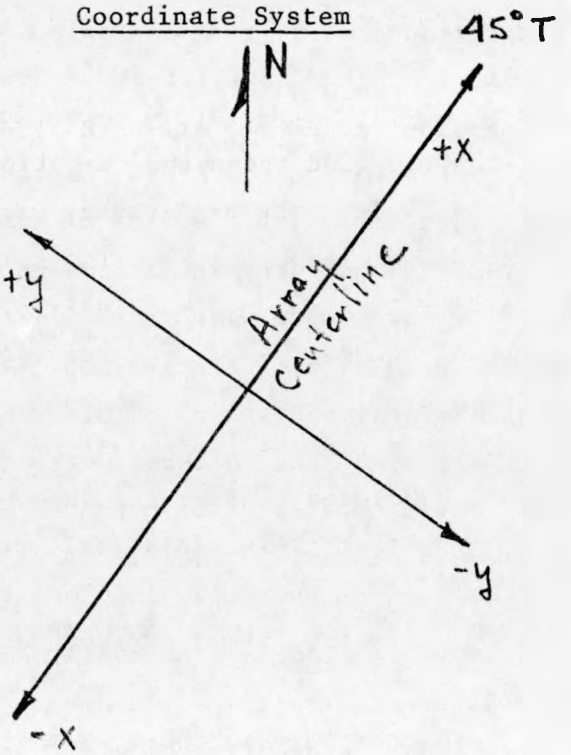

* EAG1-EAG3 positions--G02 and G20 were relocated for EAG4-EAG6 (See Section 3 for details)

2.1 The N_2O_4 Spill Facility

The two primary components of the N_2O_4 spill facility were an Air Force-supplied R-16 tanker and a LLNL N_2 gas tube trailer. A layout of the spill facility is shown in Fig. 1. The N_2 tube trailer was used to pressurize the R-16 tanker and force the N_2O_4 through the spill pipe to the spill point, to provide purge gas for cleansing the piping system after each spill, and to provide gas pressure for the pneumatically operated valves. A piping diagram of the complete system is shown in Fig. 2.

A typical spill test sequence would proceed as follows. On days with favorable weather forecasts, the diagnostic system would be checked for satisfactory operation, and the spill area would be cleared of all personnel except for the arming team. Members of the arming team would open the manual valve on the N_2 tube trailer (V10), set the pressure control valve (PCV2) to the desired drive gas pressure and open the manual valves on the R-16 tanker (V6, V9). Valves V3 and V5 would be closed. The arming team would then leave the area. All further spill operations were conducted remotely.

When the wind speed and direction were within the designated acceptable spill conditions, the R-16 tanker was pressurized by opening V1. The spill was initiated by opening V4. The spill valve had a 10 sec delay period prior to starting to open, and was fully open after a total of 17 sec. A real-time display of the volume of N_2O_4 spilled as a function of time was provided by the command and control data recording system (CCDRS) located about 1 mile upwind. When the desired amount of N_2O_4 had been spilled, valves V1 and V4 would be closed. After the vapor cloud had cleared the downwind array, the pressure in the R-16 would be relieved by opening V2. The disarming team would then enter the area and close valves V6, V9, and V10 to secure the facility. The N_2O_4 remaining in the spill pipe was purged by opening V4 and V5.

The temperature of the N_2O_4 in the R-16 was monitored by a thermocouple gauge supplied with the tanker. The R-16 tanker pressure was monitored with a Fairchild 0-200 psia pressure transducer which was also displayed in realtime at the CCDRS trailer. The tanker volume was determined by measuring the pressure difference between the ullage space and the bottom of the vessel. The flowmeter was a paddle-wheel design manufactured by Data Industrial, and although advertised as acid-proof, the paddle wheel and electrical potting compound were completely destroyed by the N_2O_4. Flow rate data were only obtained on the first spill (EAG1).

2.2 The Spill Area Diagnostics

The N_2O_4 was delivered to the spill area by a 30-m long, 7.62-cm diameter (3-in) PVC pipe where it was distributed in two different ways. The single-exit, confined spill configuration (Fig. 3a) was for the purpose of studying evaporation rates as a function of liquid pool depth and wind speed. The multi-exit, unconfined spill configuration (Fig. 3b) was designed to distribute the N_2O_4 uniformly over a large area in order that it evaporate as quickly as it was spilled. This would produce a large source of N_2O_4 vapor for the dispersion studies. A picture of the N_2O_4 spill facility with the multi-exit spill configuration is shown in Fig. 4.

Numerous measurements were made in the area of the spill. The temperature of the N_2O_4 just prior to its exit from the spill pipe was recorded. Three heat-flux sensors were placed just below the surface of the soil at locations described in Section 3. These gauges were manufactured by Hy-Cal Engineering and consisted of two layers of thermopiles separated by an aluminum plate. A thermocouple rake assembly was also installed in the spill area for the purpose of determining the temperature gradient within the liquid for the confined spills, and within the initial vapor layer of the unconfined spills. The rake assembly consisted of three chromel-alumel (Type K) thermocouples in stainless steel sheathes which were mounted on a PVC stake such that one was at ground level, and the second and third at heights of 2 and 4 cm, respectively. Provision was also made for measuring the real-time depth (pressure head) of the liquid N_2O_4 during the confined spills by use of a Validyne ± 1 psi differential pressure gauge. The locations of the spill area diagnostics for each spill are described in Section 3.

For tests Eagles 1 through 3 and Eagle 6, the N_2O_4 was spilled directly onto the ground, whereas for Eagles 4 and 5 a polyethylene plastic liner was used to help contain the liquid. Although the lakebed playa surface was clay-like and known for its impermeability to water, the N_2O_4 soaked into it quite readily. In many cases it actually caused the surface to heave up several inches. There was considerable outgassing from the surface for several hours after the spill was terminated. After each of spills Eagles 1 thru 3 and Eagle 6, a fire truck dispersed 100-1000 gallons of water to dilute the N_2O_4 absorbed by the ground to the point that its vapors were reduced to acceptable levels.

2.3 The Meteorological Array

The meteorological array consisted of nine stations with Met-One two axis, cup-and-vane anemometers, plus a 20-m tall tower located directly upwind of the spill area. The locations of the wind-field stations are shown in Fig. 5. The Met-One anemometers were mounted at a height of 2 m, had a starting threshold of 0.2 m/sec, a response distance constant of 4.6 m, and an accuracy of ± 1% (∿ 0.07 m/sec). Data taken by these instruments were averaged for 10 sec, and this result, plus the standard deviation of direction for the same period, was transmitted back to the CCDRS trailer. The wind-field data were displayed in realtime and were the primary information used to determine the optimum time for the spill. A typical wind-field station is shown in Fig. 6.

The meteorological boundary layer data were obtained from measurements mounted on a 20-m tower located 50 m directly upwind of the spill point (Fig. 5). This tower (G01) was outfitted with four temperature gauges and three Gill bivane anemometers. The temperature gauges were resistive temperature detectors (RTDs) composed of 1000 ohm platinum resistance elements mounted in aspirated solar shields. These RTD gauges are estimated to be accurate to within ± 0.1°C if the electronic drift of the amplifiers is properly accounted for. The G01 bivane anemometers were manufactured by the R.M. Young Co., and have a starting threshold of about 0.2 m/sec with a response distance constant of 1 m.

Station G01 also measured the ground heat flux with a Hy-Cal heat flux plate similar in design to those located in the spill area. Provision was also made to measure the local humidity, however the heavy rains which occurred during the NH_3 spill series ruined this gauge. As a result, the humidities reported in the experiment summary section were obtained from the NTS Weather Support Group. The humidity data (and the barometric pressure) were measured at a station located near the CCDRS trailer park. A picture of station G01 is shown in Fig. 7.

2.4 The Mass Flux Array

The purpose of the mass flux array was to determine the evaporation rate, or vapor source strength, of the N_2O_4. This was to be accomplished by measuring the N_2O_4 concentration, vapor cloud temperature and velocity as

it passed through the array. The N_2O_4/NO_2 ratio would be determined using a well-documented equilibrium reaction rate constant.[1,2] The cloud temperature data is required for calculations of the rate constant and the conversion from concentration to mass density. The product of the mass density and velocity integrated over the vapor cloud cross-section yields the total mass flux passing through the array at any instant. If the entire cloud is "captured" by the array, this mass flux should be equivalent to the vapor source strength of the spilled N_2O_4.

The mass flux array was located 25 m downwind of the spill area and consisted of seven gas stations (G02-G08) and two wind speed stations (W11, W12). A picture of this array is shown in Fig. 8. The centerline station (G05) was a 10 m tall tower outfitted with three R.M. Young Co. bivane anemometers, three LLNL IR gas sensors, and three thermocouples. The three anemometers were located at heights of 1.3, 3, and 6 m for the entire Eagle series. The IR gas sensors and thermocouples were located at various heights as indicated in Section 3 (they were all lowered after EAG2).

There were three stations located at 5 m intervals to either side of the G05 centerline station (G02-G04, G06-G08). These stations had 6 m tall masts and each was outfitted with three LLNL IR gas sensors and three thermocouples. The gas sensors and thermocouples were located at approximately the same heights on each of the mass flux stations. In addition, two of the stations (G04, G06) also had Hy-Cal heat flux gauges for the purpose of measuring the heat input from the ground to the N_2O_4 vapors. The heights of the gas sensors and thermocouples for these stations for each spill are documented in Section 3.

A detailed description of the LLNL IR gas sensor is given in Ref. 3, hence only a cursory description is presented here. A cross section of the sensor is shown in Fig. 9. The radiation from the IR source is attenuated by molecular absorption of the N_2O_4 vapors as they pass through the 15 cm sample region. The magnitude of this attenuation is recorded by a pyroelectric detector in four different spectral bandpasses between 3 and 4 μm. The sensor was calibrated by recording the IR attenuation for known concentrations of N_2O_4. The sensor was originally designed for the detection of liquefied natural gas (LNG) vapors and was not optimized for the Eagle series experiments. The species of most interest here was NO_2, however when it was discovered that the IR sensors could be used to detect N_2O_4 vapors without any

modifications, the cost savings dictated that this approach be taken. Unfortunately, this required placing the sensors very close to the source, which resulted in the loss of several of them as a result of exposure to nitric acid. An absorption spectra of commercial grade N_2O_4/NO_2 is shown in Fig. 10, along with the four spectral bandpasses of the IR sensor. The M bandpass was the most sensitive to the presence of N_2O_4 vapors and was used in conjunction with the F bandpass for a reference or baseline. A detailed discussion of the data processing for the IR sensors is given in Section 5.

The thermocouples were used to measure the temperature fluctuations as the N_2O_4 vapors passed through the 25 m array. The temperature was required to calculate the equilibrium ratio of N_2O_4 to NO_2 and the total mass density necessary for the vapor flux computation. The thermocouples were 20-mil diameter, Type K, with a response time of about 1.5 sec. The reference junction and amplifiers for the thermocouples would tend to drift over the long periods of time in the field. It was not uncommon that the temperature readings throughout the array would incorrectly show a spread of 5-10°C. However, the relative temperature variations during vapor cloud passage are felt to be quite accurate ($\pm$ 0.5°C). Consequently, all of the thermocouple data of the mass flux array were shifted to correspond to the average value of the G01 RTD prespill temperature.

Two wind speed stations (W11, W12) were located at $\pm$ 7.5 m to either side of the array centerline. These were similar to the Met-One wind-field stations described in Section 2, except that these anemometers were placed at a height of 1 m above the ground. The purpose of these measurements was to determine if there was an appreciable wind speed variation during the passage of the vapor cloud.

2.5 The Dispersion Array

The dispersion array consisted of five 10 m towers (G20-G24) located 785 m downwind of the spill area (see Fig. 5). The purpose of this array of sensors was to record the vertical cross-section of the NO_2 vapors during each spill. Each of the towers had three NO_2 gas sensors and three thermocouples located at heights of 1, 3.5, and 8.5 m above the ground. The towers were separated by a distance of 100 m, with G22 located on the array centerline (see Table 1). A picture of the dispersion array is shown in Fig. 11.

Nine NO_2 gas sensors were furnished by the Shuttle Activation Task Force, Vandenburg AFB for use during the Eagle series. These sensors were initially manufactured for NASA/KSC by Energetic Sciences, Inc. All of the sensors were dual channel instruments, i.e., capable of making two separate concentration measurements. Four were dual NO_2 sensors, while the other five were NO_2 and MMH sensors. This resulted in the capability of 13 separate NO_2 concentration measurements. All instruments were capable of full-scale measurements of 0-5, 0-50, and 0-500 ppm concentrations. The detector cell was an electrochemical transducer and required that a sample of the gas be pumped down to the instrument, through the cell, and exhausted. The sample lines were all the same length (10 m) regardless of the height of the intake port. This was done to keep the delay in the lines the same for all sensors. The instrument's internal pump was not adequate to sample through this length of tubing, consequently each sensor channel was provided with its own 1/8 hp Air Cadet pump. The total sample delay time with these pumps was only about 2 sec, which was small compared to the instruments response time (10-15 sec to 90% of full scale). A portion of the exhaust from the Air Cadet pumps was forced through the ESI sensors at the prescribed flow rate. The ESI sensors were outfitted with new transducer cells and checked for accuracy prior to installation in the field. These sensors were quite reliable and demonstrated minimal baseline drift throughout the entire test series.

A 20 mil, Type K thermocouple was located at the sample intake of each sensor, however, no temperature variations were observed during any of the spill tests.

Station G24 had an ESI NO_2 sample port at the 1 m level, and two International Sensor Technology (IST) NO_2 sensors at 3.5 and 8.5 m. The accuracy of the IST NO_2 sensors was found to be greatly effected by small variations in the relative humidity, and they required continual zero-span adjustments. Furthermore, the IST response was not linear over the desired 0-500 ppm range. Consequently, the data obtained by these two sensors was not felt to be of sufficient accuracy to publish in this report.

2.6 The Portable NO_2 Gas Sensors

In addition to the gas sensors mounted on the towers of the 25 m and the 785 m downwind stations, two portable Interscan Model 140D NO_2 gas sensors

were also used during the tests. These sensors used an electro-chemical transducer, and drew the gas sample through a short ($\sim$ 1.0 m) tube located about 1 m above the ground. The analog signal from these sensors was recorded on a Russtrack stripchart recorder operating at a speed of 48 in/hr. These recorders were quite old and the chart speed was not very accurate ($\pm$ 10 min over a 4-hr period). Both sensors had a maximum concentration range of 10 ppm NO_2, and were refurbished and recalibrated by the manufacturer just prior to the Eagle test series.

The portable NO_2 sensors were used to obtain data both during the spill tests, and to monitor the CCDRS trailer park and the Frenchman Flat access roads overnight after the spills. Their spill test positions were at various locations in a 2800 m row previously used for the NH_3 tests.

2.7 Photographic Coverage

Photographic and video coverage of EAG1-EAG3 were provided by LLNL. Photographic coverage of the PFVSS tests were the responsibility of Hill AFB. There was only video coverage of the EAG6 spill.

The LLNL cameras were located as shown in Fig. 5. For EAG2 and EAG3 there were a total of five cameras. At the upwind location there were an Aeroflex 16 mm movie camera (#1), a Nikon FM 35 mm programmable framing camera (#2), and a Pentax programmable framing camera (#5) used for slides only. For the EAG1 spill the Pentax was not available. There were two cameras at the crosswind location, an Aeroflex 16 mm movie camera (#3), and a Nikon FM 35 mm programmable camera (#4). All cameras were remotely controlled and began operating at the time the spill valve was opened. The programmable cameras provided coverage for up to 30 min at differing framing rates. The motion picture coverage was for a duration of about 20 min.

Black and white video coverage was provided by a TV camera located 20 m directly upwind of the spill area. This camera was equipped with a remote zoom, pan and tilt capabilities, and was also used to monitor the facility arming and disarming procedure. Data were recorded with a Sony U-matic video cassette recorder

2.8 Data Acquisition and Processing

The control of the spills and the data acquisition and storage was all performed in the CCDRS trailer located at Well 5B (see Fig. 5). This system

utilizes UHF radio telemetry for command and data transmission and is designed to acquire data from sensors distributed over an area with a diameter of up to 10 miles [4]. All of the remote data acquisition stations and sensors are battery-powered, portable, sealed, and ruggedized. Batteries are recharged by solar cells. This network of 24 stations acquired data from up to 270 channels at a rate of one sample per second for the gas and control stations and one sample per 10 sec for the wind-field stations. There are three subsystems (gas, control, and wind-field), each of which functions independently and communicates with its own minicomputer in the CCDRS trailer. These minicomputers sequentially poll the remote stations in their network requesting that they transmit their full data buffers back to the CCDRS trailer. Each system in the CCDRS trailer consists of a DEC LSI-11/23 minicomputer, a 10-MB disk unit, and a graphics display video terminal, with shared magnetic tape and floppy disk units. The data are recorded on disk for subsequent processing. The wind field and some of the spill system data are presented in real time. A picture of the CCDRS trailer park is shown in Fig. 12.

After each test, raw data are converted to fully calibrated data sets on the LSI-11 using sensor calibration tables. These reduced data are written to an ASCII magnetic tape and transferred to the LLNL Computation Center for archival preservation. In order to be able to manipulate this large amount of data, i.e. select data from the data base and perform an operation on it, we employ an LLNL-developed, data base management system. The data base tables are stored on an off-line mass storage system, and are readily available for analysis.

Data manipulation, IR sensor data processing, and plotting are done on a CDC 7600 computer, using existing computational and graphics output devices available at LLNL. In some cases, the data have been averaged over various time periods, condensed to single values for each test, or interpolated/extrapolated to produce the final product. These manipulations of the data are all described in detail in the sections of this report where the final results are presented (Sections 3-6).

3.0 EXPERIMENT SUMMARIES

The purpose of this section is to summarize all of the pertinent parameters associated with each spill test, along with a few general remarks about the evaporation and vapor cloud dispersion. Also included are the exact locations of the operational spill area and array diagnostics. The nomenclature for the various instruments is given in Table 2.

TABLE 2.
Measurement Nomenclature

Gxx	gas/temperature station
PHFF-x	spill area ground heat flux
TGND	spill area ground temperature
TPOOL1	spill area pool (vapor) temperatures at first height
TPOOL2	spill area pool (vapor) temperatures at second height
Wxx	wind field station
σ_θ	wind variability (standard deviation of wind direction)

The average wind speed and direction variability (σ_θ) reported in the experiment summary tables are averages of the entire (nine-station) wind-field data for the three-minute period immediately after the spill valve was opened. The average spill rate is simply the total volume spilled divided by the spill duration. The 10 sec spill valve opening delay is not included in the spill duration. The N_2O_4 spill temperature was measured near the spill pipe exit and was averaged over the spill duration. Pictures of the single-exit, confined spill (EAG1), the multi-exit, unconfined spill (EAG3), and the PFVSS spill configuration are shown in Figs. 13-15, respectively.

The experiment summaries follow and are in order of occurrence (EAG1-EAG6). The wind-field array did not change during the entire test series. The location of the spill area diagnostics varied according to the spill configuration. The spill area heat flux sensors, thermocouples, and N_2O_4 exit thermocouple were operational for all tests except for EAG6, when only TGND and TPOOL1 were deployed. The x,y locations of the mass flux array stations were identical for EAG1-EAG3, however, the sensor's heights were lowered prior to the EAG3 spill.

For the PFVSS tests, gas stations G02 and G20 were removed from their respective arrays and combined to provide both high-concentration N_2O_4 and low-concentration NO_2 measurements at three locations immediately downwind of the spill area. As a result of the severe acid damage of EAG3, gas station G08 was sacrificed to provide spare IR gas sensors for those lost at stations G03-G07.

The EAG6 spill was conducted primarily to dump the N_2O_4 remaining after the PFVSS tests. As a result, only a small level of effort was available to ready the array for dispersion measurements, and stations G02 and G20 were not returned to their original array locations. Also, some of the spill area diagnostics were not installed and there was no photographic coverage of EAG6.

EXPERIMENT SUMMARY: EAGLE 1

Date:	17 September 1983
Time:	2:07 pm PDT
Test Objective:	Spill system checkout, source strength data
Spill Configuration:	Single-exit, confined (7 m dia)
Spill Volume:	1.3 m^3 (340 gal)
Average Spill Rate:	1.75 m^3/min
Spill Duration:	45 sec
N_2O_4 Spill Temperature:	19°C
Prespill Ground Temperature:	43°C
Average Wind Speed:	6.15 m/sec
Average Wind Variability:	σ_θ = 13.3°

Remarks

1) Considerable cloud meander, but appeared to be contained within the 785 m array.

2) Surface vapor temperature indicates N_2O_4 freezing.

3) Short spill, did not establish steady state at 785 m.

4) Peak concentration of 19 ppm NO_2 at 785 m.

5) Cloud appeared to lift off the surface at 785 m.

6) Much outgassing from surface for several hours after the spill was terminated.

MEASUREMENT SUMMARY: EAG1

WIND ARRAY

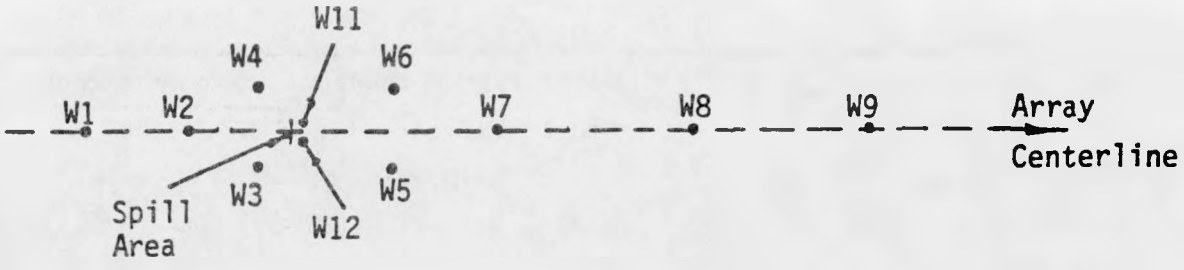

SPILL AREA

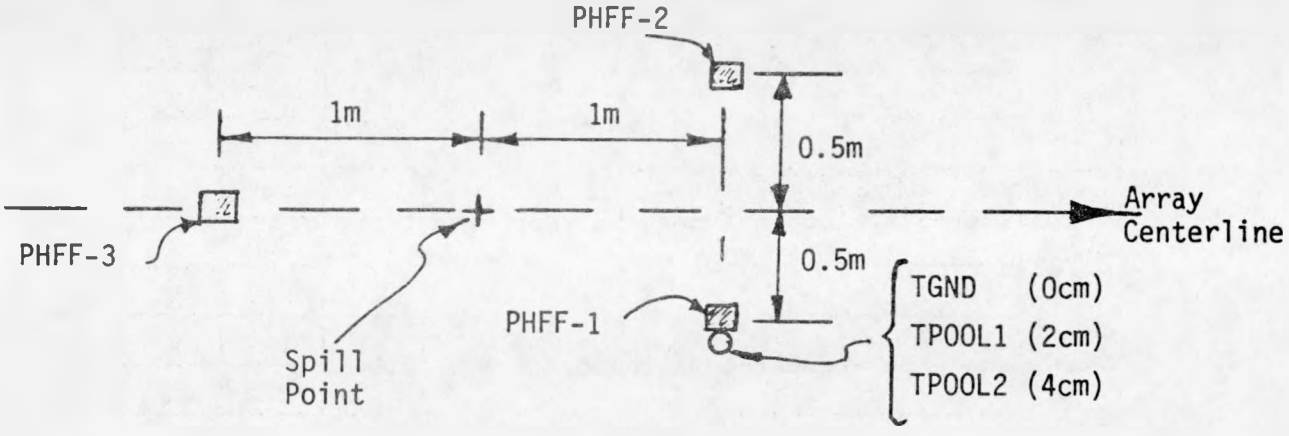

MET. STATIONS

Station (y position)	height (m)	air temp.	wind speed	wind direction	heat flux
G01 (-50)	0				X
	0.82	X			
	2.46	X			
	6.13	X			
	16.2	X			
	3.36		X	X	
	5.83		X	X	
	12.1		X	X	
G05 (+25)	1.3			X	
	3.0			X	
	6.0		X	X	

MEASUREMENT SUMMARY: EAG1

25m ARRAY

station (y position)	height (m)	N_2O_4 conc.	temp.	heat flux
G02 (+15)	0.5	X	X	
	1.5	X	X	
	3.0	X	X	
G03 (+10)	0.5	X	X	
	1.5	X	X	
	3.0		X	
G04 (+5)	0		X	
	0.5	X	X	
	1.5	X	X	
	3.0	X	X	
G05 (0)	0.5	X	X	
	1.5	X	X	
	3.0	X		
G06 (-5)	0		X	
	0.5		X	
	1.5	X	X	
	3.0		X	
G07 (-10)	0.5	X	X	
	1.5	X	X	
	3.0	X	X	
G08 (-15)	0.5	X	X	
	1.5	X	X	
	3.0	X	X	

785m ARRAY

station (y position)	height (m)	NO_2 conc.	temp.
G20 (+200)	1.0	X	X
	3.5	X	X
	8.5	X	X
G21 (+100)	1.0	X	X
	3.5	X	X
	8.5	X	X
G22 (0)	1.0	X	X
	3.5	X	X
	8.5	X	X
G23 (-100)	1.0	X	X
	3.5	X	X
	8.5	X	X
G24 (-200)	1.0	X	X
	3.5		X
	8.5		X

EXPERIMENT SUMMARY: EAGLE 2

Date:	23 September 1983
Time:	5:02 pm PDT
Test Objective:	Multi-exit evaluation test, dispersion data
Spill Configuration:	Multi-exit, unconfined
Spill Volume:	1.5 m^3
Average Spill Rate:	1.4 m^3/min
Spill Duration:	65 sec
N_2O_4 Spill Temperature:	25.2°C
Prespill Ground Temperature:	28.3°C
Average Wind Speed:	5.80 m/sec
Average Wind Variability:	σ_θ = 35.1°

Remarks

1) Multi-exit appeared to distribute fluid nicely.

2) Surface vapor temperature indicates N_2O_4 freezing.

3) Short spill, did not establish steady state at 785 m.

4) Vapor cloud passed over only G24 producing a 60 ppm peak concentration.

5) Still much outgassing from soil after spill was terminated.

MEASUREMENT SUMMARY: EAG2

WIND ARRAY

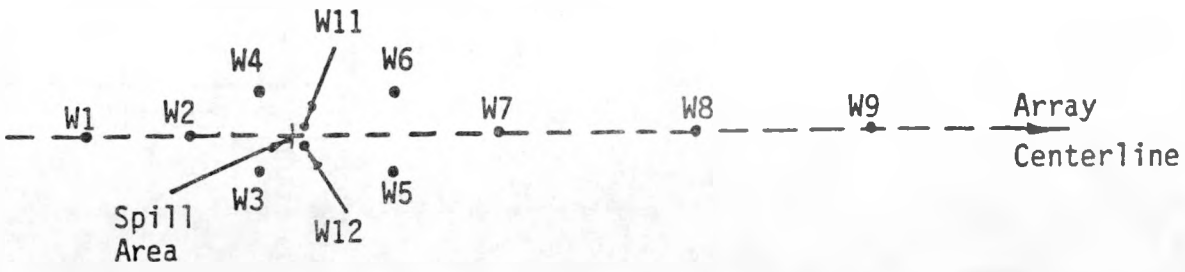

SPILL AREA

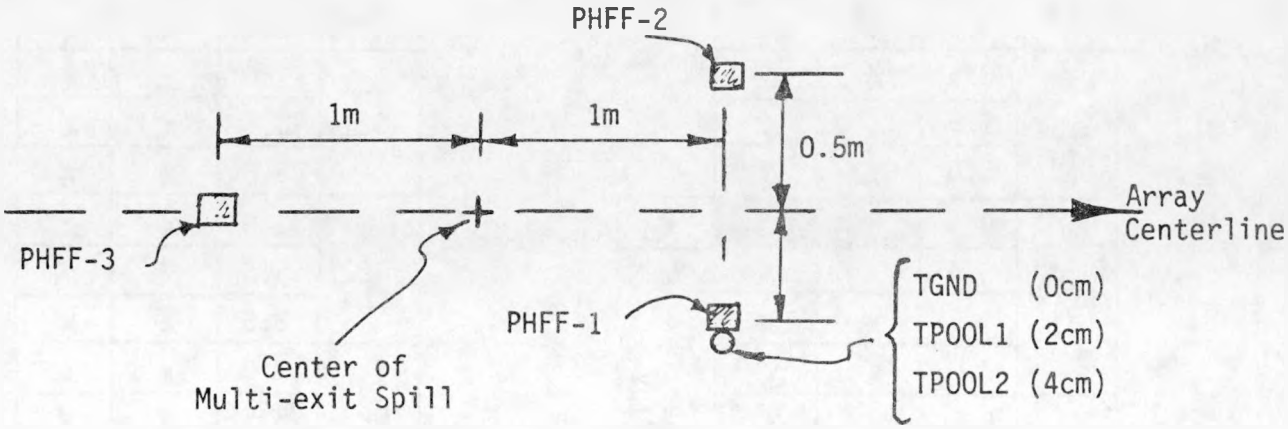

MET. STATIONS

Station (y position)	height (m)	air temp.	wind speed	wind direction	heat flux
G01 (-50)	0				X
	0.82	X			
	2.46	X			
	6.13	X			
	16.2	X			
	3.36		X	X	
	5.83		X	X	
	12.1		X	X	
G05 (+25)	1.3			X	
	3.0			X	
	6.0		X	X	

MEASUREMENT SUMMARY: EAG2

25m ARRAY

station (y position)	height (m)	N_2O_4 conc.	temp.	heat flux
G02 (+15)	0.5	X	X	
	1.5	X	X	
	3.0	X	X	
G03 (+10)	0.5	X	X	
	1.5	X	X	
	3.0	X	X	
G04 (+5)	0		X	
	0.5	X	X	
	1.5	X	X	
	3.0	X	X	
G05 (0)	0.5	X	X	
	1.5	X	X	
	3.0	X		
G06 (-5)	0		X	
	0.5	X	X	
	1.5	X	X	
	3.0	X	X	
G07 (-10)	0.5	X	X	
	1.5	X	X	
	3.0	X	X	
G08 (-15)	0.5	X	X	
	1.5	X	X	
	3.0	X	X	

785m ARRAY

station (y position)	height (m)	NO_2 conc.	temp.
G20 (+200)	1.0	X	X
	3.5	X	X
	8.5	X	X
G21 (+100)	1.0	X	X
	3.5	X	X
	8.5	X	X
G22 (0)	1.0	X	X
	3.5	X	X
	8.5	X	X
G23 (-100)	1.0	X	X
	3.5	X	X
	8.5	X	X
G24 (-200)	1.0	X	X
	3.5		X
	8.5		X

EXPERIMENT SUMMARY: EAGLE 3

Date:	7 October 1983
Time:	4:48 PDT
Test Objective:	Dispersion data
Spill Configuration:	Multi-exit, unconfined
Spill Volume:	4.2 m^3
Average Spill Rate:	1.4 m^3/min
Spill Duration:	188 sec
N_2O_4 Spill Temperature:	19°C
Prespill Ground Temperature:	27°C
Average Wind Speed:	3.14 m/sec
Average Wind Variability:	σ_θ = 13.2°

Remarks

1) Surface vapor temperature indicates N_2O_4 freezing.

2) Severe acid damage to optics on low-level IR sensors at 25 m.

3) Vapor cloud was totally confined within the 785 m array.

4) Long spill, good steady state data at 785 m.

5) NO_2 concentration exceeds 500 ppm at 785 m.

6) No cloud lift off at 785 m.

7) Portable NO_2 sensor at 2800 m shows 9 ppm at ground level.

MEASUREMENT SUMMARY: EAG3

WIND ARRAY

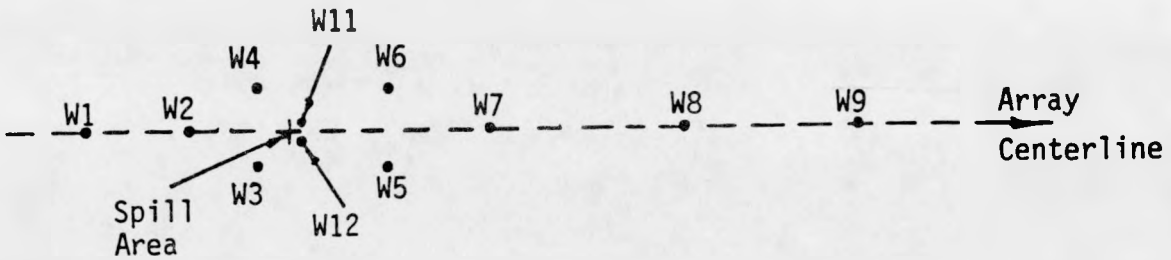

SPILL AREA

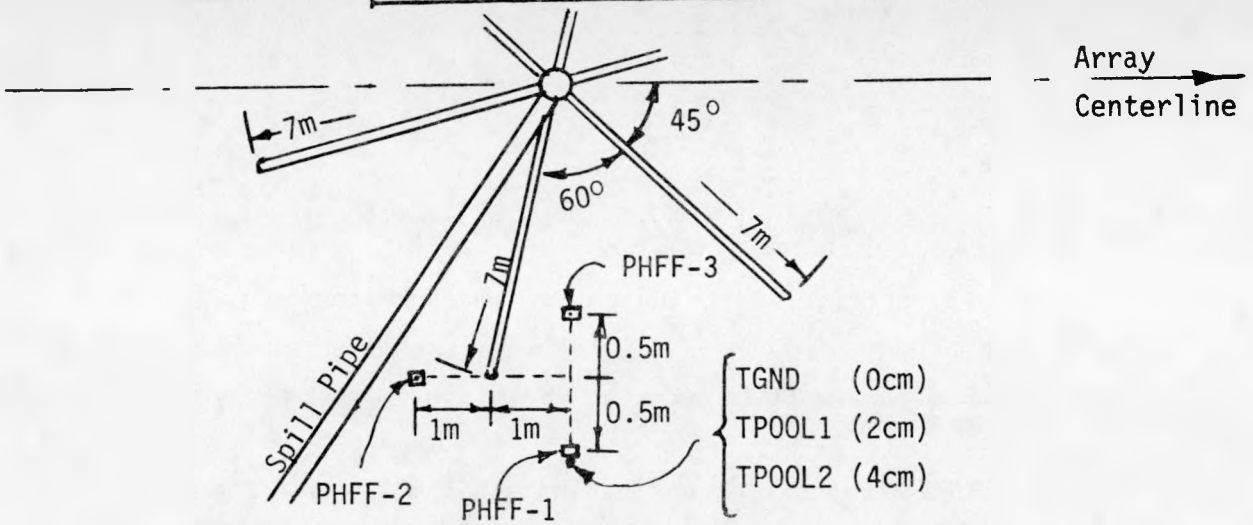

MET. STATIONS

Station (y position)	height (m)	air temp.	wind speed	wind direction	heat flux
G01 (-50)	0				X
	0.82	X			
	2.46	X			
	6.13	X			
	16.2	X			
	3.36		X	X	
	5.83		X	X	
	12.1		X	X	
G05 (+25)	1.3			X	
	3.0			X	
	6.0		X	X	

MEASUREMENT SUMMARY: EAG3

25m ARRAY

station (y position)	height (m)	N_2O_4 conc.	temp.	
G02 (+15)	0.30	X	X	
	0.75	X	X	
	1.25	X	X	
G03 (+10)	0.30	X	X	
	0.75	X	X	
	1.25	X	X	
G04 (+5)	0			X
	0.30	X	X	
	0.75	X	X	
	1.25	X	X	
G05 (0)	0.30	X	X	
	0.75	X	X	
	1.25	X	X	
G06 (-5)	0			X
	0.30	X	X	
	1.0	X	X	
	1.5	X	X	
G07 (-10)	0.30	X	X	
	0.75	X	X	
	1.25	X	X	
G08 (-15)	0.30	X	X	
	0.75	X	X	
	1.25	X	X	

heat flux

785m ARRAY

station (y position)	height (m)	NO_2 conc.	temp.
G20 (+200)	1.0	X	X
	3.5	X	X
	8.5	X	X
G21 (+100)	1.0	X	X
	3.5	X	X
	8.5	X	X
G22 (0)	1.0	X	X
	3.5	X	X
	8.5	X	X
G23 (-100)	1.0	X	X
	3.5	X	X
	8.5	X	X
G24 (-200)	1.0	X	X
	3.5		X
	8.5		X

EXPERIMENT SUMMARY: EAGLE 4

Date:	13 October 1983
Time:	1:22 pm PDT
Test Objective:	PFVSS system evaluation
Spill Configuration:	Single-exit, confined, with plastic liner
Spill Volume:	2.8 m^3
Average Spill Rate:	0.5 m^3/min
Spill Duration:	341 sec
N_2O_4 Spill Temperature:	19.8°C
Prespill Ground Temperature:	53.0°C
Average Wind Speed:	4.94 m/sec
Average Wind Variability:	σ_θ = 12.2°

Remarks

1) Cloud passed through 785 m array producing a 20 ppm peak concentration.

2) The initial and reapplications of the foam appeared to adequately suppress the vapors.

3) The diluted N_2O_4 was successfully pumped into the storage bladder, after some pump intake clogging.

MEASUREMENT SUMMARY: EAG4

WIND ARRAY

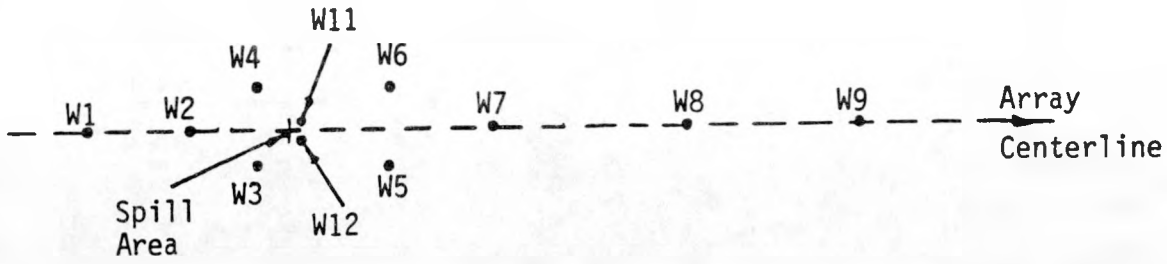

SPILL AREA

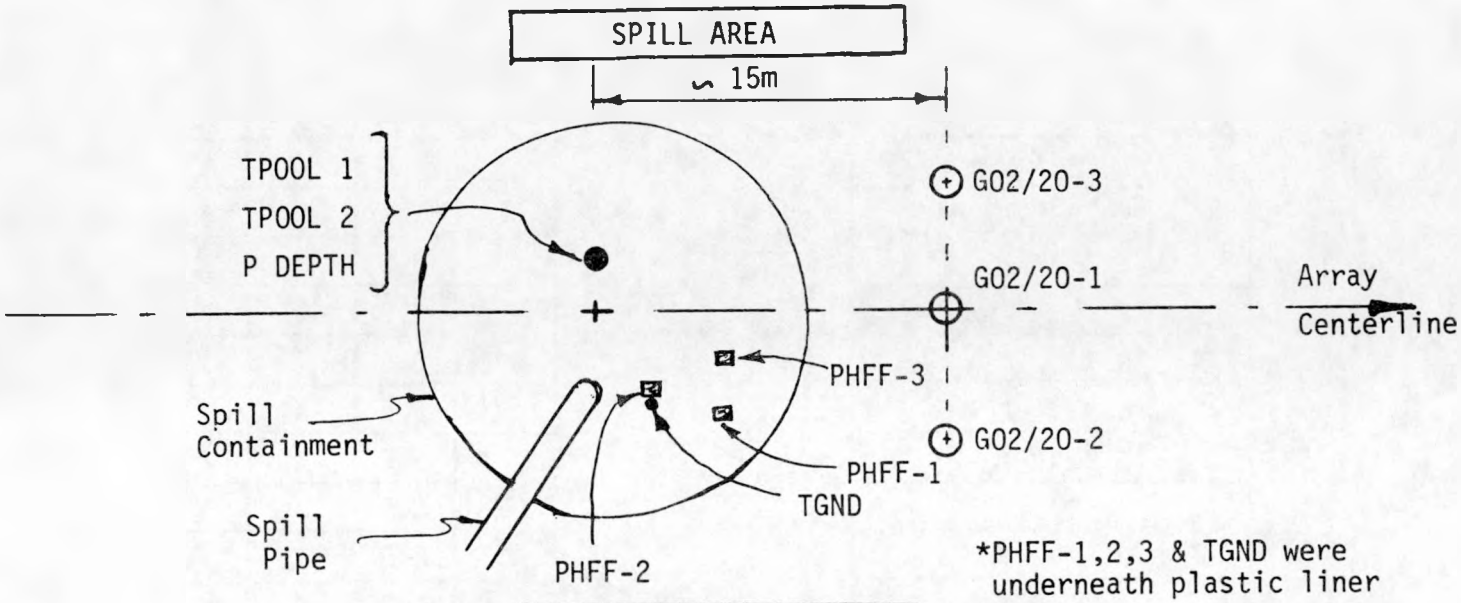

*PHFF-1,2,3 & TGND were underneath plastic liner

MET. STATIONS

Station (y position)	height (m)	air temp.	wind speed	wind direction	heat flux
GO1 (-50)	0				X
	0.82	X			
	2.46	X			
	6.13	X			
	16.2	X			
	3.36		X	X	
	5.83		X	X	
	12.1		X	X	
GO5 (+25)	1.3			X	
	3.0			X	
	6.0		X	X	

MEASUREMENT SUMMARY: EAG4

25m ARRAY

station (y position)	height (m)	N_2O_4 conc.	temp.	
G02	1.0	X	X	located immediately downwind of spill area
	1.0	X	X	
	1.0	X		
G03 (+10)	0.30	X	X	
	0.75	X	X	
	1.25	X	X	
G04 (+5)	0		X	heat flux
	0.30	X	X	
	0.75	X	X	
	1.25	X	X	
G05 (0)	0.30	X	X	
	0.75	X	X	
	1.25	X	X	
G06 (-5)	0		X	
	0.30		X	
	0.75	X	X	
	1.25	X	X	
G07 (-10)	0.30	X	X	
	0.75	X	X	
	1.25	X	X	

785m ARRAY

station (y position)	height (m)	NO_2 conc.	temp.
G20	1.0	X	
	1.0	X	
	1.0	X	
G21 (+100)	1.0	X	X
	3.5	X	X
	8.5	X	X
G22 (0)	1.0	X	X
	3.5	X	X
	8.5	X	X
G23 (-100)	1.0	X	X
	3.5	X	X
	8.5	X	X
G24 (-200)	1.0	X	X
	3.5		X
	8.5		X

EXPERIMENT SUMMARY: EAGLE 5

Date:	16 October 1983
Time:	4:11 pm PDT
Test Objective:	PFVSS system evaluation
Spill Configuration:	single-exit, confined, with plastic liner
Spill Volume:	1.3 m^3
Average Spill Rate:	0.6 m^3/min
Spill Duration:	130 sec
N_2O_4 Spill Temperature:	17°C
Prespill Ground Temperature:	41°C
Average Wind Speed:	2.21 m/sec
Average Wind Variability:	σ_θ = 38.5°

Remarks

1) Wind direction at 261°, the vapor cloud missed the 785 m array.

2) Liquid pool temperature down to -4°C.

3) Pump intake still had clogging problems, however the foam appeared to suppress the vapors quite effectively.

MEASUREMENT SUMMARY: EA5

WIND ARRAY

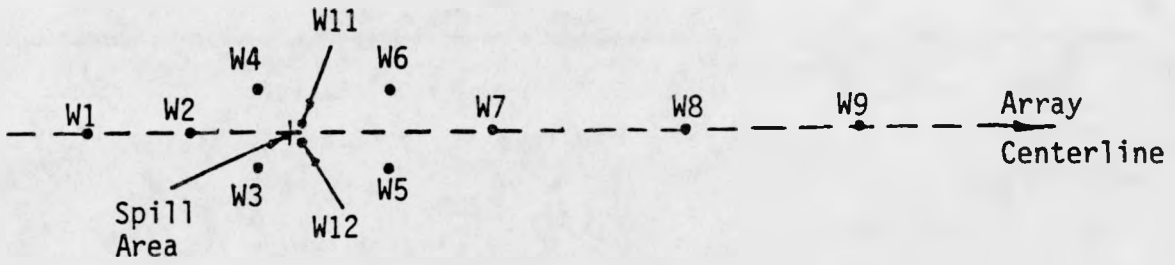

SPILL AREA

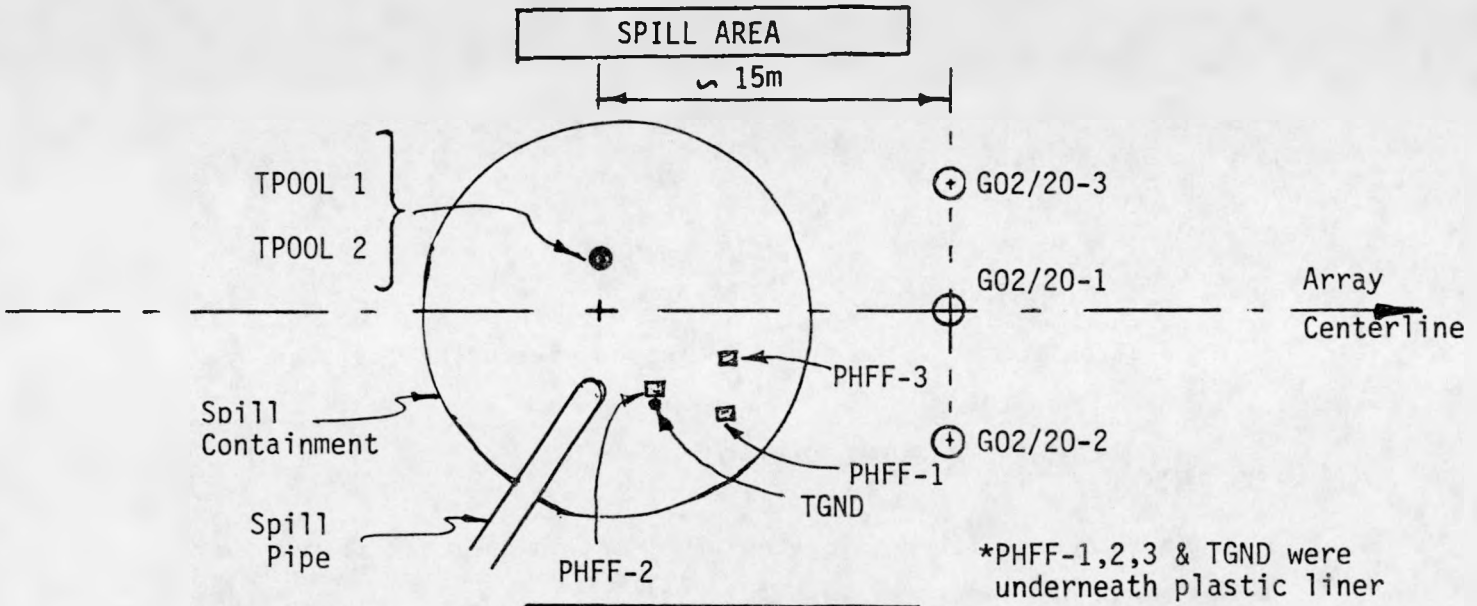

*PHFF-1,2,3 & TGND were underneath plastic liner

MET. STATIONS

Station (y position)	height (m)	air temp.	wind speed	wind direction	heat flux
GO1 (-50)	0				X
	0.82	X			
	2.46	X			
	6.13	X			
	16.2	X			
	3.36		X	X	
	5.83		X	X	
	12.1		X	X	
GO5 (+25)	1.3			X	
	3.0			X	
	6.0		X	X	

MEASUREMENT SUMMARY: EAG5

25m ARRAY

station (y position)	height (m)	N_2O_4 conc.	temp.	
G02	1.0	X	X	located immediately downwind of spill area
	1.0	X	X	
	1.0	X	X	
G03 (+10)	0.30	X	X	
	0.75	X	X	
	1.25	X	X	
G04 (+5)	0		X	heat flux
	0.30	X	X	
	0.75	X	X	
	1.25	X	X	
G05 (0)	0.30	X	X	
	0.75	X	X	
	1.25		X	
G06 (-5)	0		X	heat flux
	0.30		X	
	0.75	X	X	
	1.25	X	X	
G07 (-10)	0.30	X	X	
	0.75	X	X	
	1.25	X	X	

785m ARRAY

station (y position)	height (m)	NO_2 conc.	temp.
G20	1.0	X	
	1.0	X	
	1.0	X	
G21 (+100)	1.0	X	X
	3.5	X	X
	8.5	X	X
G22 (0)	1.0	X	X
	3.5	X	X
	8.5	X	X
G23 (-100)	1.0	X	X
	3.5	X	X
	8.5	X	X
G24 (-200)	1.0	X	X
	3.5		X
	8.5		X

EXPERIMENT SUMMARY: EAGLE 6

Date:	30 October 1983
Time:	2:37 pm PST
Test Objective:	Dump remaining N_2O_4; dispersion data if possible
Spill Configuration:	Multi-exit, unconfined
Spill Volume:	3.4 m^3
Average Spill Rate:	0.7 m^3/min
Spill Duration:	296 sec
N_2O_4 Spill Temperature:	17.5°C
Prespill Ground Temperature:	28.0°C
Average Wind Speed:	4.96 m/sec
Average Wind Variability:	σ_θ = 7.5°

Remarks

1) A very long spill (296 s) at low rate, good steady state data.

2) Vapor cloud contained within the 785 m array, maximum NO_2 concentration greater than 500 ppm.

3) There was no photographic coverage coverage of this spill, nor were there any NO_2 sensors at 2800 m.

MEASUREMENT SUMMARY: EAG6

WIND ARRAY

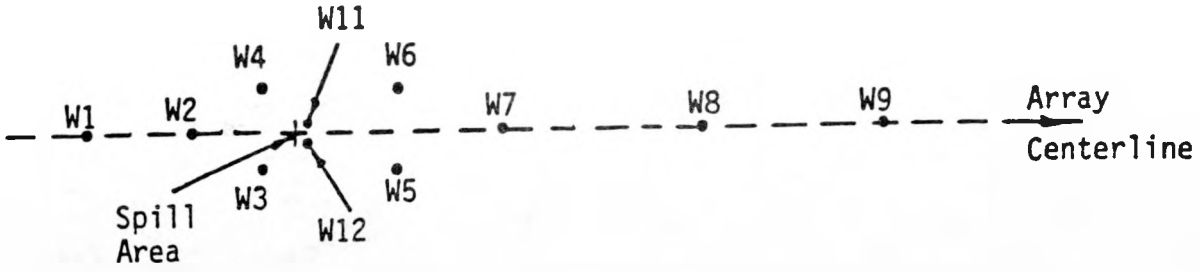

SPILL AREA

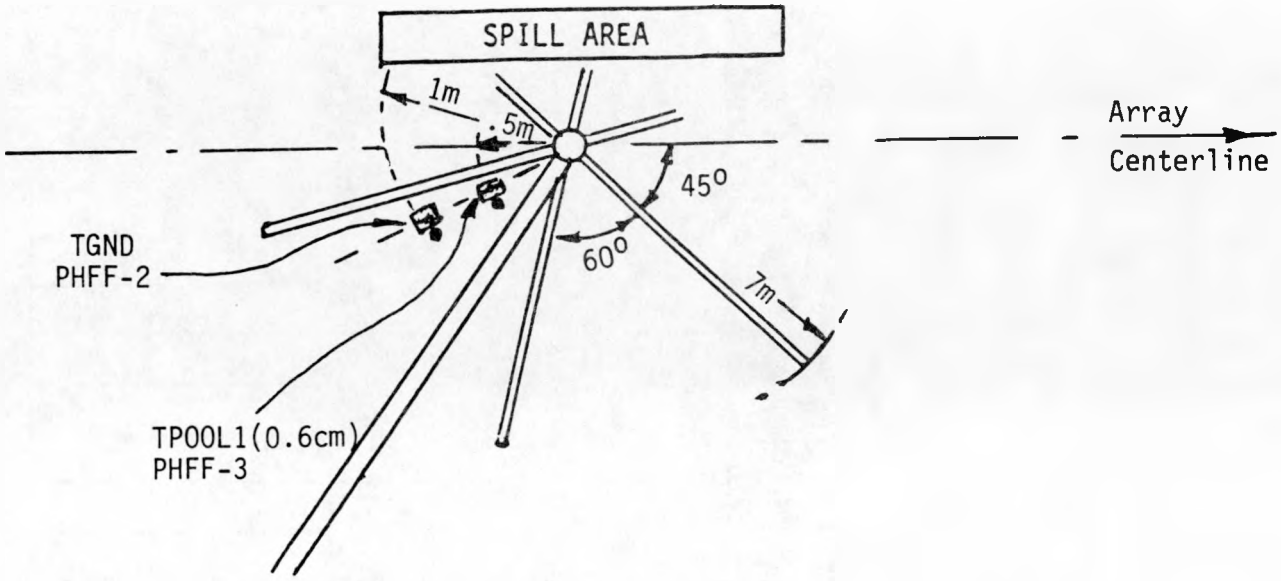

MET. STATIONS

Station (y position)	height (m)	air temp.	wind speed	wind direction	heat flux
G01 (-50)	0				X
	0.82	X			
	2.46	X			
	6.13	X			
	16.2	X			
	3.36		X	X	
	5.83		X	X	
	12.1		X	X	
G05 (+25)	1.3			X	
	3.0			X	
	6.0		X	X	

MEASUREMENT SUMMARY: EAG6

25m ARRAY

station (y position)	height (m)	N_2O_4 conc.	temp.	
G02	0.30			
	0.30			
	0.30			
G03 (+10)	0.30	X	X	
	0.75	X	X	
	1.25	X	X	
G04 (+5)	0			X
	0.30	X		
	0.75	X	X	
	1.25	X	X	
G05 (0)	0.30	X	X	heat flux
	0.75	X	X	
	1.25		X	
G06 (-5)	0			X
	0.30	X		
	0.75	X	X	
	1.25	X	X	
G07 (-10)	0.30	X	X	
	0.75	X	X	
	1.25	X	X	

785m ARRAY

station (y position)	height (m)	NO_2 conc.	temp.
G21 (+100)	1.0	X	X
	3.5	X	X
	8.5	X	X
G22 (0)	1.0	X	X
	3.5	X	X
	8.5	X	X
G23 (-100)	1.0	X	X
	3.5	X	X
	8.5	X	X
G24 (-200)	1.0	X	X
	3.5		X
	8.5		X

4.0 THE METEOROLOGICAL RESULTS

The data contained in this section includes summaries of the atmospheric boundary layer conditions in effect during each spill, estimates of the center-line trajectory of the dispersing vapor cloud as predicted by the wind-field data, and a measure of the atmospheric turbulence immediately upwind of the spill area.

4.1 The Atmospheric Boundary Layer Data

A summary of the atmospheric boundary layer data for each of the six Eagle series tests is presented in Tables 3 - 8 in the form of widely recognized meteorological parameters. The background and physical significance of these parameters is adequately described elsewhere (5,6,7) and only a brief description of each is presented here.

The average wind direction, its standard deviation (sigma theta), the average wind speed, and its standard deviation (sigma speed) were taken from the wind-field data from the nine anemometer stations averaged over a three-minute period starting at zero time. The wind speed profile and the temperature profile were calculated respectively from the bivane data and the temperature data of station G01 for the same three-minute interval.

The friction velocity u_*, scaling potential temperature θ_*, zero level potential temperature θ_o, and the Monin-Obukhov length L are determined from a least squares fit of the wind-speed profile and temperature profile data to the assumed velocity profile, Eq.(1a), and temperature profile, Eq.(2a), as given below.

$$u(z) = (u_*/k)\cdot[\ln(z/z_o) - \psi_m(z/L)] \tag{1a}$$

$$\frac{\partial u(z)}{\partial z} = \frac{u_* \cdot \phi_m(z/L)}{k \cdot z} \tag{1b}$$

$$\theta(z) = \theta_o + (\theta_*/k)\cdot[\ln(z/z_o) - \psi_h(z/L)] \qquad (2a)$$

$$\frac{\partial\theta(z)}{\partial z} = \frac{\theta_*\cdot\phi_h(z/L)}{k\cdot z} \qquad (2b)$$

In these equations u(z) is the wind speed at height z, $\theta(z)$ is the potential temperature at height z, and k = 0.41 is the von Karman constant. The surface roughness z_o was estimated from the zero wind-speed intercept under neutral stability conditions ($\psi_m = 0$) and was found to be approximately .0003 m for these tests.

The similarity functions used in Eqs.(1 & 2) are defined such that when $L \geq 0$:

$$\psi_m(z/L) = \psi_h(z/L) = -5\cdot z/L$$

$$\phi_m(z/L) = \phi_h(z/L) = 1 + 5\cdot z/L$$

and when $L < o$; (3)

$$\psi_m(z/L) = 2\cdot\ln[(1+x)/2] + \ln[(1+x^2)/2] - 2\cdot\tan^{-1}(x) + \pi/2$$

$$\psi_h(z/L) = 2\cdot\ln[(1+x^2)/2]$$

$$\phi_m(z/L) = 1/x$$

$$\phi_h(z/L) = 1/x^2 \text{ where } x = (1-16\cdot z/L)^{1/4}$$

The parameters u_*, θ_*, θ_o and L are all related by the Monin-Obukhov length definition

$$L = u_*^2\cdot\theta_o/g\cdot k\cdot\theta_* \qquad (4)$$

where $g = 9.8\ m/s^2$ is the acceleration of gravity. Equation (4) is used as a constraint on the least squares fit of the profile data to the analytic curves of Eqs.(1a & 2a).

The potential temperature is defined to be

$$\theta = T \cdot (p_o/p)^{\kappa} \tag{5a}$$

where T = ambient temperature
p = ambient pressure
p_o = standard pressure = 1000 mb
$\kappa = R/c_p = .285.$

Differentiating Eq.(5a) with respect to height z, using the hydrostatic approximation, $\partial p = -g \cdot \rho \cdot \partial z$, and the ideal gas law, $p = \rho \cdot R \cdot T$, assuming that the ratio θ/T is essentially constant over the height range of interest, and then integrating with respect to height yields the following equation for potential temperature as a function of temperature and height

$$\theta = (p_o/p_r)^{\kappa} \cdot [T + \gamma \cdot (z - z_r)] \tag{5b}$$

where $\gamma = g/c_p$

and sub "r" denotes reference value. Eq. (5b) was used to calculate the potential temperatures from the temperature data.

The sensible heat flux, H, defined to be negative upward, is calculated from

$$H = \rho \cdot c_p \cdot u_* \cdot \theta_* \tag{6}$$

where $\rho = 1.13\ kg/m^3$ ($\pm$ 1% for 30 to 40°C) and $c_p = 1005$ W sec/kg°C are respectively the density and specific heat of the ambient atmosphere. The momentum diffusivity K_m and the heat diffusivity K_h are calculated from the formulas

$$K_m(z) = u_* \cdot k \cdot z/\phi_m(z/L) \qquad (7a)$$

$$K_h(z) = u_* \cdot k \cdot z/\phi_h(z/L) \quad . \qquad (7b)$$

The Richardson number is defined and calculated from the similarity functions as follows

$$Ri(z/L) = (g/\theta_o) \cdot (\partial\theta/\partial z)/(\partial u/\partial z)^2 = (z/L) \cdot \phi_h(z/L)/\phi_m^2(z/L) \quad . \qquad (8)$$

In addition to the LLNL data, the relative humidity, barometric pressure, and boundary layer temperatures and speeds were also recorded by the Weather Service Nuclear Support Office (WSNSO) of the National Oceanic and Atmospheric Administration, Las Vegas, Nevada. The relative humidity and barometric pressure were recorded at a WSNSO station located just downwind of the CCDRS trailer park. The atmospheric temperature and wind speed were also measured by WSNSO at heights of 10 and 30 m at a location about 6 km south-southwest of the spill area. Unfortunately, the 10 and 30 m measurements were made using two different towers separated by about 100 m. The horizontal wind speed and temperature recorded at these two locations (stations #38 and #39) for the day of each spill are presented in Figs. 16 - 20. The WSNSO stations were not operational for EAG4. The local time is Pacific Standard Time (PST) in all plots.

Table 3
Boundary Layer Data: Eagle 1

Average wind direction at 2 m	233 degrees
Sigma theta	13.3 degrees
Average wind speed at 2 m	6.15 m/sec
Sigma speed	1.39 m/sec
Wind speed profile (G01)	
at 3.36 m	7.39 $\pm$ 1.09 m/sec
at 5.83 m	7.78 $\pm$ 1.05 m/sec
at 12.10 m	8.16 $\pm$ 1.01 m/sec
U star	0.307 m/sec
Percent cloud cover	5%
Temperature profile (G01)	
at 0.82 m	34.28°C
at 2.46 m	33.57°C
at 6.13	33.17°C
θ star	-0.374°C
Barometric pressure	904.5 mbars
Relative humidity	26%
Sensible heat flux	-118.4 watt/m^2
Momentum diffusivity at 2 m	0.319 m^2/sec
Heat diffusivity at 2 m	0.404 m^2/sec
Monin-Obukhov length	-20.2 m
Richardson number at 2 m	-.0990
Roughness length	.0003 m

Table 4
Boundary Layer Data: Eagle 2

Average wind direction at 2 m	223 degrees
Sigma theta	35.1 degrees
Average wind speed at 2 m	5.80 m/sec
Sigma speed	1.02 m/sec
Wind speed profile (G01)	
at 3.36 m	6.15 $\pm$ 1.00 m/sec
at 5.83 m	6.50 $\pm$ 1.05 m/sec
at 12.10 m	6.87 $\pm$ 0.90 m/sec
U star	0.284 m/sec
Percent cloud cover	5%
Temperature profile (G01)	
at 0.82 m	29.00°C
at 2.46 m	28.77°C
at 6.13	28.89°C
θ star	-0.0315°C
Barometric pressure	905.6 mbars
Relative humidity	23%
Sensible heat flux	-9.37 watt/m^2
Momentum diffusivity at 2 m	0.242 m^2/sec
Heat diffusivity at 2 m	0.251 m^2/sec
Monin-Obukhov length	-198. m
Richardson number at 2 m	-0.101
Roughness length	.0003 m

Table 5
Boundary Layer Data: Eagle 3

Average wind direction at 2 m	229 degrees
Sigma theta	13.2 degrees
Average wind speed at 2 m	3.13 m/sec
Sigma speed	0.48 m/sec
Wind speed profile (G01)	
at 3.36 m	3.16 ± 0.53 m/sec
at 5.83 m	3.94 ± 0.59 m/sec
at 12.10 m	4.16 ± 0.62 m/sec
U star	0.129 m/sec
Percent cloud cover	95%
Temperature profile (G01)	
at 0.82 m	22.01°C
at 2.46 m	22.31°C
at 6.13	22.58°C
θ star	0.075°C
Barometric pressure	907.9 mbars
Relative humidity	45%
Sensible heat flux	10.43 watt/m²
Momentum diffusivity at 2 m	0.066 m²/sec
Heat diffusivity at 2 m	0.066 m²/sec
Monin-Obukhov length	16.8 m
Richardson number at 2 m	.0746
Roughness length	.0003 m

Table 6
Boundary Layer Data: Eagle 4

Average wind direction at 2 m	233 degrees
Sigma theta	12.2 degrees
Average wind speed at 2 m	4.94 m/sec
Sigma speed	1.14 m/sec
Wind speed profile (G01)	
at 3.36 m	4.48 ± 0.81 m/sec
at 5.83 m	4.79 ± 0.74 m/sec
at 12.10 m	5.11 ± 0.68 m/sec
U star	0.245 m/sec
Percent cloud cover	5%
Temperature profile (G01)	
at 0.82 m	24.56°C
at 2.46 m	24.23°C
at 6.13	24.08°C
θ star	-0.139°C
Barometric pressure	898.8 mbars
Relative humidity	17%
Sensible heat flux	-36.0 watt/m²
Momentum diffusivity at 2 m	0.238 m²/sec
Heat diffusivity at 2 m	0.282 m²/sec
Monin-Obukhov length	-33.4 m
Richardson number at 2 m	-.0599
Roughness length	.0003 m

Table 7
Boundary Layer Data: Eagle 5

Average wind direction at 2 m	261 degrees
Sigma theta	38.5 degrees
Average wind speed at 2 m	2.21 m/sec
Sigma speed	0.85 m/sec
Wind speed profile (G01)	
at 3.36 m	2.49 $\pm$ 0.82 m/sec
at 5.83 m	2.59 $\pm$ 0.78 m/sec
at 12.10 m	2.58 $\pm$ 0.81 m/sec
U star	0.114 m/sec
Percent cloud cover	1%
Temperature profile (G01)	
at 0.83 m	22.65°C
at 2.46 m	22.57°C
at 6.13	22.69°C
θ star	.008°C
Barometric pressure	906.9 mbars
Relative humidity	23%
Sensible heat flux	1.00 watt/m^2
Momentum diffusivity at 2 m	0.086 m^2/sec
Heat diffusivity at 2 m	0.086 m^2/sec
Monin-Obukhov length	119. m
Richardson number at 2 m	.0155
Roughness length	.0003 m

Table 8
Boundary Layer Data: Eagle 6

Average wind direction at 2 m	223 degrees
Sigma theta	7.5 degrees
Average wind speed at 2 m	4.96 m/sec
Sigma speed	0.68 m/sec
Wind speed profile (G01)	
at 3.36 m	5.42 $\pm$ 0.63 m/sec
at 5.83 m	5.75 $\pm$ 0.60 m/sec
at 12.10 m	6.10 $\pm$ 0.51 m/sec
U star	0.233 m/sec
Percent cloud cover	85%
Temperature profile (G01)	
at 0.83 m	22.44°C
at 2.46 m	22.45°C
at 6.13	22.46°C
θ star	.014°C
Barometric pressure	909.3 mbars
Relative humidity	35%
Sensible heat flux	3.50 watt/m^2
Momentum diffusivity at 2 m	0.185 m^2/sec
Heat diffusivity at 2 m	0.185 m^2/sec
Monin-Obukhov length	293. m
Richardson number at 2 m	.0066
Roughness length	.0003 m

4.2 The Wind-field Data

The wind field during all of the Eagle Series spills was measured by an array of nine anemometers each mounted at a height of 2 m above the ground. The array covered an area from 1000 m upwind of the spill point to 2800 m downwind, as shown in Fig. 5. Wind speed and direction were measured every second and averaged within each remote station for a 10-sec period. Mean values of speed and direction, and RMS values (σ_θ) about the mean wind direction for the 10-sec period were calculated and transmitted to the data-recording trailer.

The wind field is a primary factor in estimating the dispersion of the N_2O_4 vapor cloud. In order to provide a preliminary estimate of cloud transport and dispersion, trajectory plots were constructed from the wind-field data. Data from the nine wind-field stations were interpolated and extrapolated to a 200-m wide by 2800-m long grid beginning at the spill point and straddling the array centerline. These data were then used to track hypothetical particles released every 10 sec during the spill. These computer-generated centerline trajectories at selected times during each spill are shown in Figs. 21 - 26. The centerline of cloud travel is indicated in each plot by a solid line. Using the interpolated σ_θ data, trajectories were also constructed for hypothetical particles tracked along wind directions of the centerline trajectory $\pm \sigma_\theta$. These ever-widening trajectories, indicated by dotted lines, display the lateral cloud dispersion associated with a spreading rate equal to the measured wind-field fluctuations. The "concentrations" at the dotted boundaries represent about 60% of the centerline value.

These results should closely estimate the position of the vapor cloud centerline as it passes through the dispersion array.

4.3 The Turbulence Data

Turbulence data were recorded (one sample/sec) at two stations, G01 and G05. Both of these stations were equipped with three bivane anemometers capable of measuring the wind speed and its horizontal and vertical direction components. The anemometer data of G01 were used to calculate the wind speed profiles of Tables 4 - 9. The purpose of station G05 was to determine if

there was any measurable wind-field displacement or turbulence perturbations as a result of the presence of the N_2O_4 vapors. Unfortunately, the two lower-level anemometers (1.3 and 3 m) of G05 were damaged during the NH_3 spills and never produced usable results for the Eagle series.

The 2.46-m high anemometer data of station G01 are presented in Figs. 27 - 32 and are felt to be representive of the local wind-field turbulence.

5.0 THE N_2O_4 SOURCE STRENGTH RESULTS

This section presents the data obtained in the spill area and by the mass flux array. These data are required to determine the evaporation rate of the spilled N_2O_4. Unfortunately, as explained in Section 5.2, the formation of nitric acid mist has made accurate determination of the source strength via the mass flux array very difficult. As a result, a great deal of attention has been spent in the processing and display of both the spill area and mass flux data.

5.1 The Spill Area Data

The spill area data are presented by individual test, and consist of the ground heat flux results and the ground surface, 2- and 4-cm high temperature results. The temperature of the spilled N_2O_4, the spill volume, duration, and average spill rate are given in Section 3. The exact locations of the heat flux gauges and the thermocouple rake system are also given in Section 3. Included in this section (where appropriate) is the N_2O_4 pool depth measurement as determined by the liquid pressure head.

The temperature profile data are given in °C and the spill area heat flux data are in units of kwatt/m^2 where a positive value indicates heat flow into the ground.

Some of the important physical and chemical properties of N_2O_4 are given in Table 9.

Table 9

N_2O_4 Properties

Molecular weight	92.016 gm/mole
Normal boiling point	21.15°C
Normal freezing Point	-12.2°C
Liquid density @ 20°C	1.45 gm/cm^3
Vapor density (S.T.P.)	3.62×10^{-3} gm/cm^3
Heat of vaporization	99 cal/gm
Heat capacity (liquid)	0.378 cal/gm°C
Thermal conductivity (liquid)	3.13×10^{-4} cal/cm-sec-°K

Eagle 1

The temperature profile data and ground heat flow data for the EAG1 test are shown in Figs. 33 and 34, respectively. The EAG1 test was the only spill during which flow rate data were obtained. The EAG1 flowmeter data is shown in Fig. 35.

Eagle 2

The temperature profile data and the ground heat flow data for test EAG2 are shown in Figs. 36 and 37, respectively.

Eagle 3

The temperature profile data and ground heat flow data for the EAG3 test are given in Figs. 38 and 39, respectively.

Eagle 4

The temperature profile and ground heat flow data for test EAG4 are given in Figs. 40 and 41, respectively. The temperature levels of Fig. 40 are too high due to a reference junction amplifier drift problem. Since the PFVSS tests (EAG4 and EAG5) were both confined spills of large volumes of N_2O_4, the liquid did pool to some depth. The results of the pool depth measurement are given in Fig. 42. The pool depth was calculated from the liquid pressure head measurement array using a liquid density of 1.45 gm/cm^3.

Eagle 5

The temperature profile and ground heat flow data for test EAG5 are given in Figs. 43 and 44, respectively. The pool depth system was installed for the EAG5 spill, but the data was of no use.

Eagle 6

The temperature profile and ground heat flow data for test EAG6 are given in Figs. 45 and 46, respectively. For this test there were only two thermocouples (surface and 0.5-cm high), and two heat flux gauges.

5.2 The Vapor Flux Data

As mentioned in Section 2.4, the primary purpose of the mass flux array was to determine the source strength of each spill. This was to be accomplished by measuring the vapor density and velocity as it passed through the 21 gas sensors located in the vertical plane 25 m downwind of the spill area. The mass flux ($\dot{m}$) at any instant in time is calculated by integrating the product of the density and velocity over the entire cross-section of the vapor cloud, i.e.,

$$\dot{m} = {}_A\int \rho u dA \qquad (9)$$

where ρ is the density, u is the vapor velocity component normal to the plane of the array, and A is the cloud cross-sectional area. The summation of the instantaneous mass flux ($\dot{m}$) over the entire vaporization period should equal the amount spilled. This total mass evaporation calculation assumes no N_2O_4 is lost due to permeation into, or deposition onto the ground.

It became immediately obvious upon examination of the EAG1 spill results that something other than N_2O_4 and/or NO_2 vapors were present in the vapor cloud. The four spectral band passes of the LLNL IR gas sensor are shown in Fig. 10. If only N_2O_4 or NO_2 vapors were to pass through the sensor absorption region, one would expect to see strong attenuation in the M and R channels and essentially none in the F and E channels. The four-channel transmission results from station G04 for the EAG1 spill are shown in Fig. 47. As can be seen, the attenuation in the F and E channels, is almost equivalent to that of the M and R channels.

Prior to the EAG3 spill, the IR sensors were tested using N_2O_4 vapors directly from the R16 tanker. The sensors behaved as expected, showing little attenuation in the F and E channels. During the EAG2 and EAG3 spills, grab samples of the vapors were obtained as the cloud passed through the 25 m array. A grab sample of the vapors of the N_2O_4 in the spill pipe was also obtained. These grab samples were analyzed later at LLNL by both mass and IR spectroscopy. None of the grab sample results indicated the presence of a foreign gas capable of producing the broad-band (4-channel) attenuation observed in the Eagle series tests. It was concluded that the attenuation was the result of aerosol scattering which does produce broad-band attenuation.

Furthermore, the photography of the spills show what appears to be a definite two-phase region within the vapor cloud.

The source of the aerosol is believed to be a result of the gas-phase reaction of NO_2 with the ambient humidity, i.e.,

$$3\ NO_2 + H_2O \rightarrow 2\ HNO_3 + NO\ . \qquad (10)$$

This reaction, and the resulting HNO_3 mist formation, has been studied in the past in regards to the scrubbing of NO_2 from exhaust stacks (8-11). The reaction is extremely fast and experiments have shown that for typical atmospheric humidities and NO_2 concentrations greater than 50 ppm, a HNO_3 mist is quickly formed. A HNO_3 mist would also explain the severe acid damage which occurred to the instrumentation and structures in the 25 m array during the spills.

There are serious implications for the 25 m array source strength estimates as a result of the HNO_3 mist. It is well known that the N_2O_4 vapors dissociate quite rapidly to NO_2.[1,2] The scavenging of the NO_2 by the reaction of Eq. (10) will tend to increase the N_2O_4 dissociation. This is in agreement with the observed N_2O_4 concentrations which were much less than expected. Furthermore, since the IR gas sensors were not calibrated for HNO_3 mists, they can only produce estimates of the N_2O_4 vapor content of the cloud. That portion of the total mass flux due to the HNO_3 mist is not known.

The effect of the mist on the downwind dispersion is not known at this time. It is known that NO (Eq. (10)) combines with molecular oxygen (O_2) to form NO_2 at a rate which is dependent on the O_2 concentration and the square of the NO concentration. At very low NO concentrations the oxidation rate is slow (at 10 ppm NO, seven hours are required for 50% oxidation). However, at a concentration of 1% NO, 50% oxidation is achieved in about 24 seconds. The eventual downwind products of the HNO_3 mist are not known due to the highly reactive nature of this substance.

The N_2O_4 concentrations presented in this section pertain only to the vapor portion of the cloud. The IR gas sensor data have been processed assuming the broad band mist attenuation to be equal in both the M and F channels. The corresponding NO_2 concentration was calculated assuming NO_2/N_2O_4 equilibrium, i.e.,

$$C_{NO_2} = \sqrt{K_e \, C_{N_2O_4}} \tag{11}$$

using the equilibrium rate constant (K_e) of Giauque & Kemp[1]

$$K_e = \exp\left[\frac{33.815769 + 0.027048675\ T - 2.9114204 \times 10^{-5}\ T^2 - \frac{12875}{T}}{1.9871}\right] \tag{12}$$

where T is the temperature (°K) corresponding to the N_2O_4 concentration measurement.

The total vapor density (ρ in kg/m^3) was calculated by combining the N_2O_4 and NO_2 concentrations as per

$$\rho = \frac{12.183\ P}{T}\left[46\ C_{NO_2} + 92\ C_{N_2O_4}\right] \tag{13}$$

where P is the local pressure (atm) and C_{NO_2} and $C_{N_2O_4}$ are the NO_2 and N_2O_4 volume fractions, respectively.

One other liberty has been taken in the presentation of the N_2O_4 concentration data. The N_2O_4 data were very noisy, and in the interest of a more discernible presentation, the data have been smoothed using an 11-point sliding average. Each concentration value is replaced by the average value of itself and the five values immediately before and after. The results of this data smoothing are shown in Fig. 48. This, in effect, provides a continuous display of the average value of the data.

N_2O_4 Concentration Data (@ 25 m)

When the 25 m array was fully operational, there were a total of 21 N_2O_4 gas concentration data sets. In order to conserve space, all gas sensor data at the same height have been superimposed in each plot. This effectively removes the meander of the vapor cloud back and forth across the array. The envelope of the maximum concentration values is indicative of the temporal variation of the cloud centerline concentration. The results of the EAG1-EAG3 and EAG6 tests are presented in Figs. 49-52.

The 25 m array for EAG6 does not include stations G02 or G08 (Fig. 52). The middle and upper gas sensors of station G06, spill EAG3 (Fig. 51), are not included in the row plot data, as both were not lowered to the 0.75 m and 1.25 m heights of the other middle and upper level sensors in the array.

The source strength data for the PFVSS tests EAG4 and EAG5 are given in Figs. 53 and 54 respectively. Measurements of both N_2O_4 (G02) and NO_2 (G20) were made approximately 15 m downwind of the spill point during each of these spills.

N_2O_4 Concentration Contours @ 25 m

The N_2O_4 concentration contours in the vertical plane of the 25 m array are shown in Figs. 55-58. These data represent the N_2O_4 concentration distribution across the 25 m array at several different times during the spills. The contours are as they would appear to an observer at the spill area looking in the downwind direction. The time and concentration levels (% vol) are indicated on each plot.

The contour routine assumes a linear interpolation between the concentration values recorded at each sensor location. In order that the contours not close below the lower level of sensors, extrapolations of the data were required. Two techniques were used to extrapolate the vertical concentration data to the ground level. If the middle height concentration at a station was less than the lower height value, the ground level concentration was determined by using a quadratic curve through these two values whose slope (concentration gradient) is zero at the ground. For cases where the middle height concentration was greater than the lower height value, the ground level concentration was determined by a linear extrapolation of these two values.

The contour plots of Figs. 55-58 only represent the data of the EAG1-EAG3 and EAG6 tests. The N_2O_4 vapor concentrations were either too low, or missed most of the 25 m array during the EAG4 and EAG5 spills.

Temperature Data @ 25 m

The temperature data of the 25 m array is presented in Figs. 59-62 and is felt to be important for several reasons. First of all, it is required to calculate the NO_2 concentrations from the N_2O_4 data, and to calculate the total mass density. Secondly, it will probably be important for the analysis of the HNO_3 mist formation. Lastly, it indicates an additional

heavier-than-air aspect of the N_2O_4/NO_2 cloud dispersion characteristics, due to the increase in density of the cold vapor.

The temperature data is also presented in the form of row plots; i.e., superposition of all the 25 m row data at the same height. For EAG1-EAG3 (Figs. 59-61) this generally involves seven data sets per plot. Once again, the idea here is to remove the meander of the vapor cloud across the array from the results. For EAG6 (Fig. 62), there are only five data sets per plot as stations G02 and G08 were not set up.

The only temperature data presented for EAG4 (Fig. 63) and EAG5 (Fig. 64) is that of station G02. These data are also superimposed and represent the temperature results for the three 1 m high stations located approximately 15 m downwind of the spill point.

Wind Speed Data @ 25 m

The wind speed data (m/sec) obtained at stations W11 and W12 in the 25 m array are presented in Figs. 65-70. These data indicate the speed that the N_2O_4/NO_2 vapors passed through the 25 m array, a quantity required for the vapor flux calculations to follow. The plots represent linear connections of 10-sec average values of the wind speed.

N_2O_4 Vapor Flux Results

The estimates of the instantaneous and accumulative N_2O_4/NO_2 vapor flux through the 25 m array for the EAG1-EAG3 and EAG6 spills are given in Figs. 71-74. The values in the Figs. were calculated using Eq. (9) where the density (ρ) was calculated by Eqs. (11)-(13). The interpolation/extrapolation scheme for the density was the same as that used for generation of the contours. The distribution of the vapor velocity (u) over the array area was formulated from the windspeed data of W11 and W12. The windspeed was assumed to vary linearly between W11 (+7.5 m) and W12 (-7.5 m) and to be constant at the W11 and W12 values outside of this region. The wind speed was assumed to vary logarithmically with height according to Eq. (2).

In the case of EAG3, where the vapor cloud was not completely contained by the 25 m array, the vapor density was set to zero at ± 20 m in order to account for some of the "lost" mass flux. This increased the total integrated mass by 13%. The total mass of each spill is also indicated on each plot.

6.0 THE VAPOR DISPERSION RESULTS

The dispersion array results not only include the NO_2 vapor concentrations measured in the 785 m stations but also the vapor cloud heat flux measured at 25 m and, for EAG1 and EAG3, the NO_2 concentration data obtained at 2800 m.

6.1 The Vapor Cloud Heat Flux Data @ 25 m

It is clear that the vapor cloud produced by the evaporating N_2O_4 will demonstrate some heavy gas dispersion characteristics due to its large molecular weight. However, as a result of the evaporative cooling of the liquid N_2O_4, the density of the vapor is further increased due to its lower-than-ambient temperature. This initially cold vapor cloud is eventually warmed to ambient temperature by mixing with the air, and by heating from the ground. In an effort to better understand the surface heating process, surface heat flux measurements were made at 25 m downwind, next to stations G04 and G06.

The G04 and G06 surface-to-cloud heat flux data for the EAG1-EAG3 and EAG6 tests are presented in Figs. 75-78. Surface heat flux measurements were also made at upwind station G01. These upwind data are included with the G04 and G06 data for reference purposes. The sign convention is such that a positive value indicates heat into the ground.

6.2 The NO_2 Concentration Data @ 785 m

The NO_2 concentration data obtained at the five stations (G20-G24) located 785 m downwind of the spill area (Fig. 5) are presented in two formats; superposition of time histories at the same height (row plots), and vertical cross-wind contours. At the observed NO_2 concentration values, essentially all of the N_2O_4 has completely dissociated.

NO_2 Time Histories

The NO_2 concentration time histories for EAG1-EAG3 and EAG6 are presented in Figs. 79-82. Each plot is a superposition of the data obtained by all the sensors in the 785 m row located at the same height (1 m, 3.5 m,

or 8.5 m). No time histories of EAG2, EAG4, or EAG5 are presented because the vapor cloud missed the array for EAG5, dispersed too rapidly during EAG2, and the maximum recorded concentration for EAG4 was only 16 ppm, with a duration of only 30 sec.

For all tests, the only NO_2 concentration data obtained at station G24 were at the 1 m height. For the EAG6 test, station G20 was not operational, but the vapor cloud was contained within the remaining array of sensors.

NO_2 Vertical Contours

The NO_2 vertical concentration contours at several different times for the EAG1-EAG3 and EAG6 tests are shown in Figs. 82-84. The contours were calculated assuming a linear variation of the NO_2 concentration data between sensors, and using the same extrapolation scheme for determining the surface concentration as described in section 5.2.

The contours are as they would appear to an observer viewing them from an upwind location.

6.3 NO_2 Concentrations @ 2800 m

As described in section 2.6, the two portable NO_2 sensors were deployed during the EAG1-EAG3 tests. These sensors were placed at various locations in a row located 2800 m downwind of the spill point. The data obtained by these two sensors are given in Figs. 85 and 86. These sensors recorded no NO_2 concentrations for the EAG2 spill, and were not deployed for the EAG6 spill.

As mentioned in section 2.6, the strip chart recorders for these two sensors were only accurate to about ± 10 min. with respect to the actual time of day. The two sensor traces have been coordinated in time according to our best estimates of their scan rates.

7.0 SUMMARY

A series of six N_2O_4 spills (Eagle series) was conducted at the Frenchman Flat area of the DOE Nevada Test Site in 1983. Four of the tests (EAG1-EAG3, EAG6) were for the purpose of studying the source strength characteristics and heavy gas dispersion aspects of N_2O_4 spills on the ground. Two of the tests (EAG4, EAG5) were for the purpose of evaluation of a portable foam vapor suppression system. The tests were performed between September 8, 1983 and October 30, 1983 and involved a total of 16 m^3 (4200 gal) of N_2O_4.

This data report describes the spill facility and its operation, and all of the diagnostic instrumentation used by LLNL during these tests. All of the meteorological data necessary to adequately describe the local atmospheric conditions during each test are presented. Data pertaining to the source strength and downwind dispersion of N_2O_4 vapor are also presented, with particular emphasis on the EAG1, EAG3, and EAG6 spills. The contents of this report document the experimental system and present essentially all of the data obtained so that it may be understood and used by others in the future. An analysis of these data is currently underway and should be available by October 1984.

REFERENCES

1. Giauque, W.F. and J.D. Kemp, J. Chem. Phys., Vol 6, p 40 (1938).

2. Nordstrom, R.J. and W.H. Shan, J. Phys. Chem., Vol 80, No 8, p 847 (1976).

3. Bingham, G.E., R.D. Kiefer, C.H. Gillespie, T.G. McRae, H.C. Goldwire, Jr, and R.P. Koopman, A Portable, Fast-Response Multiwavelength Infrared Sensor for Liquefied Natural Gas Vapors, UCRL-84850, Rev. 1 (1982). Rev. Sci. Instrum., Vol 54, No 10, p 135b, (1983).

4. Baker, J., The LGF Data Acquisition System, Lawrence Livermore National Laboratory, Livermore, Calif., UCID-19431 (1982).

5. Dyer, A.J., "A Review of Flux-Profile Relationships," Boundary-Layer Meteorology, 7, 363-372 (1974).

6. Businger, J.A., Turbulent Transfer in the Atmospheric Surface Layer, Chapter 2 in Workshop on Micrometeorology, ed. Duane A. Haugen, American Meteorological Society (1973).

7. Lettau, H.H., "Wind and Temperature Profile Prediction for Diabatic Surface Layers Including Strong Inversion Cases," Boundary-Layer Meteorology, 17, 443-464 (1979).

8. Goyer, G.G., "The Formation of Nitric Acid mists," J. Colloid Sci., Vol 18, p 616-624 (1963).

9. England, C., and W.H. Corcoran, "Kinetics and Mechanisms of the Gas-Phase Reaction of Water Vapor and Nitrogen Dioxide," Ind. & Eng. Chem. Fundamentals, Vol 13, p 173 (1974).

10. Peters, M.S., and J.L. Holman, "Vapor- and Liquid-Phase Reactions Between Nitrogen Dioxide and Water," Ind. & Eng Chem., Vol 47, p 2536 (1955).

11. Chambers, F.S., Jr., and T.K. Sherwood, "Absorption of Nitrogen Dioxide by Aqueous Solutions," Ind. & Eng. Chem., Vol 29, p 1415 (1937).

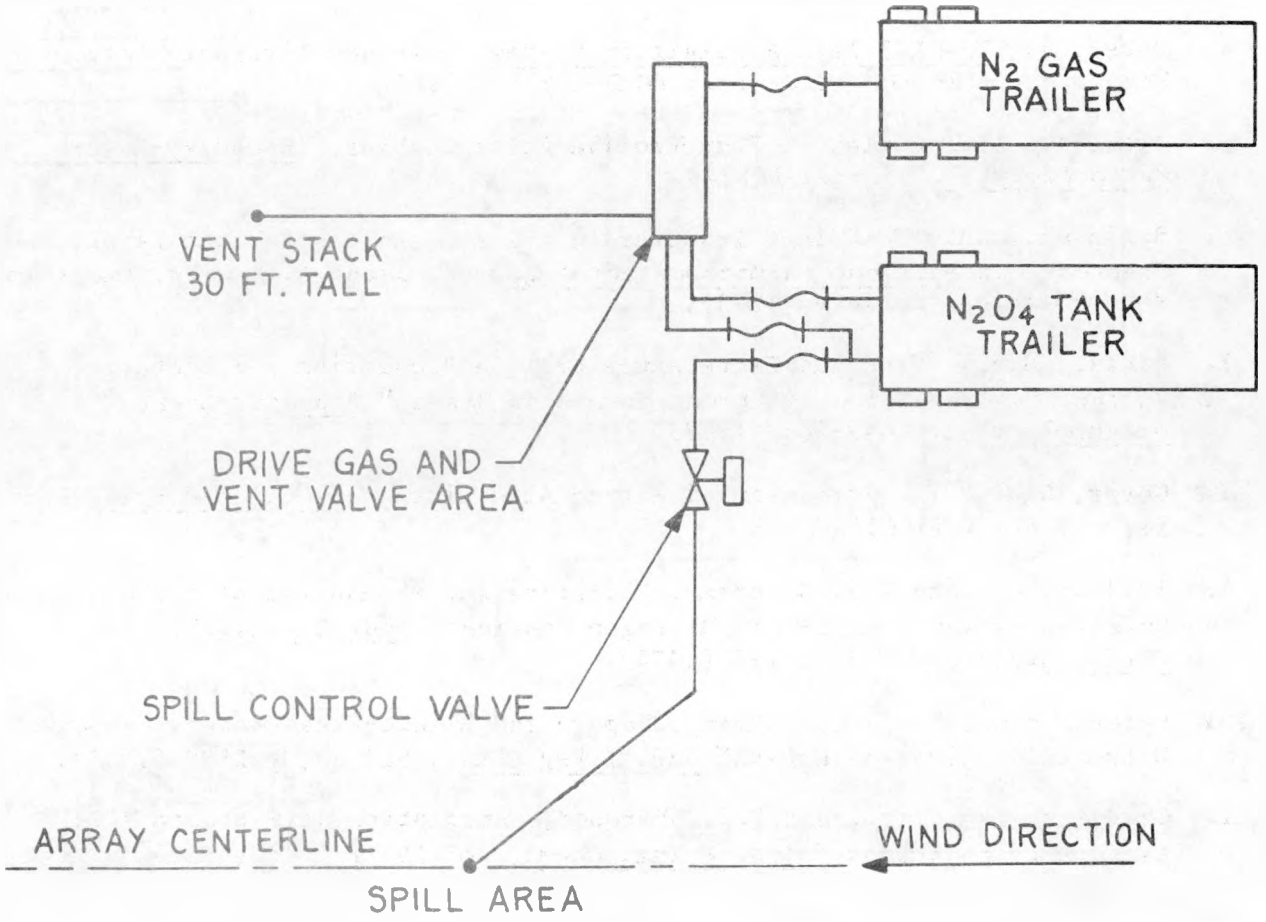

FIG. 1. SPILL FACILITY SITE LAYOUT.

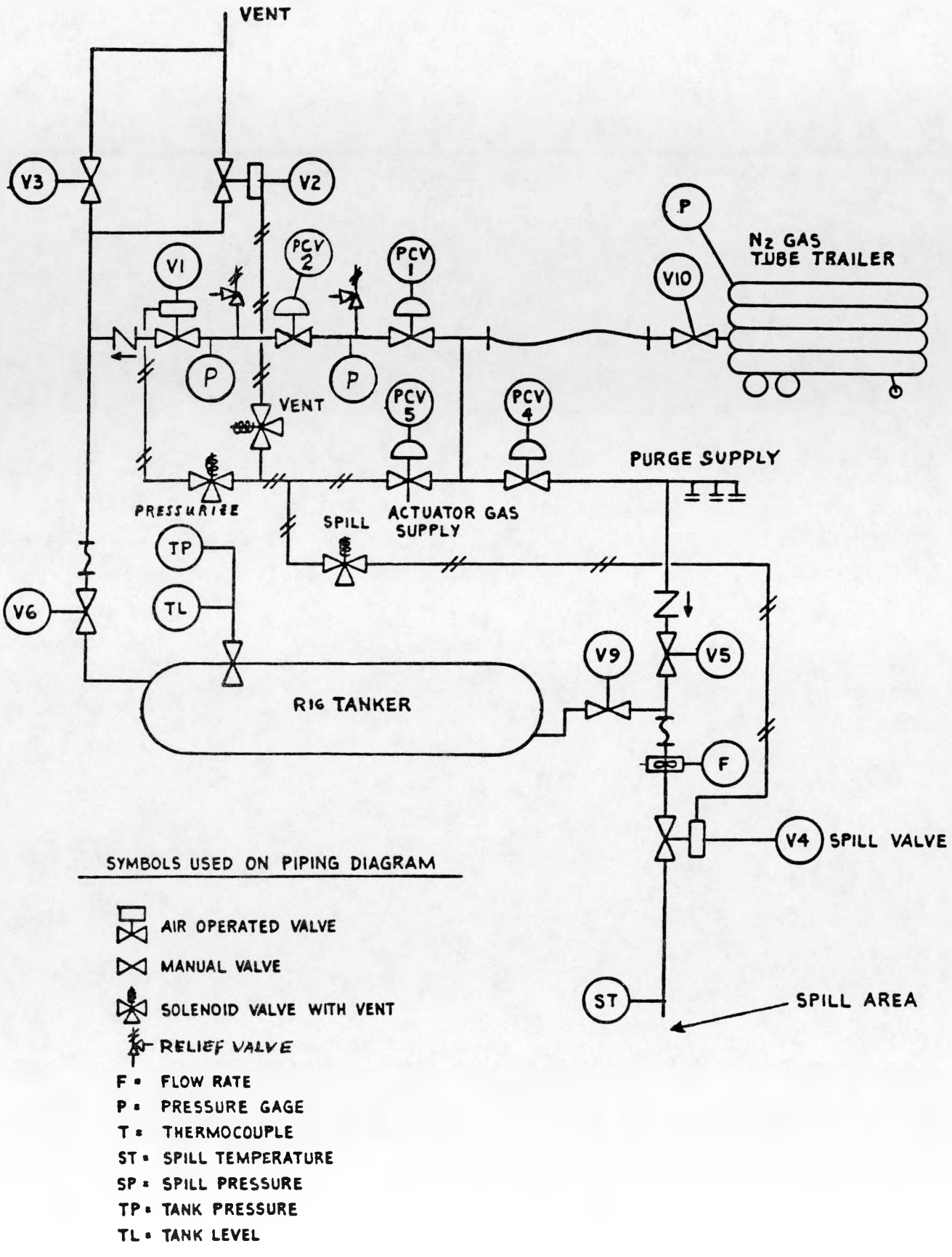

FIG. 2. SPILL FACILITY PIPING DIAGRAM.

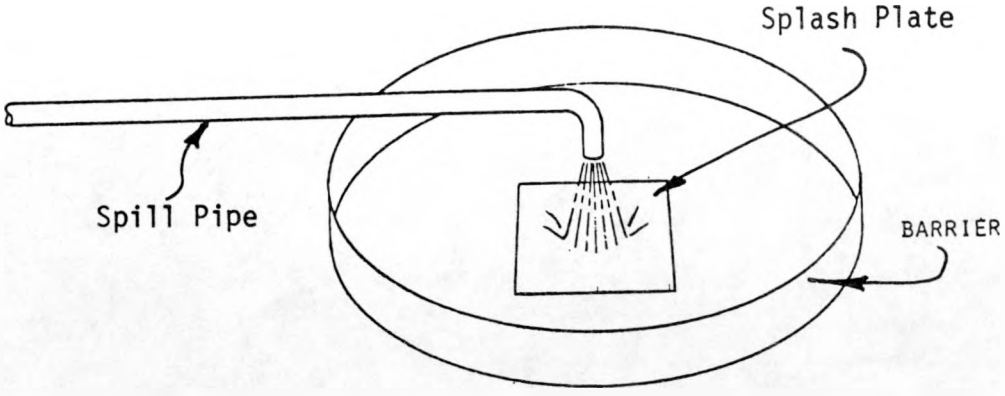

a) Single-exit confined

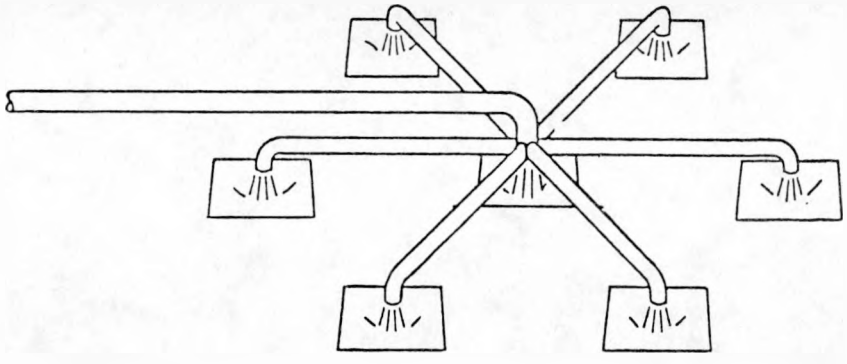

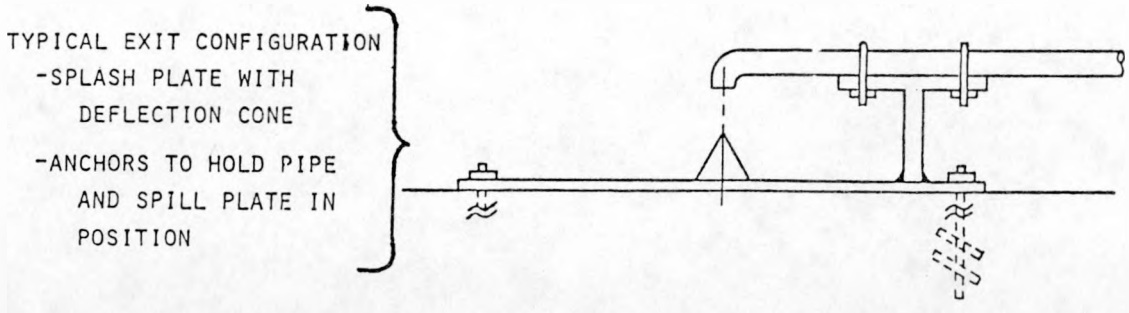

b) Multi-exit unconfined

FIG. 3. EAGLE SERIES SPILL CONFIGURATIONS.

FIG. 4. The N_2O_4 Spill Facility with the Multi-exit Spill Configuration.

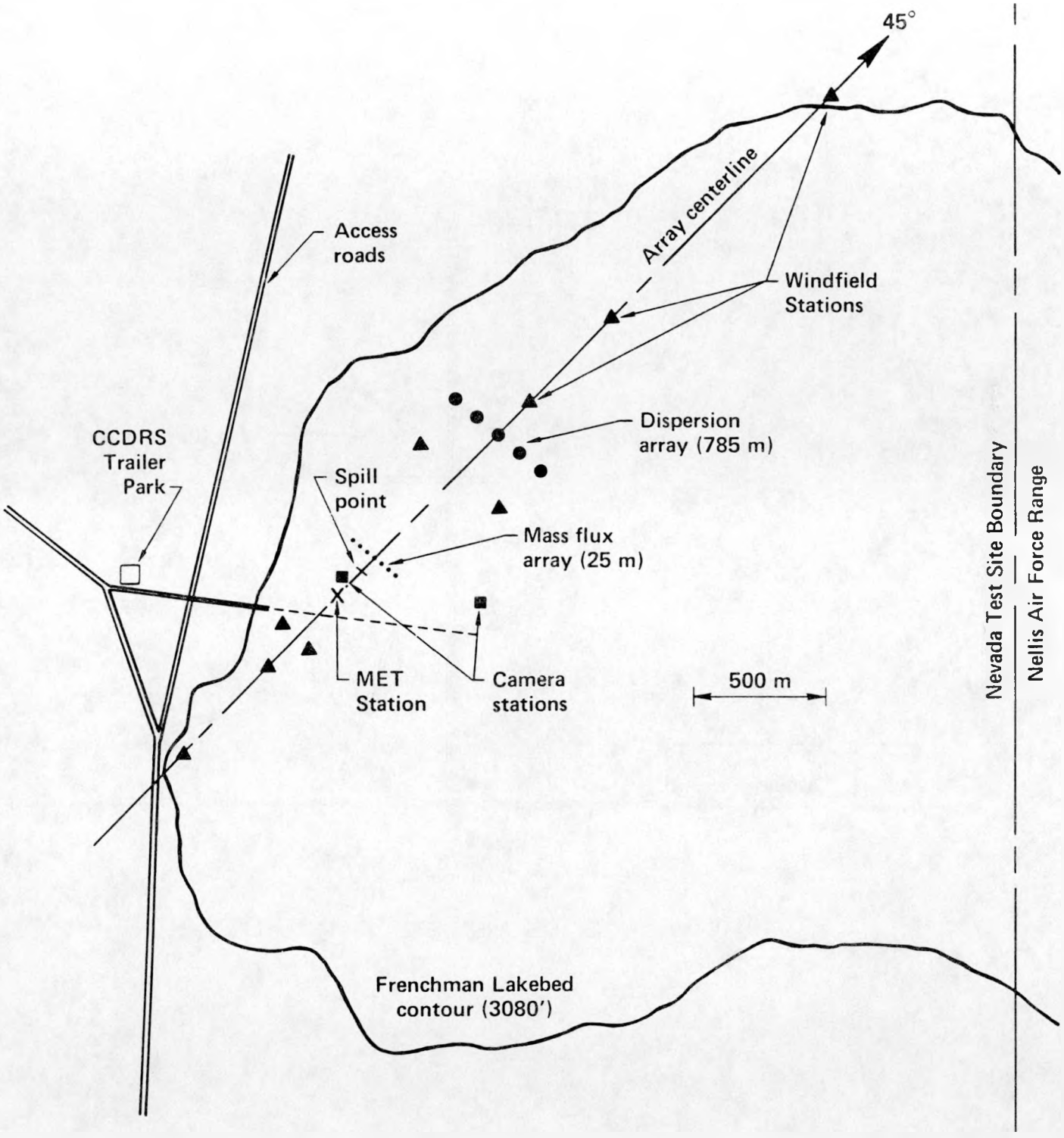

FIG. 5. Eagle Series Diagnostic System.

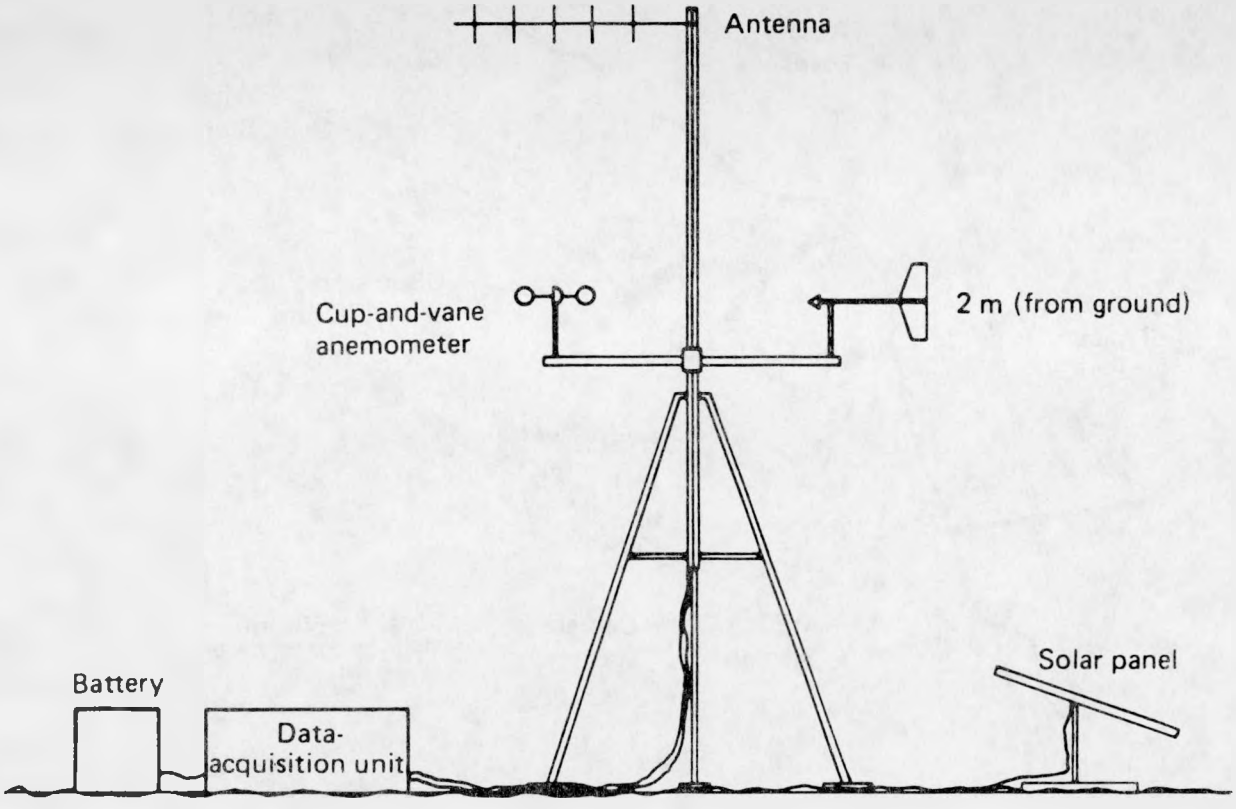

FIG. 6. WINDFIELD ANEMOMETER STATION.

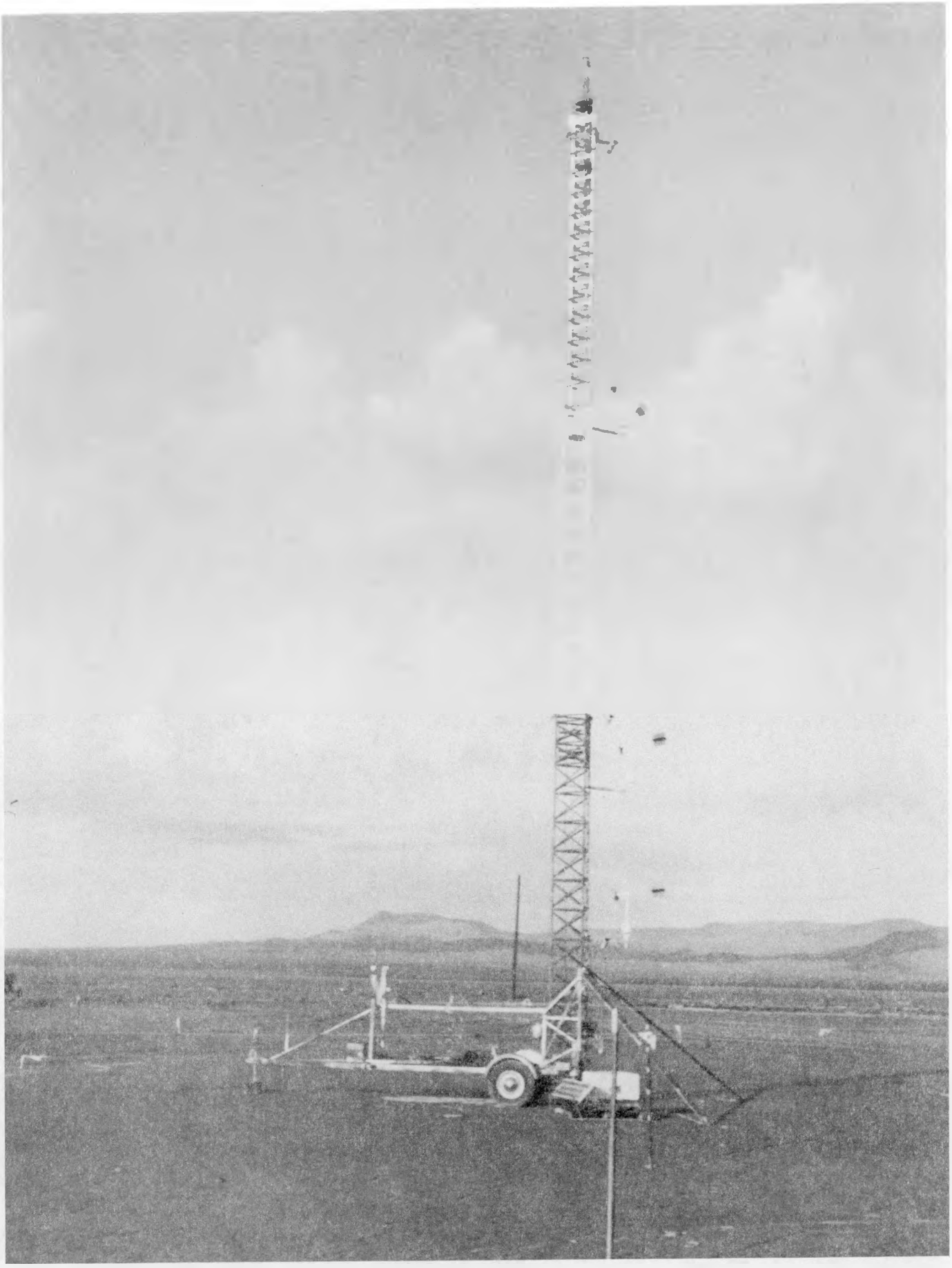

FIG. 7. The Meteorological Boundary Layer Station.

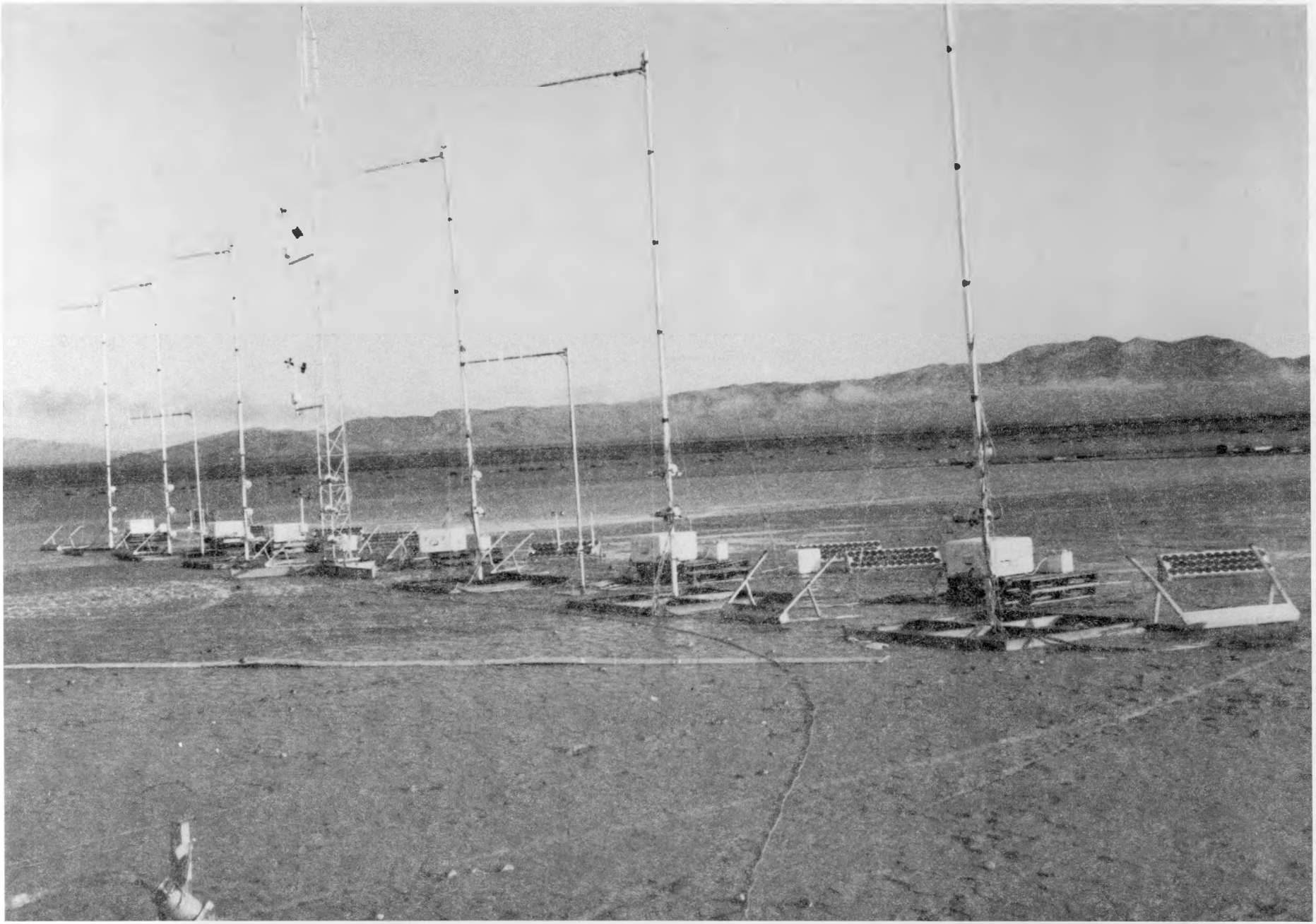

FIG. 8. The Mass Flux Array (25m)

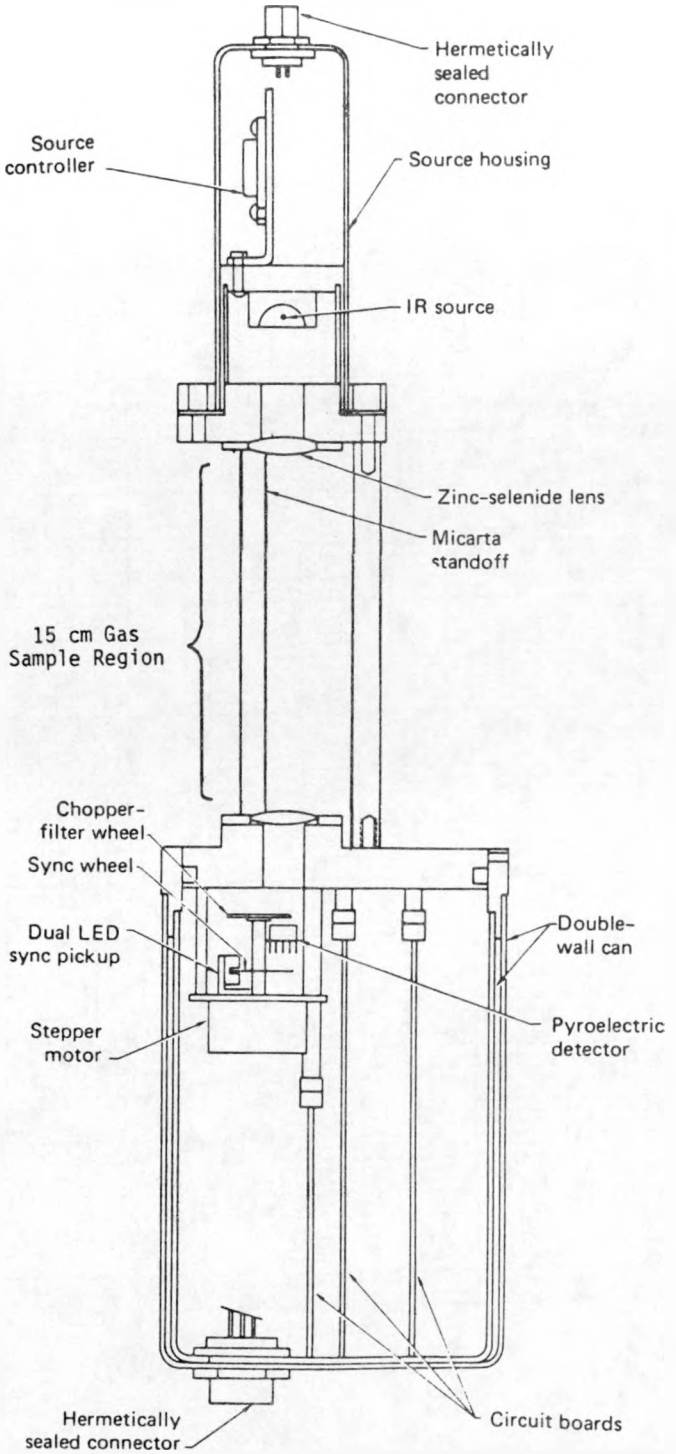

FIG. 9. CROSS SECTION OF THE LLNL IR GAS SENSOR.

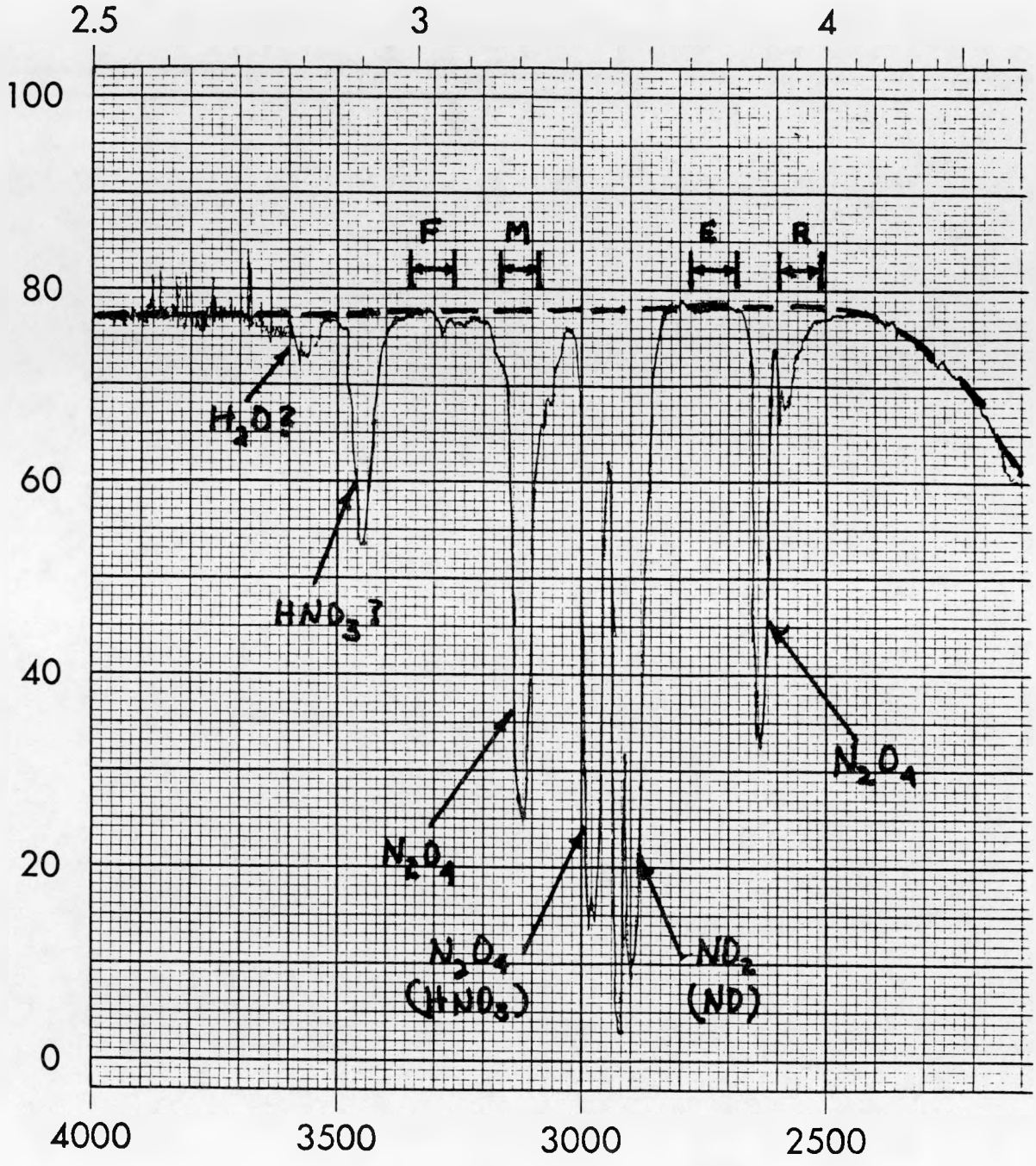

FIG. 10. N_2O_4 ABSORPTION SPECTRUM WITH LLNL IR SENSOR FILTER BANDPASSES.

FIG. 11. The Dispersion Array (785m)

FIG. 12. The CCDRS Trailer Park.

FIG. 13. Single Exit Confined Spill (EAG1)

FIG. 14. Multi-exit Unconfined Spill (EAG3)

FIG. 15. PFVSS Spill Configuration.

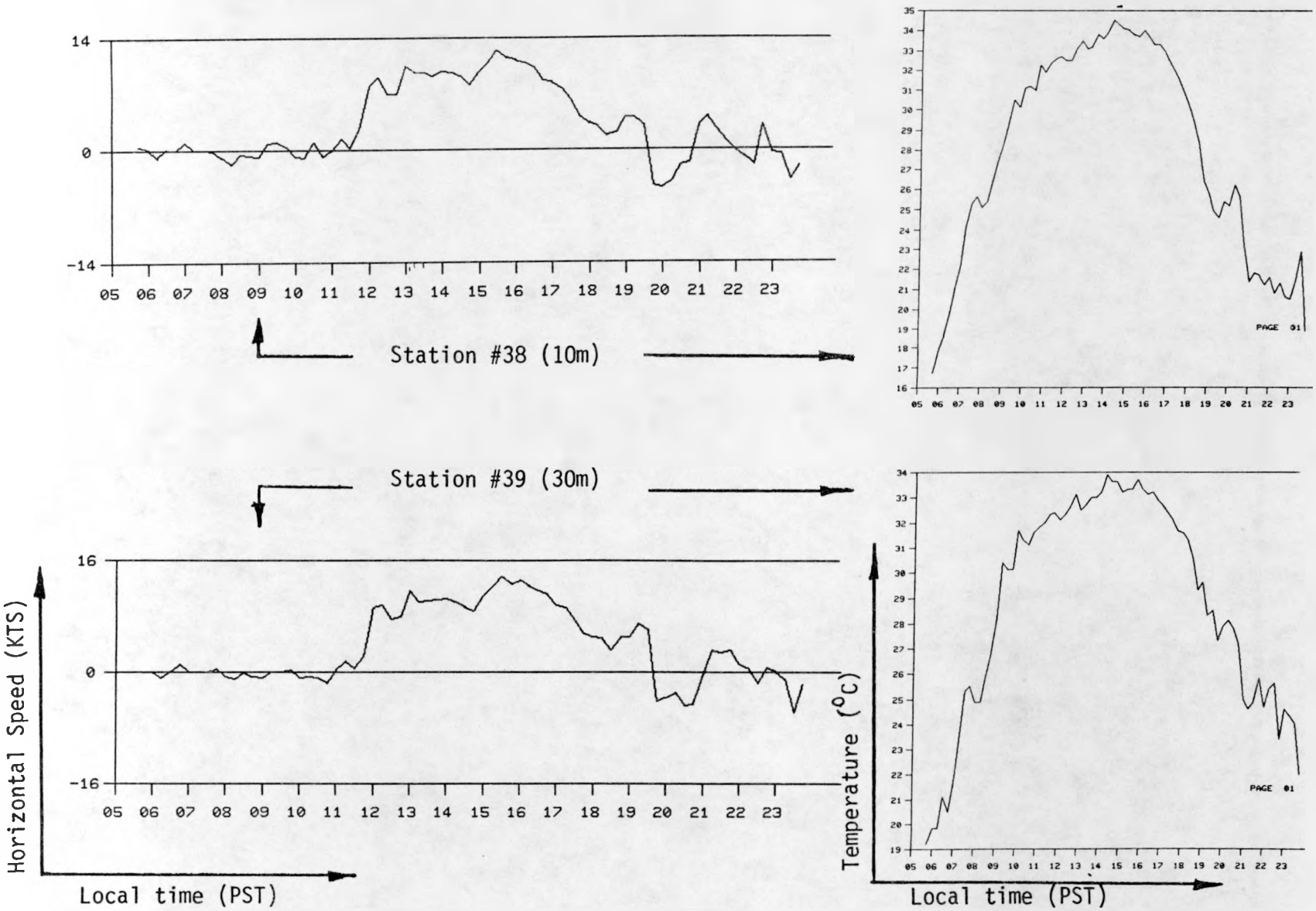

FIG. 16. EAG1 WSNSO Boundary Layer Data.

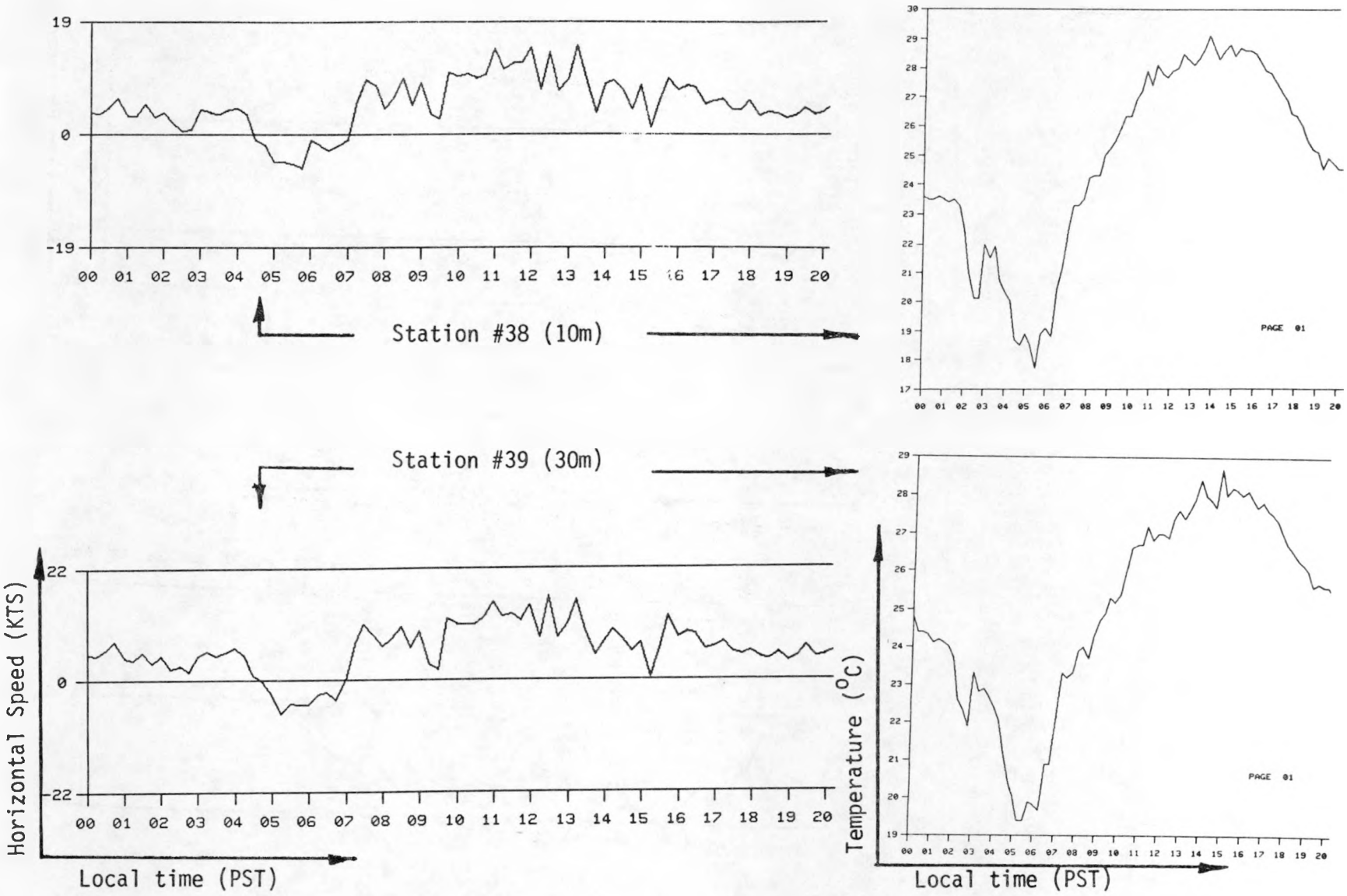

FIG. 17. EAG2 WSNSO Boundary Layer Data.

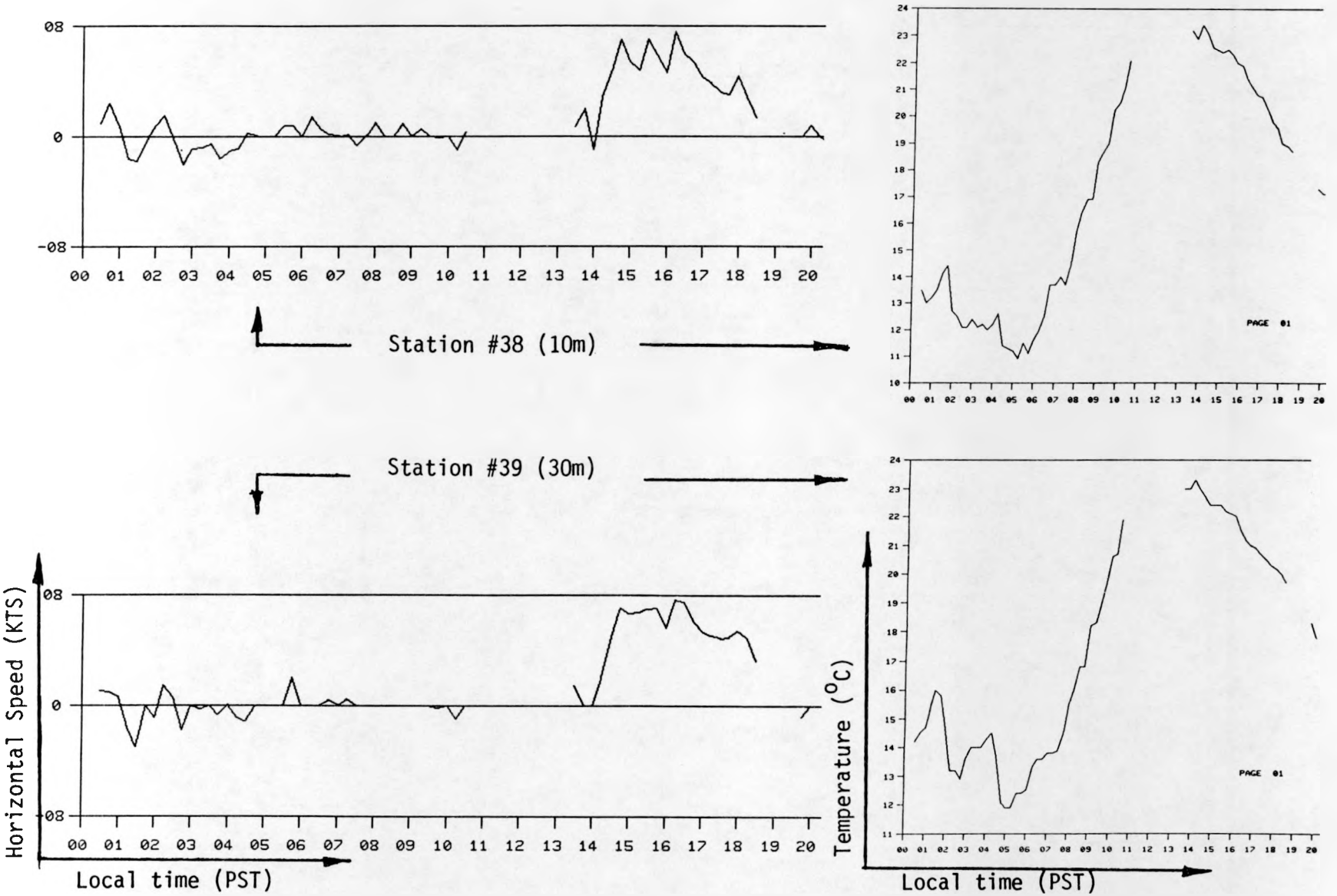

FIG. 18. EAG3 WSNSO Boundary Layer Data.

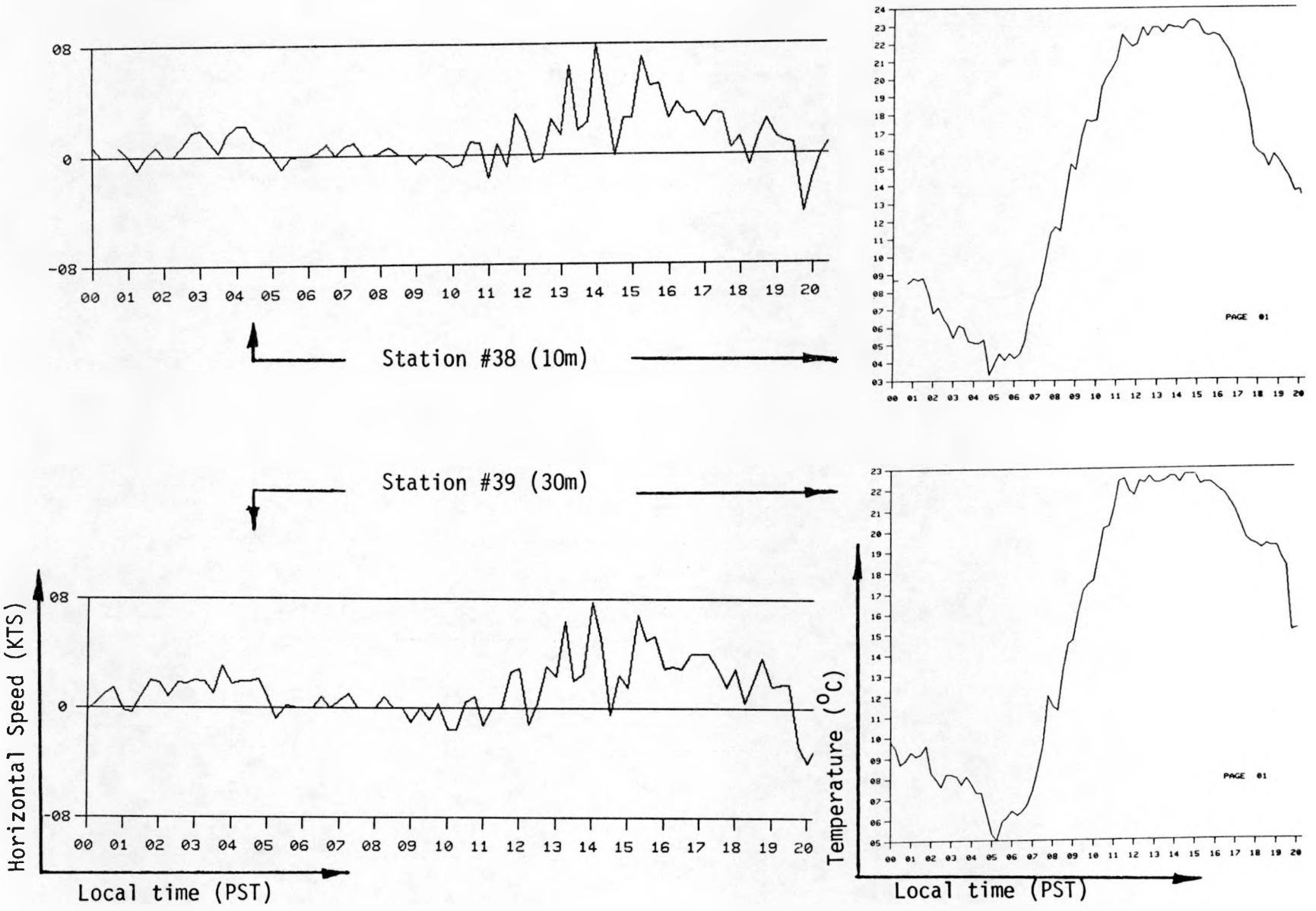

FIG. 19. EAG4 WSNSO Boundary Layer Data.

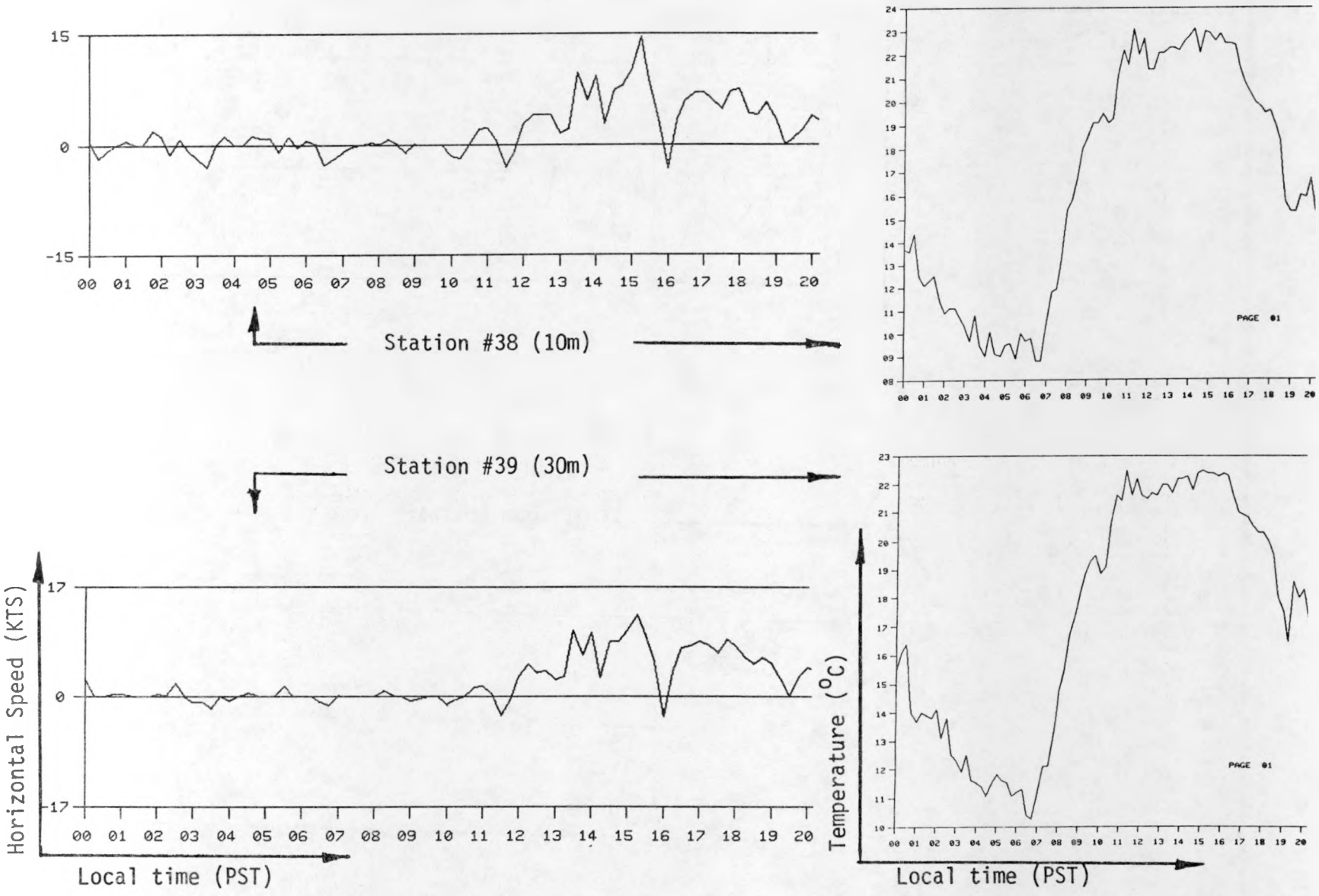

FIG. 20. EAG6 WSNSO Boundary Layer Data.

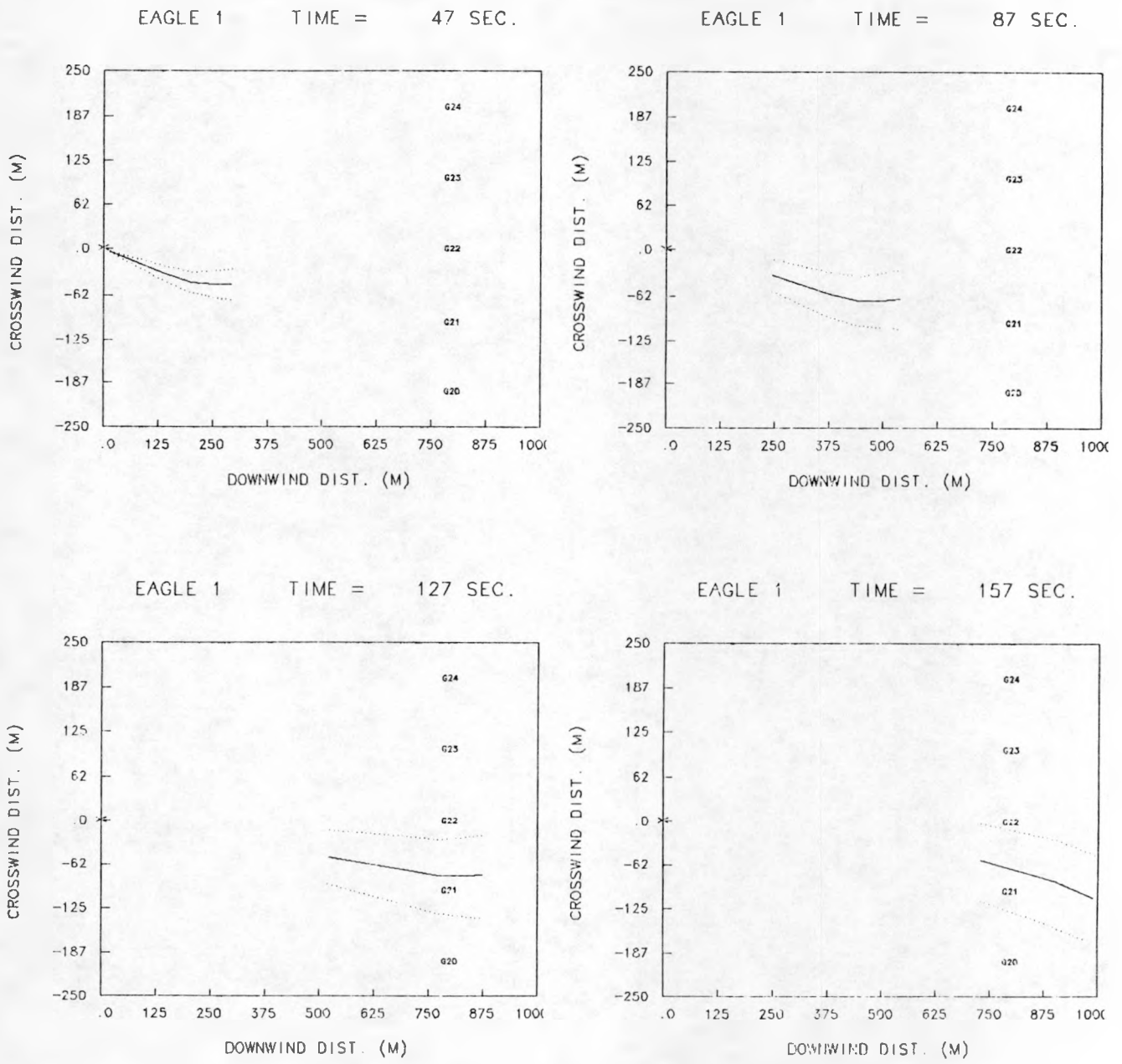

FIG. 21. EAG1 WINDFIELD CENTERLINE TRAJECTORY.

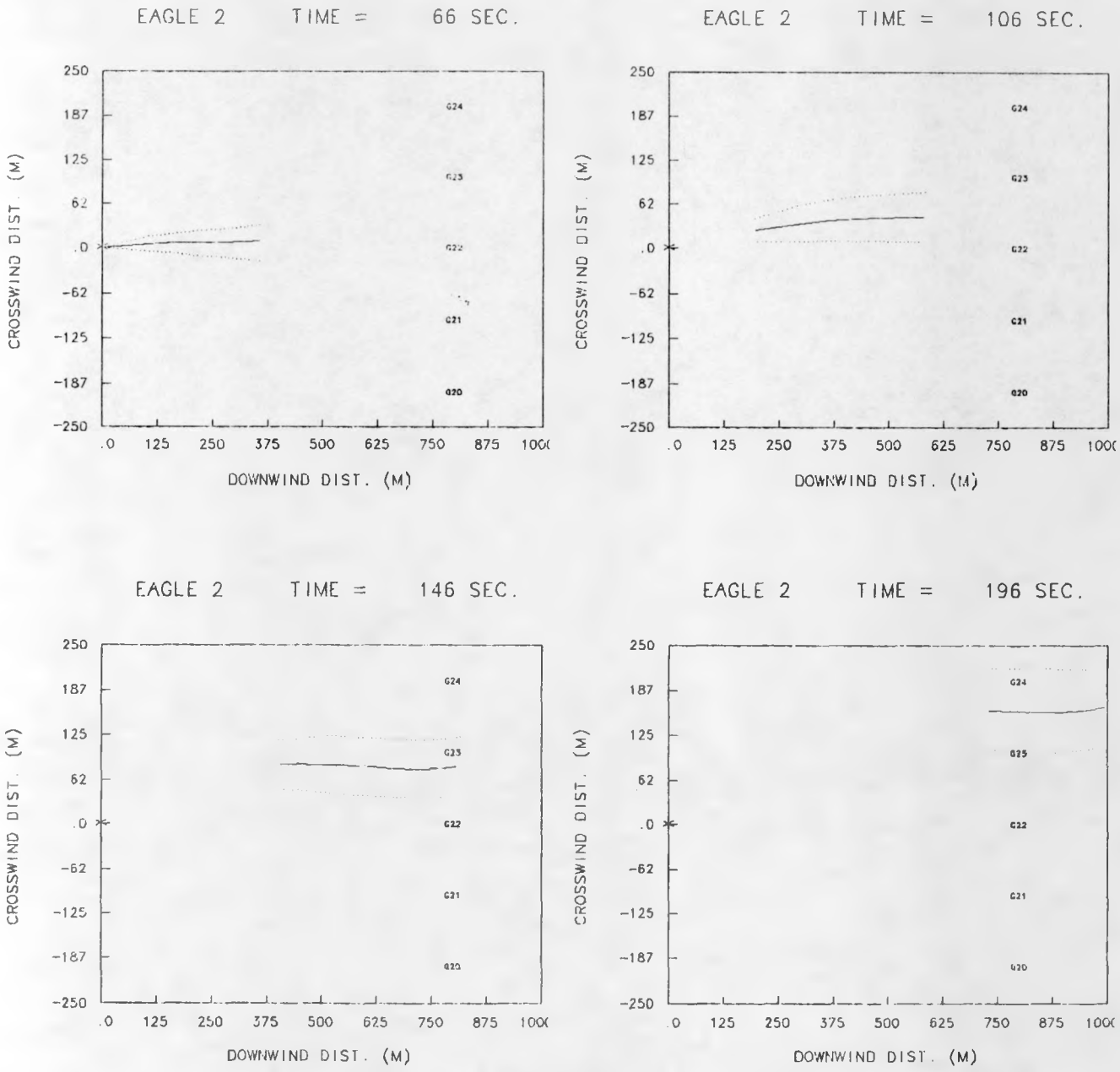

FIG. 22. EAG2 WINDFIELD CENTERLINE TRAJECTORY.

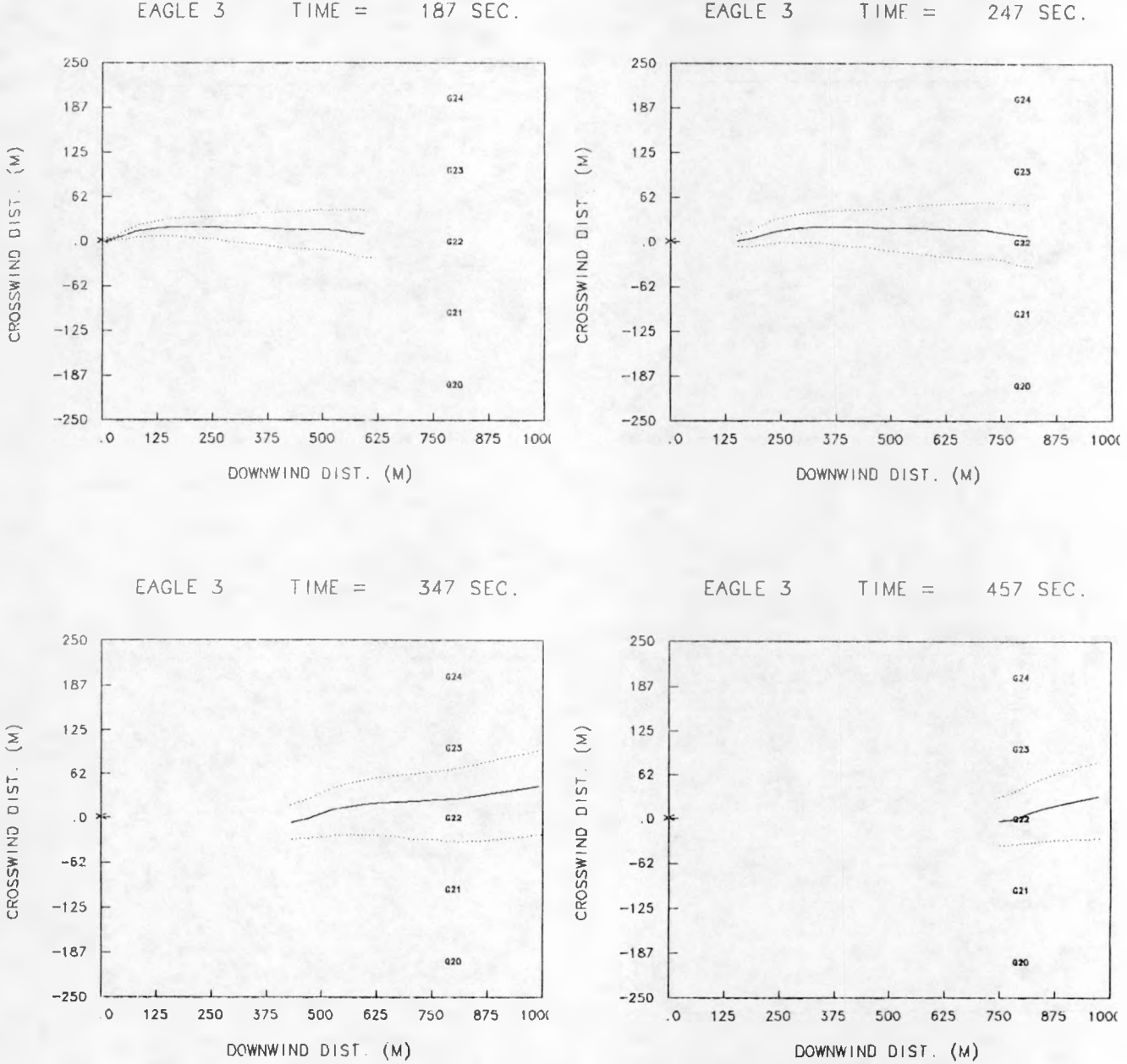

FIG. 23. EAG3 WINDFIELD CENTERLINE TRAJECTORY.

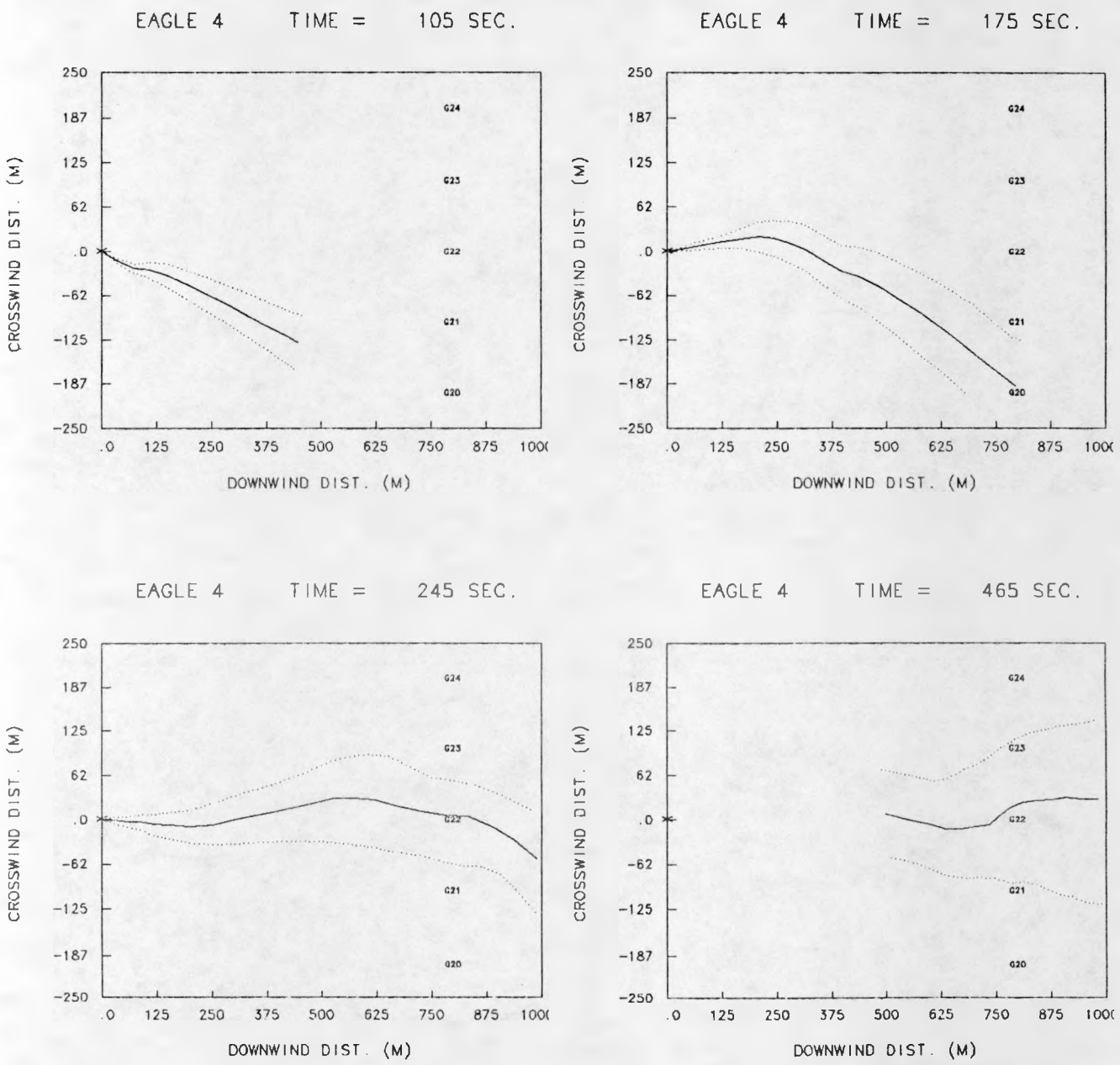

FIG. 24. EAG4 WINDFIELD CENTERLINE TRAJECTORY.

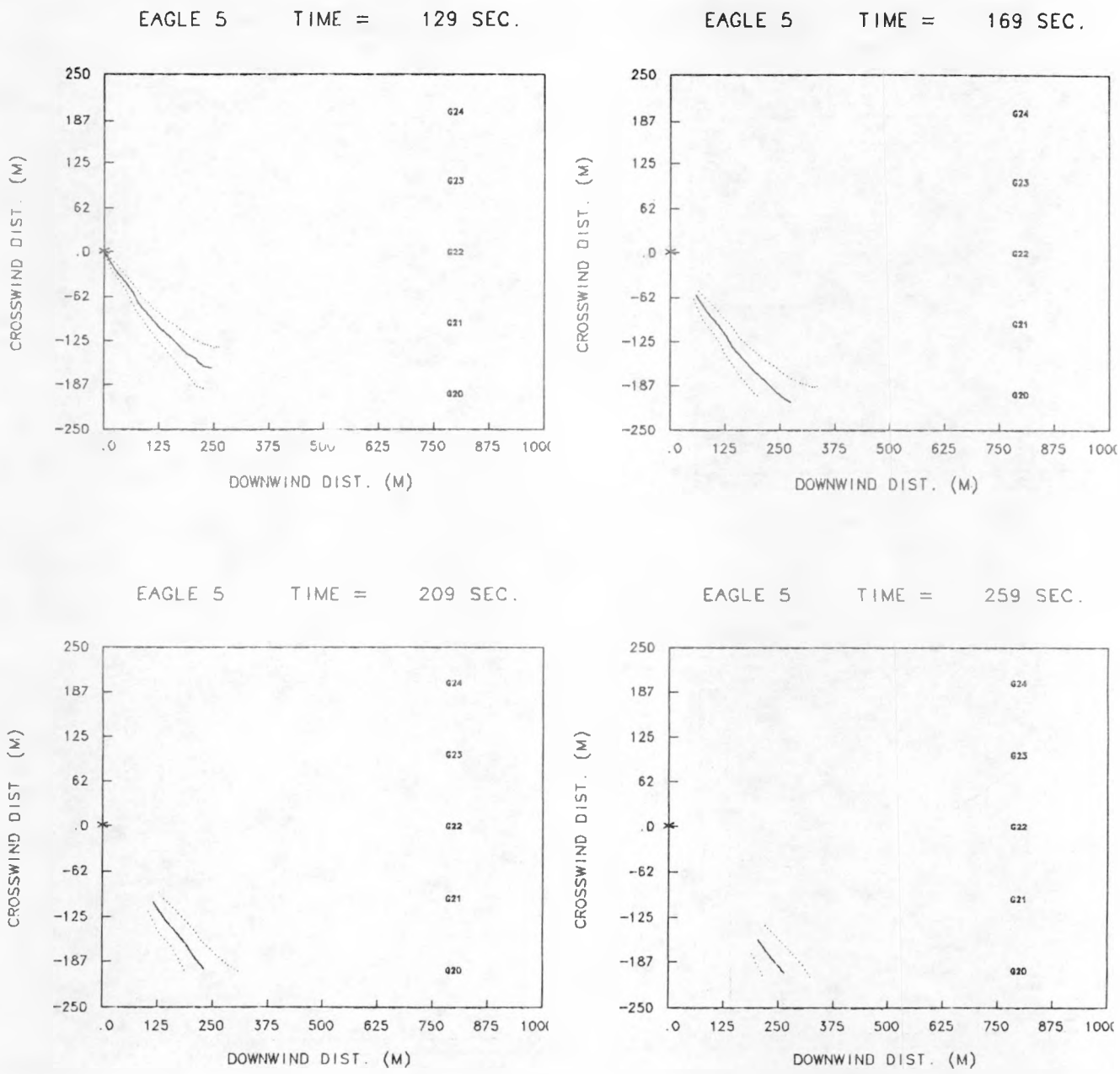

FIG. 25. EAG5 WINDFIELD CENTERLINE TRAJECTORY.

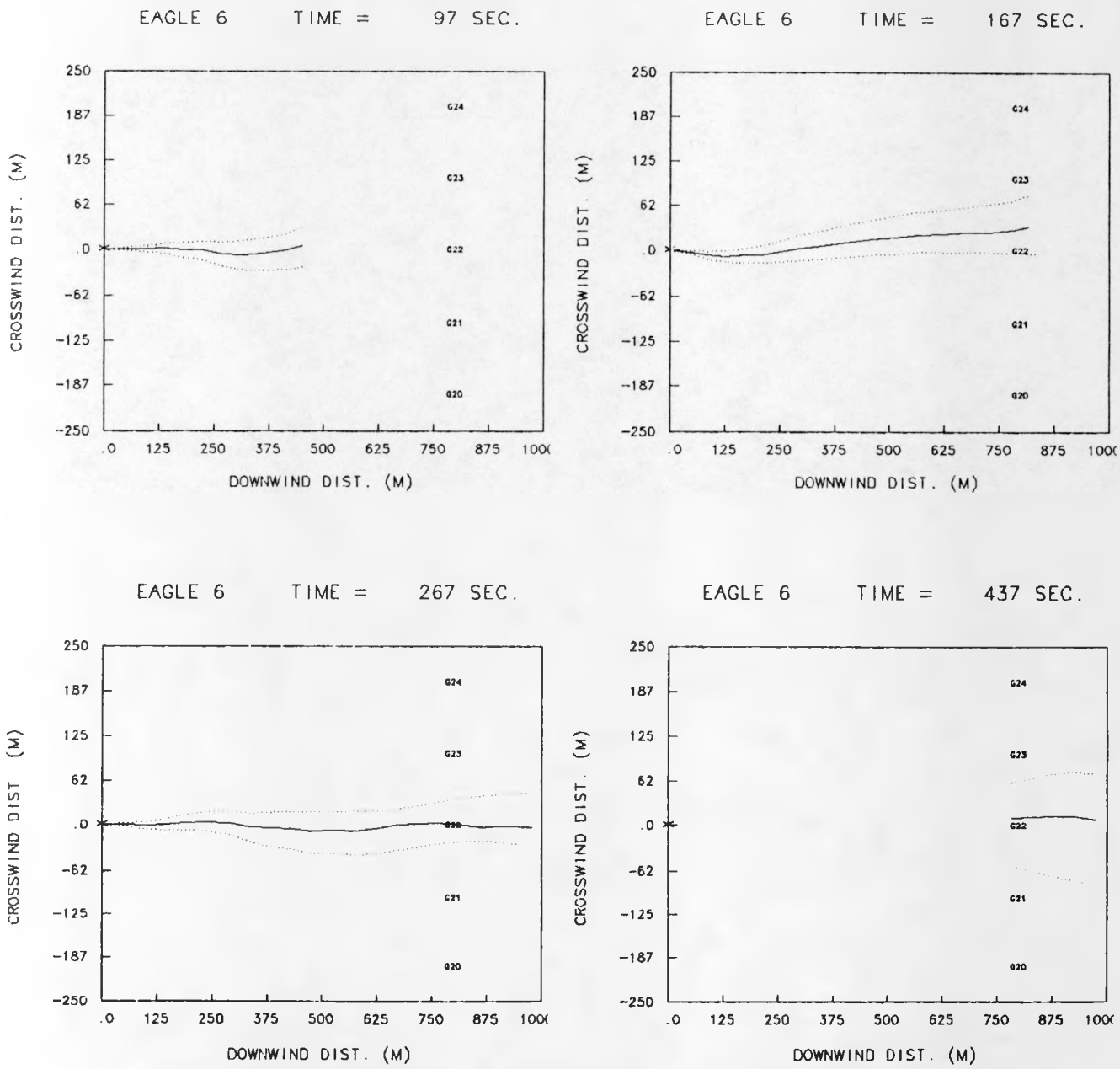

FIG. 26. EAG6 WINDFIELD CENTERLINE TRAJECTORY.

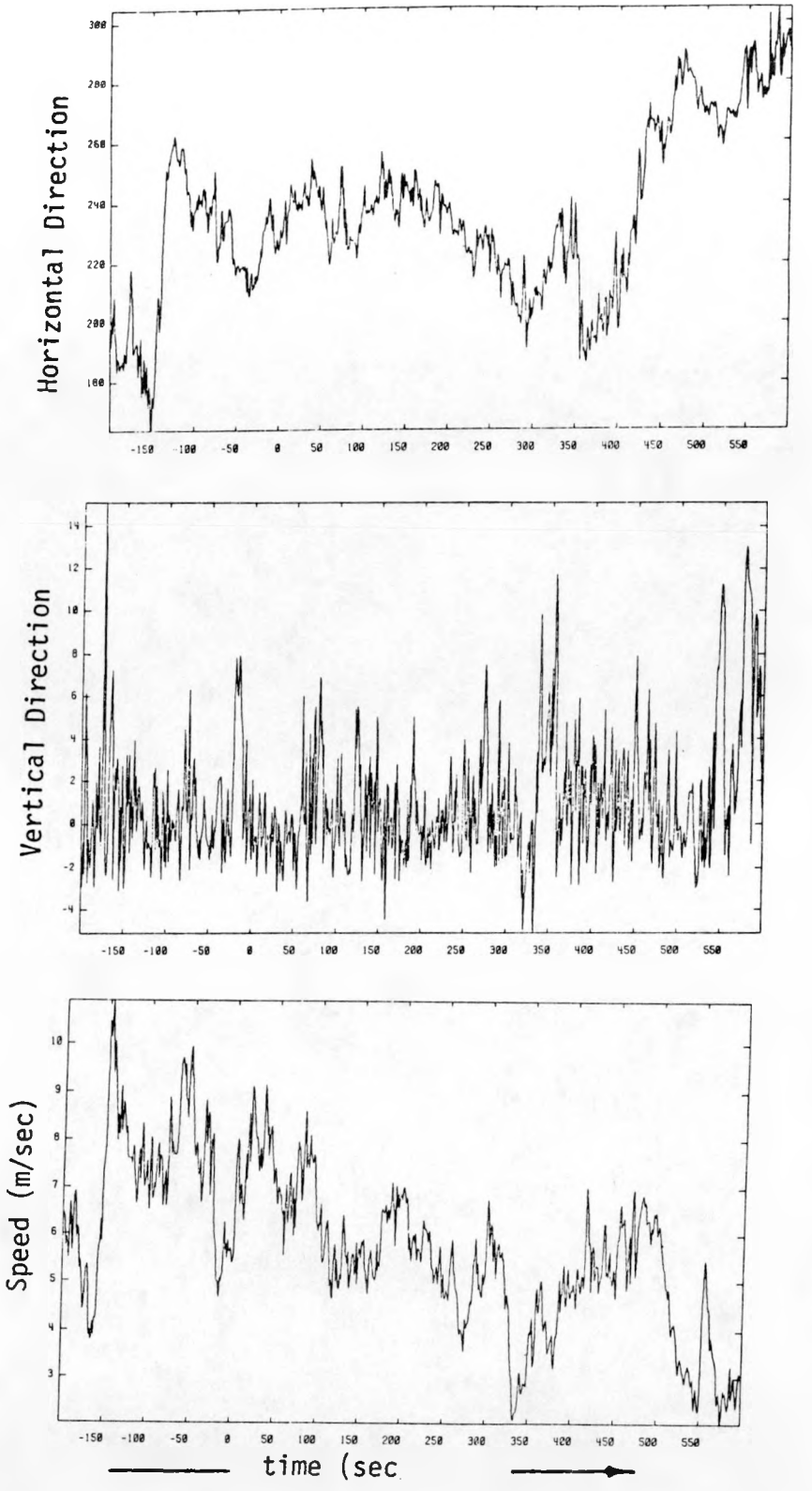

FIG. 27. EAG1 Turbulence Data (G01 @ 2.46m)

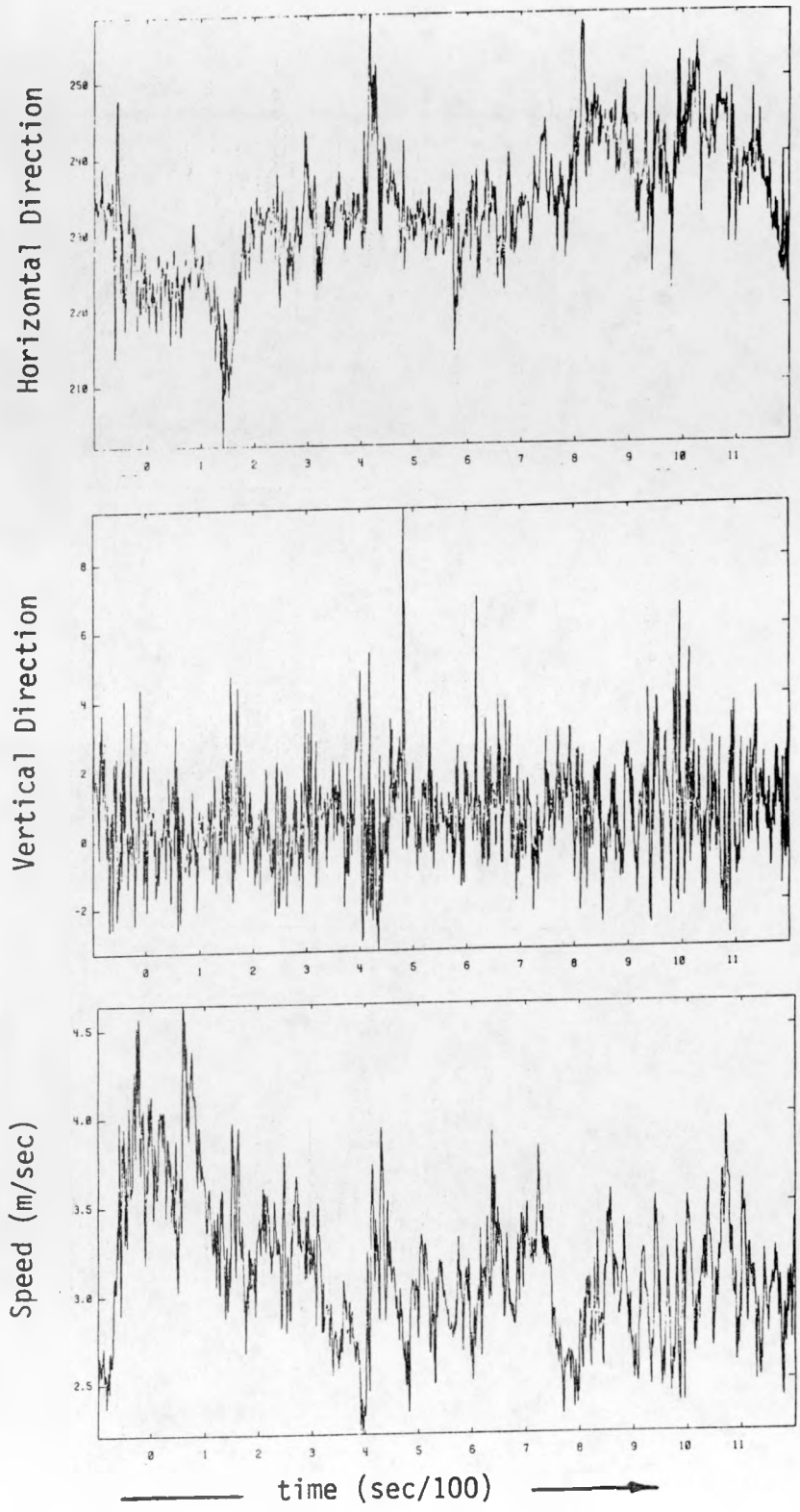

FIG. 29. EAG3 Turbulence Data (G01 @ 2.46m)

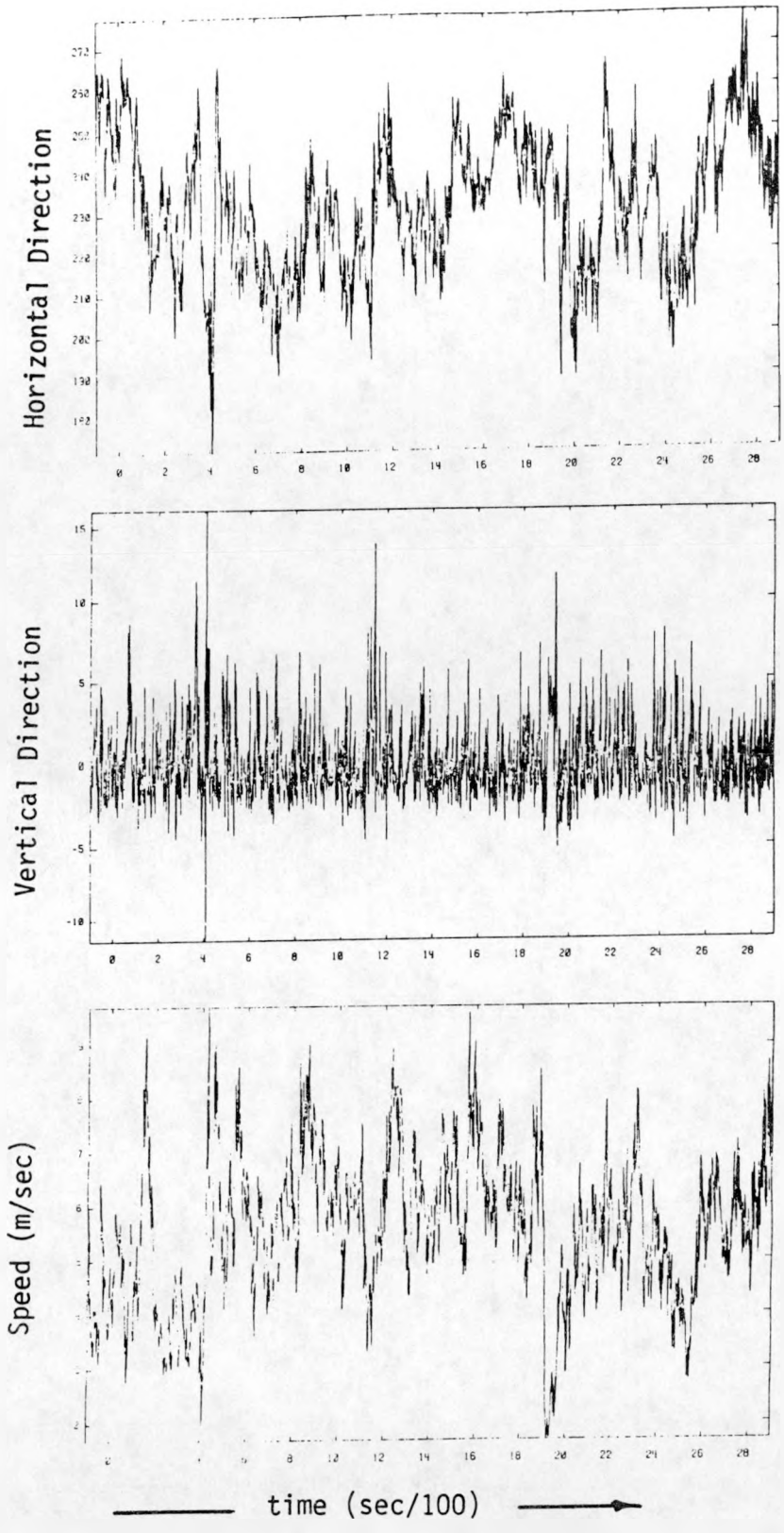

FIG. 30. EAG4 Turbulence Data (G01 @ 2.46m)

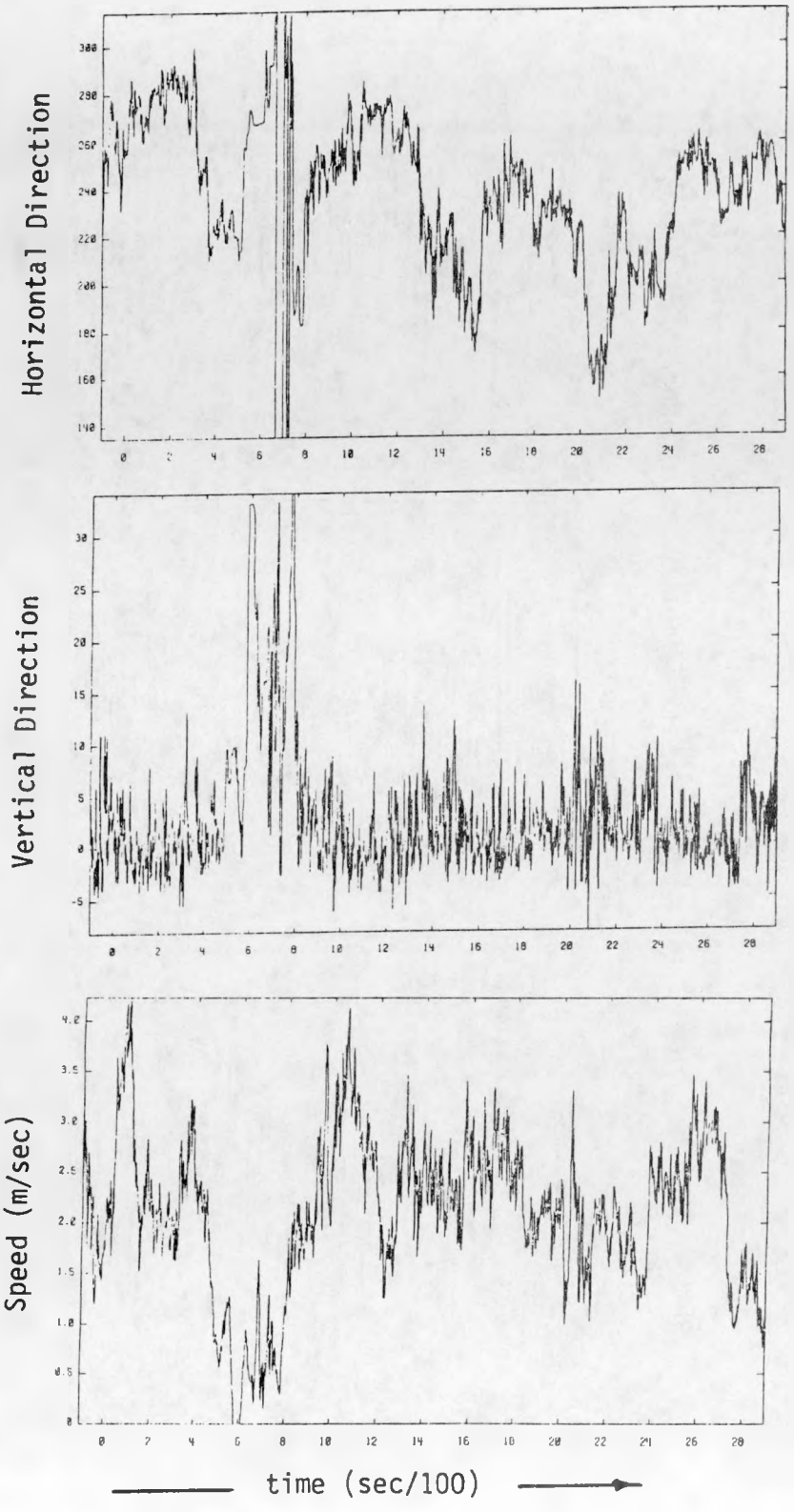

FIG. 31. EAG5 Turbulence Data (G01 @ 2.46m)

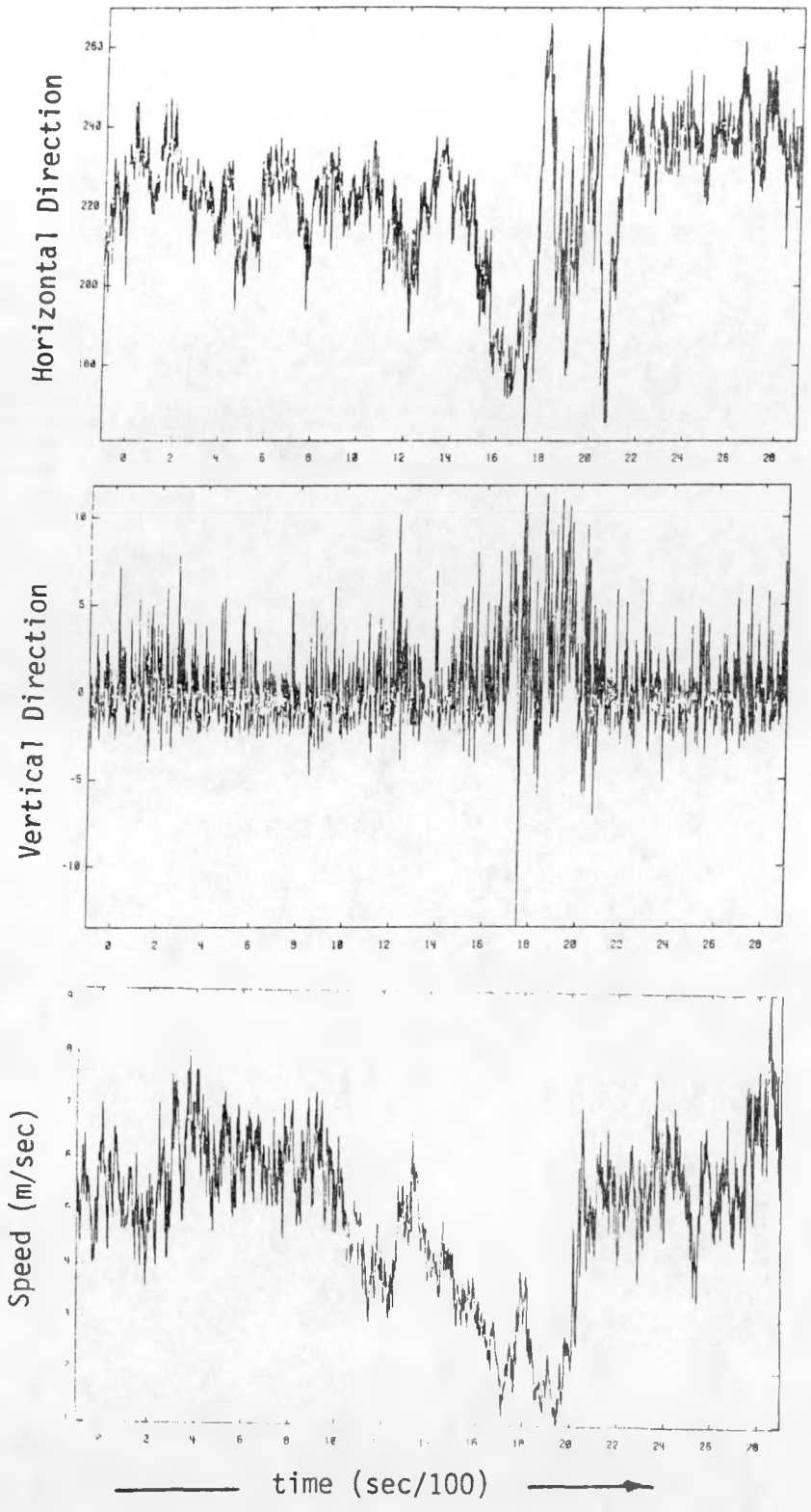

FIG. 32. EAG6 Turbulence Data (G01 @ 2.46m)

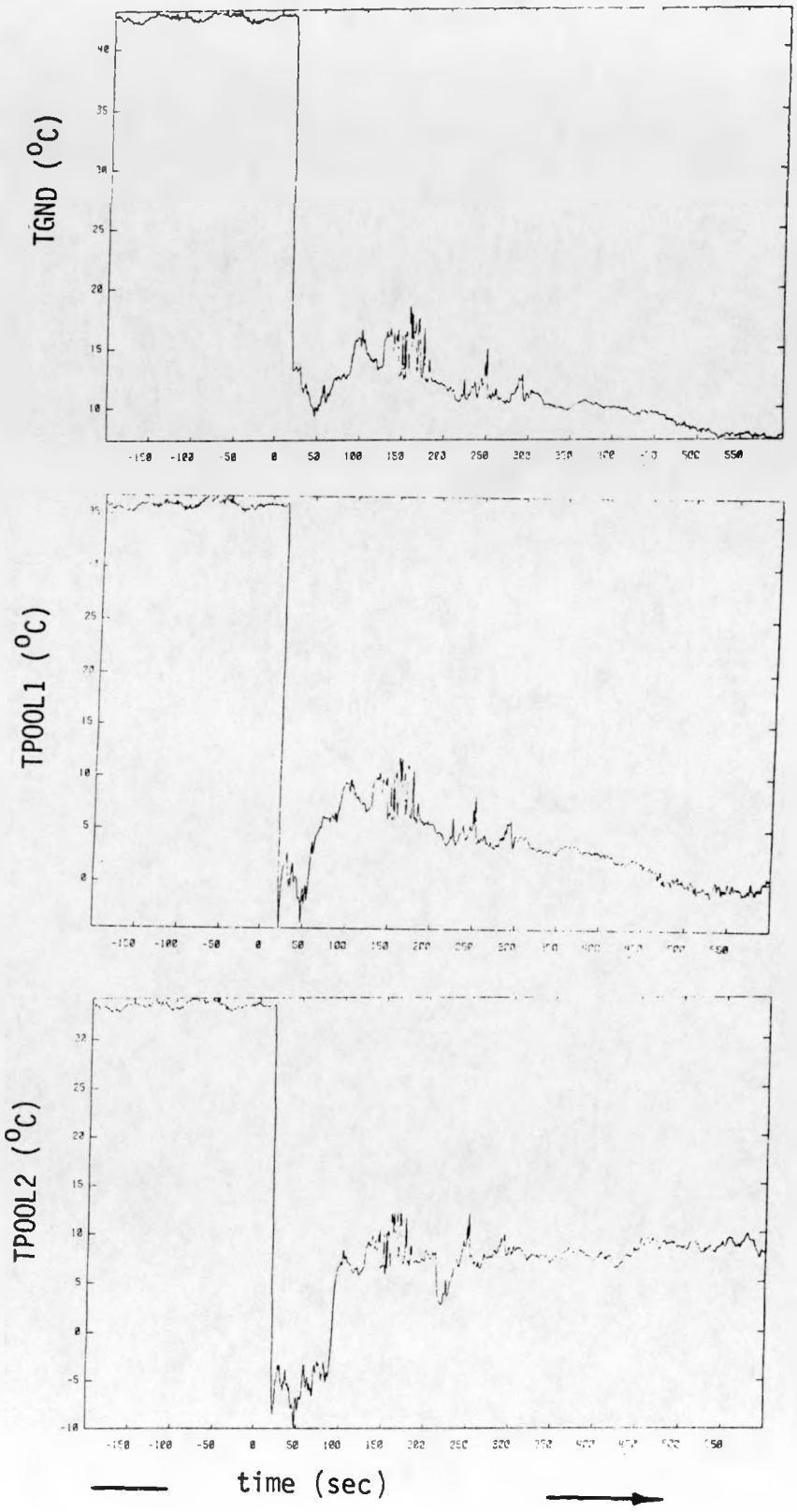

FIG. 33. EAG1 Temperature Profile Data

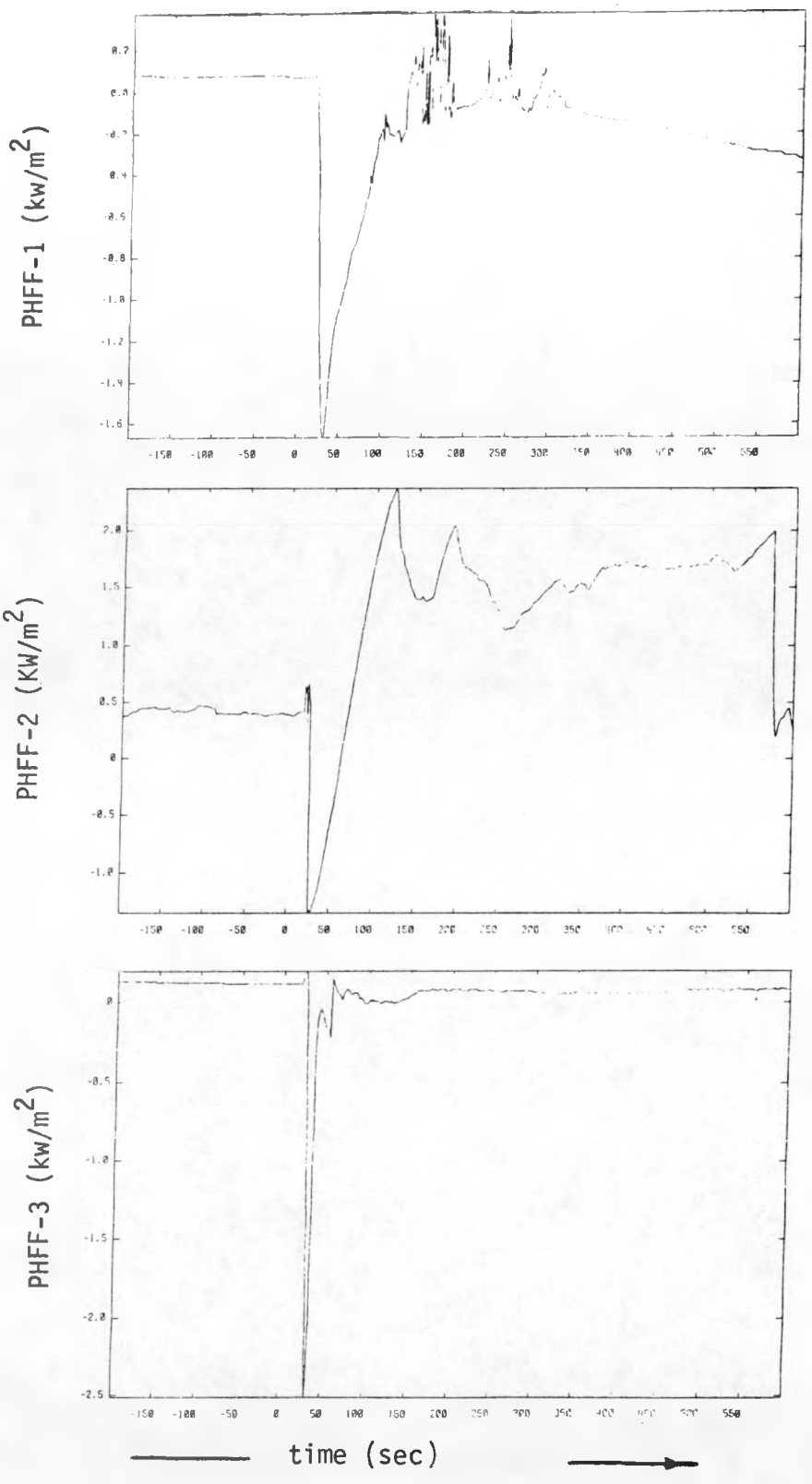

FIG. 34. EAG1 Spill Area Heat Flow Data

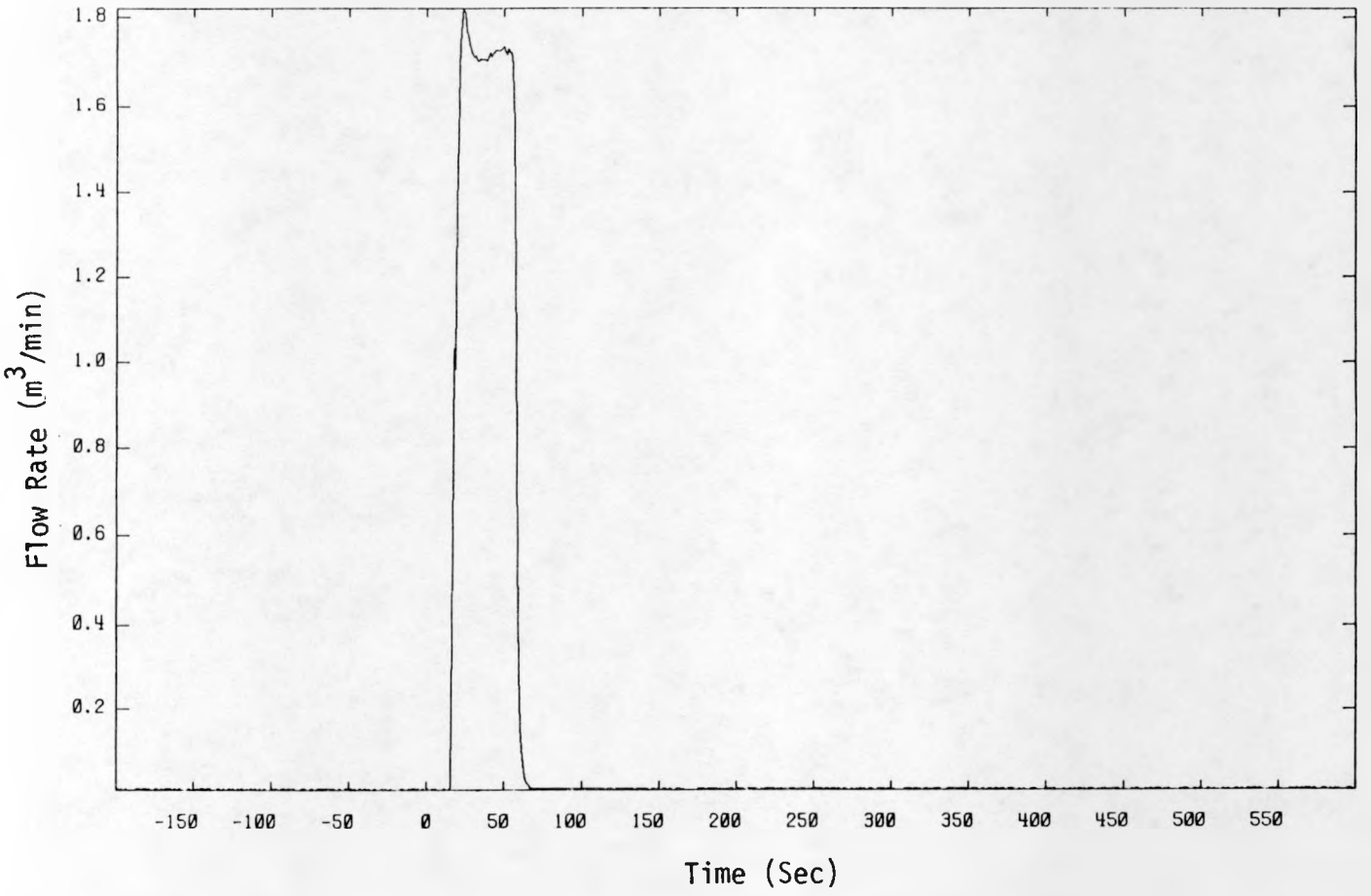

FIG. 35. EAG1 FLOWMETER DATA.

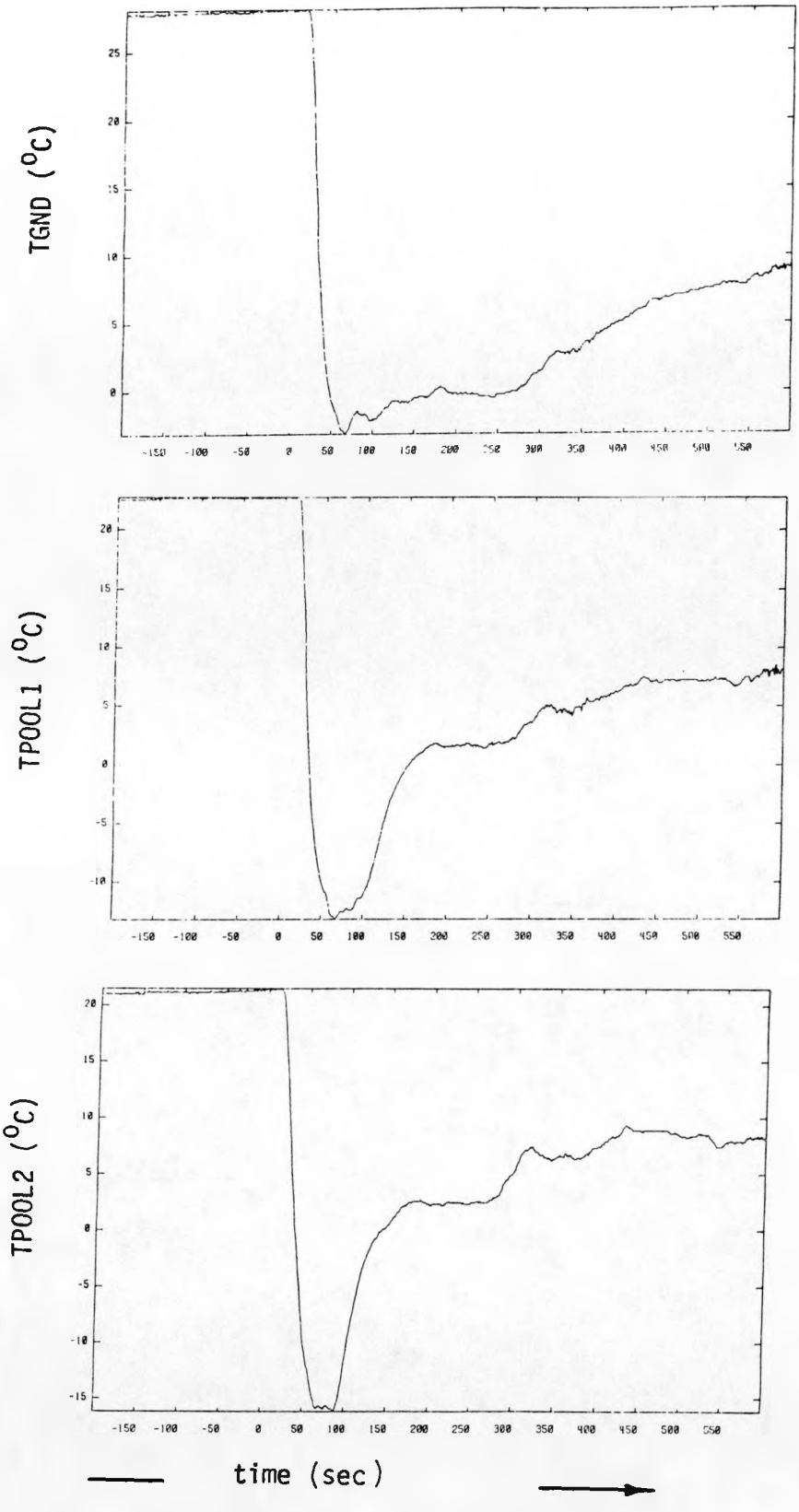

FIG. 36. EAG2 Temperature Profile Data

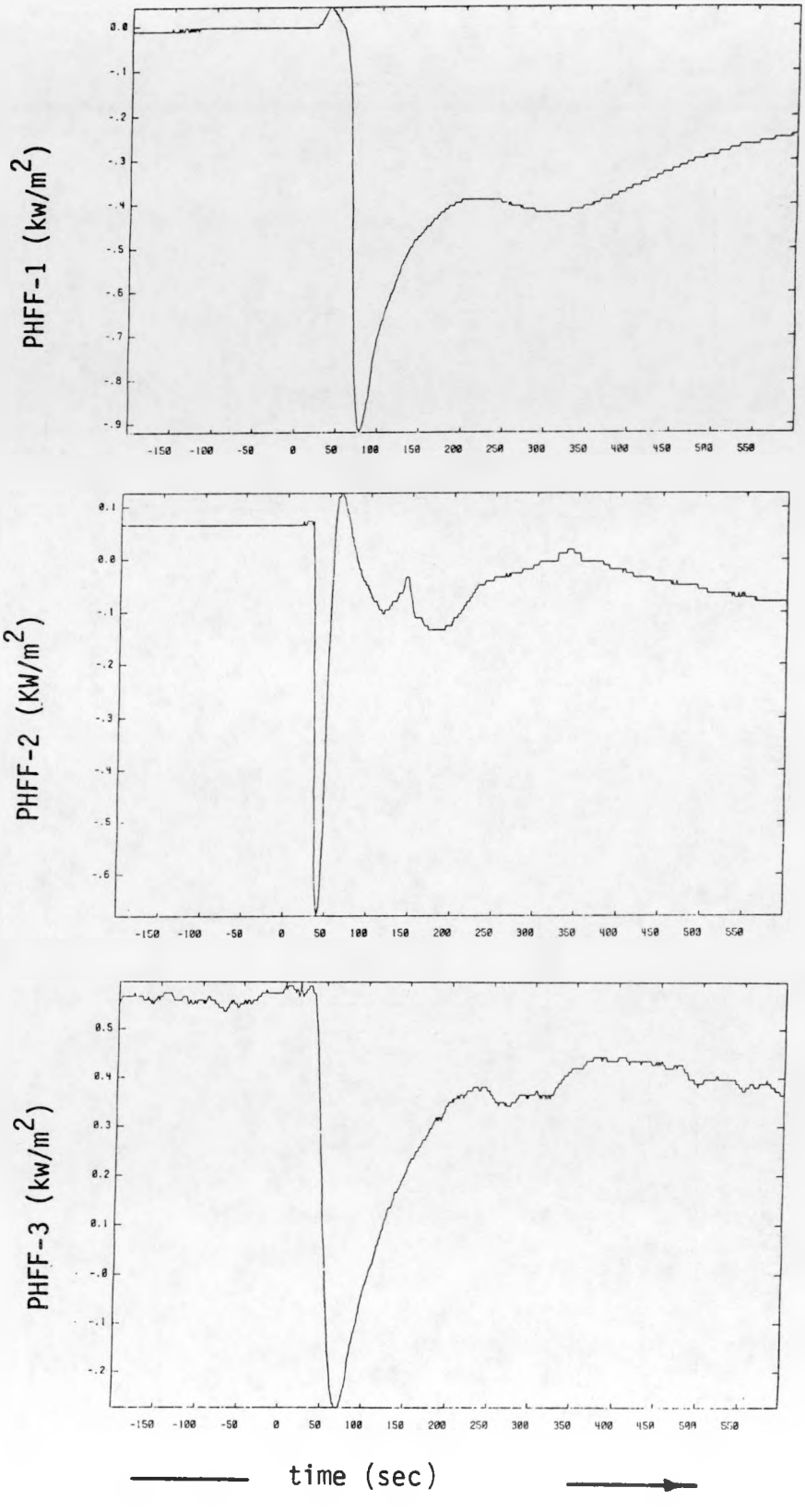

FIG. 37. EAG2 Spill Area Heat Flow Data

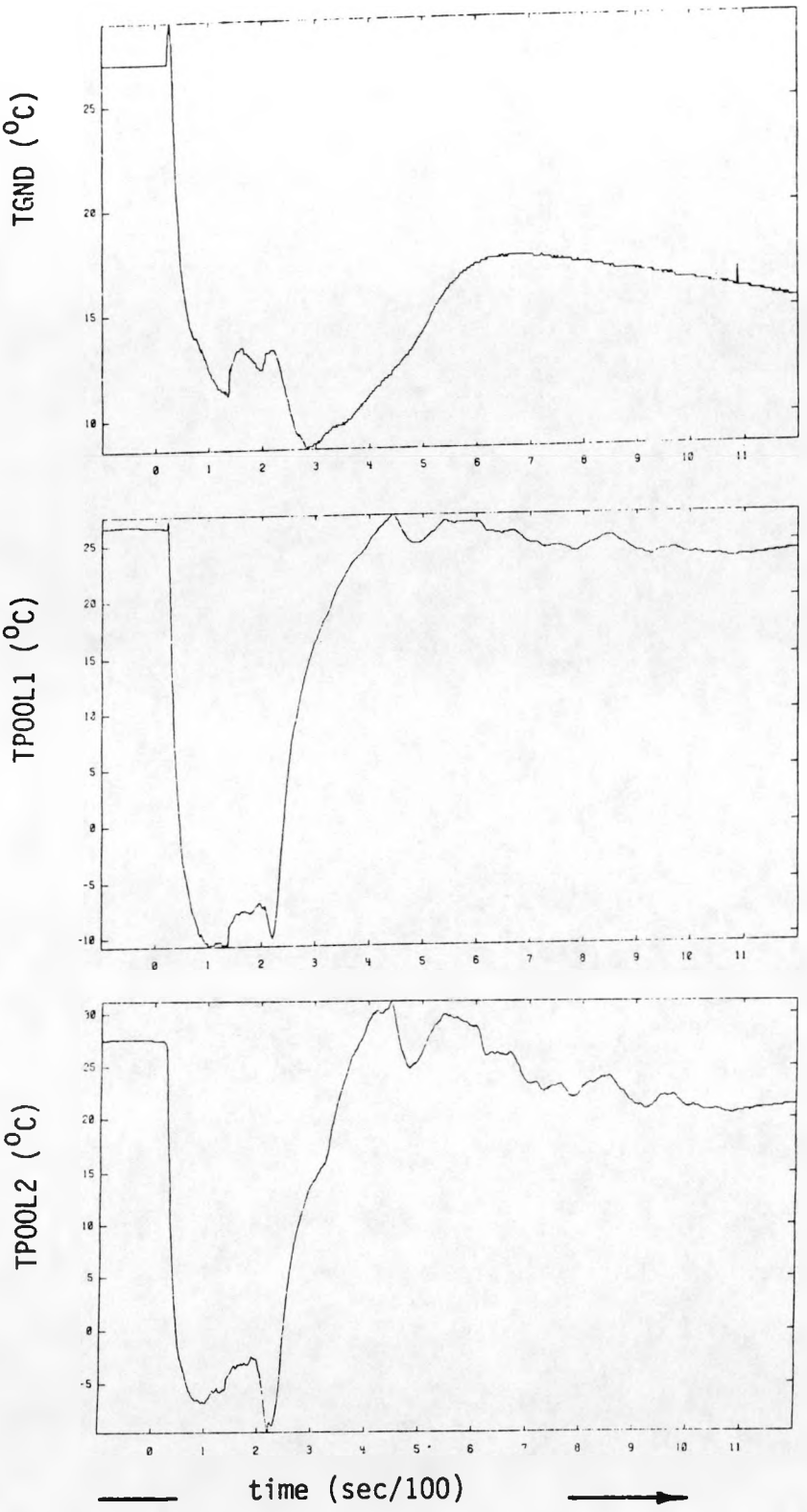

FIG. 38. EAG3 Temperature Profile Data

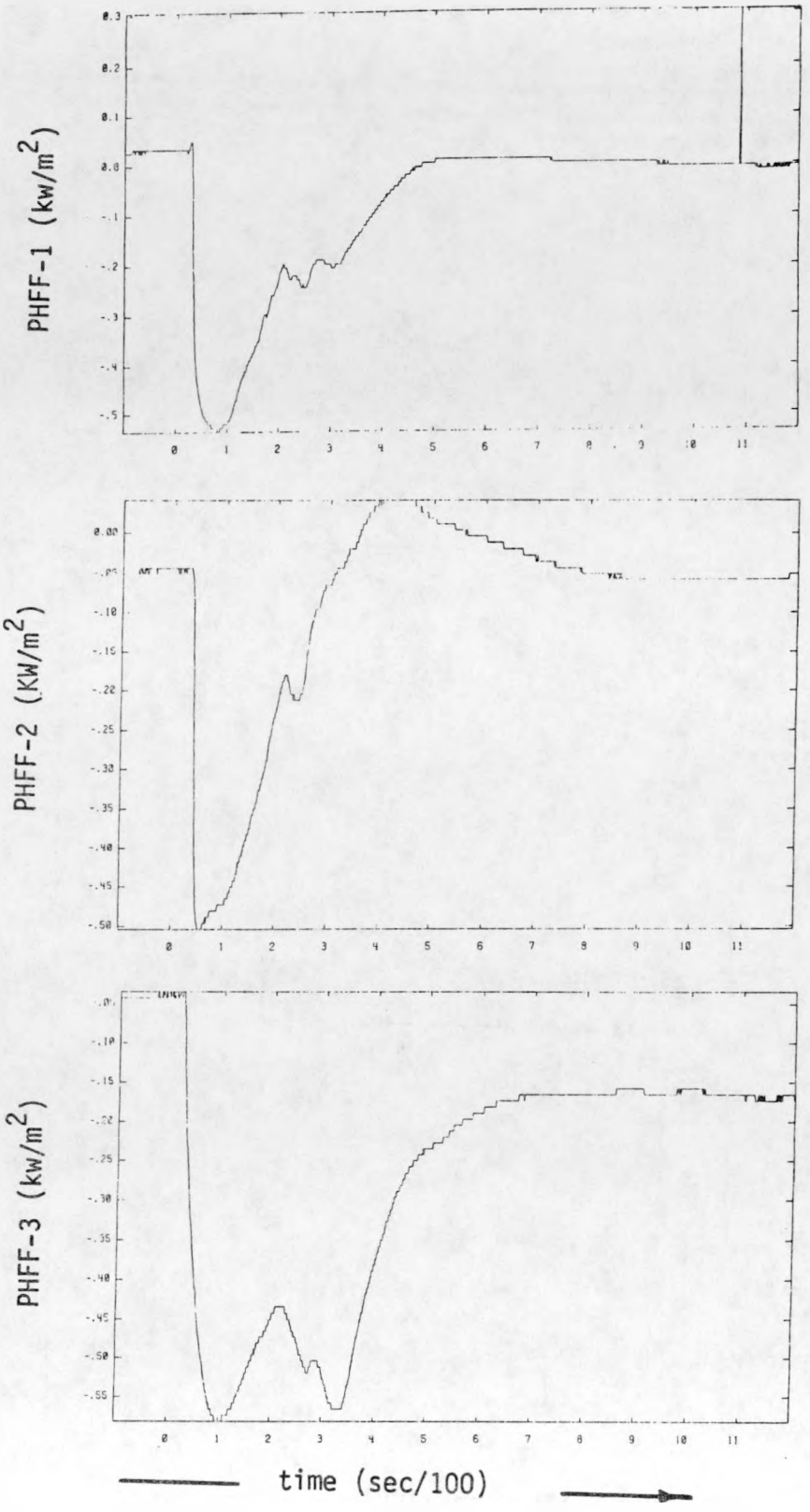

FIG. 39. EAG3 Spill Area Heat Flow Data

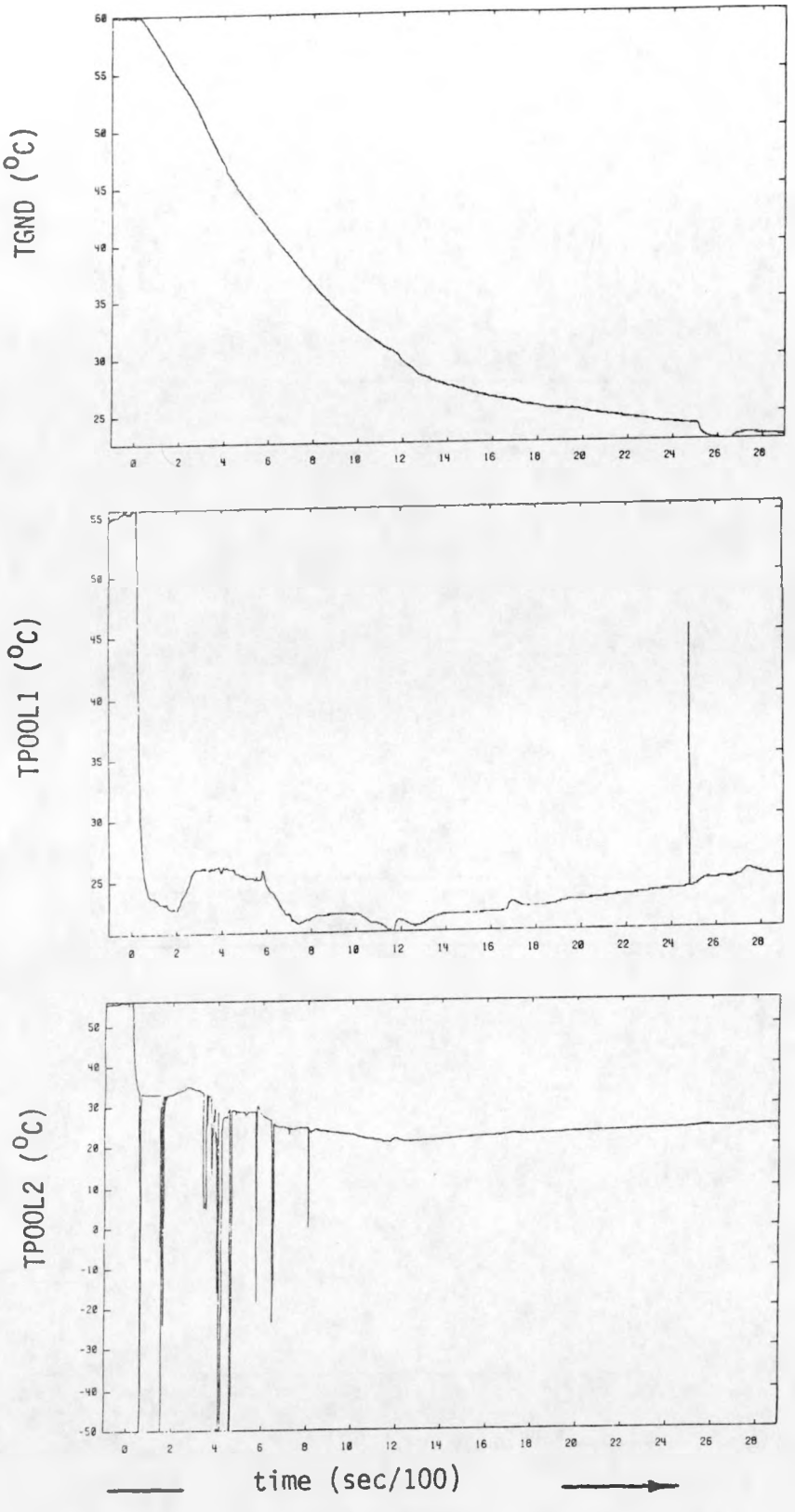

FIG. 40. EAG4 Temperature Profile Data

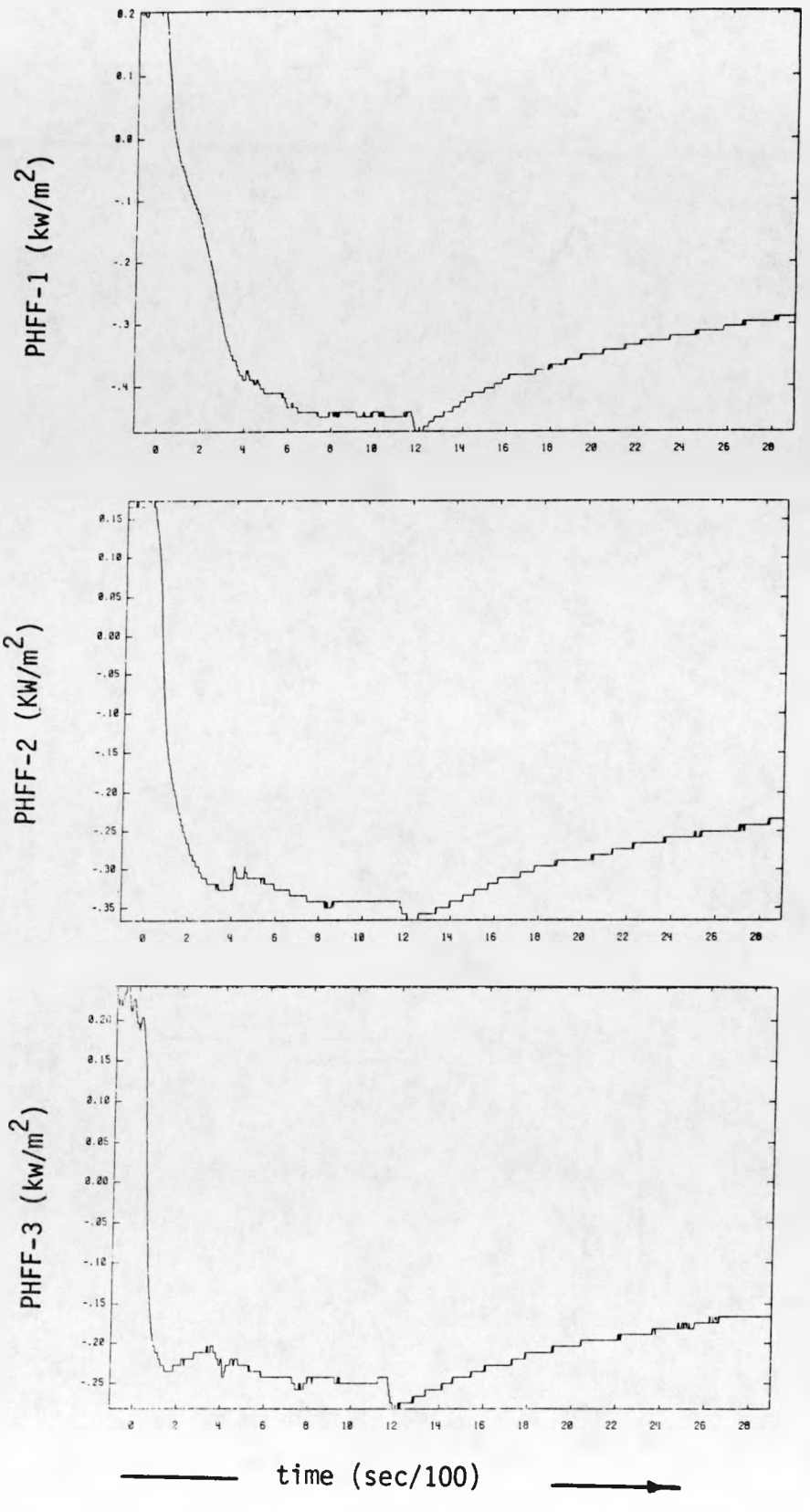

FIG. 41. EAG4 Spill Area Heat Flow Data

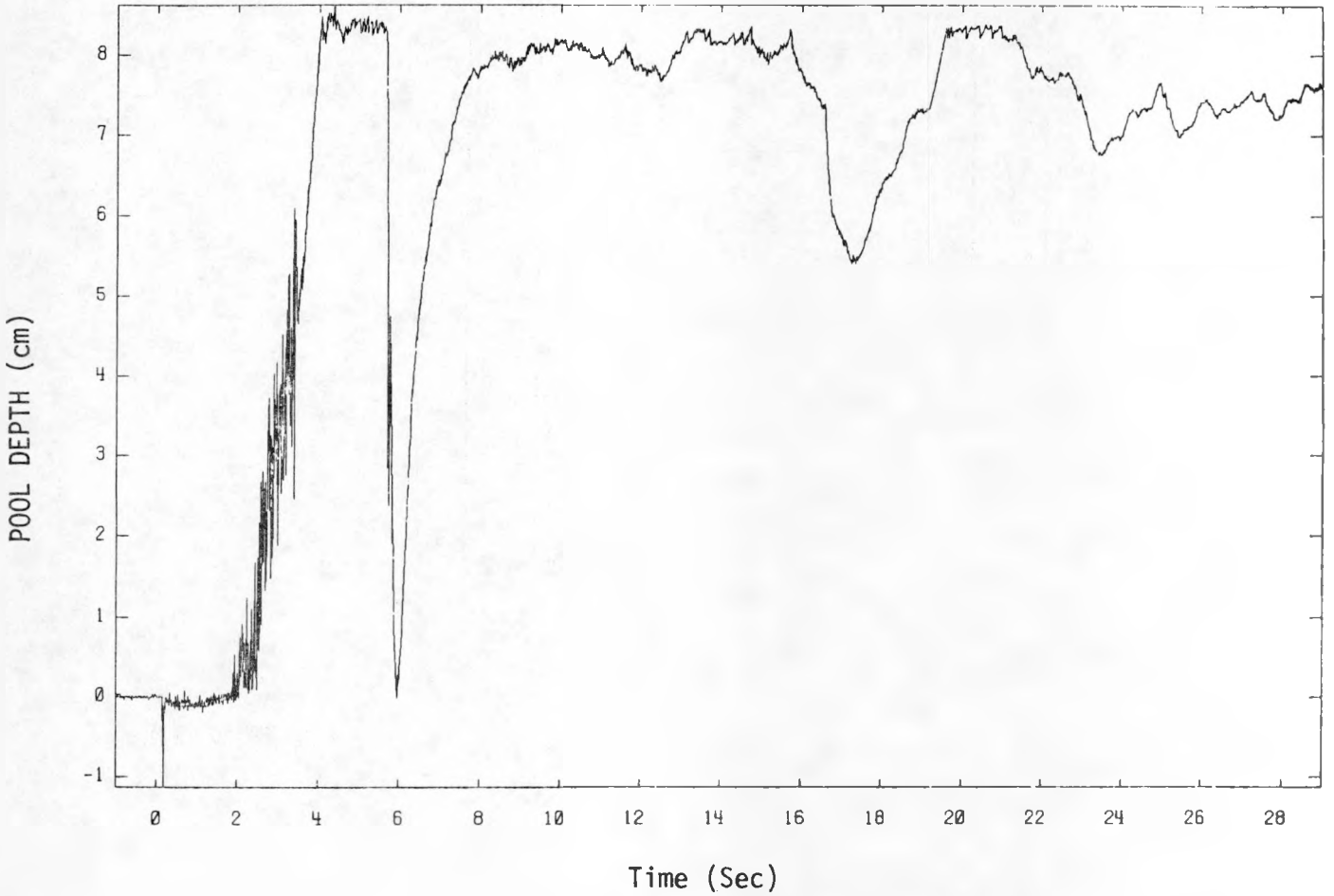

FIG. 42. EAG4 POOL DEPTH DATA

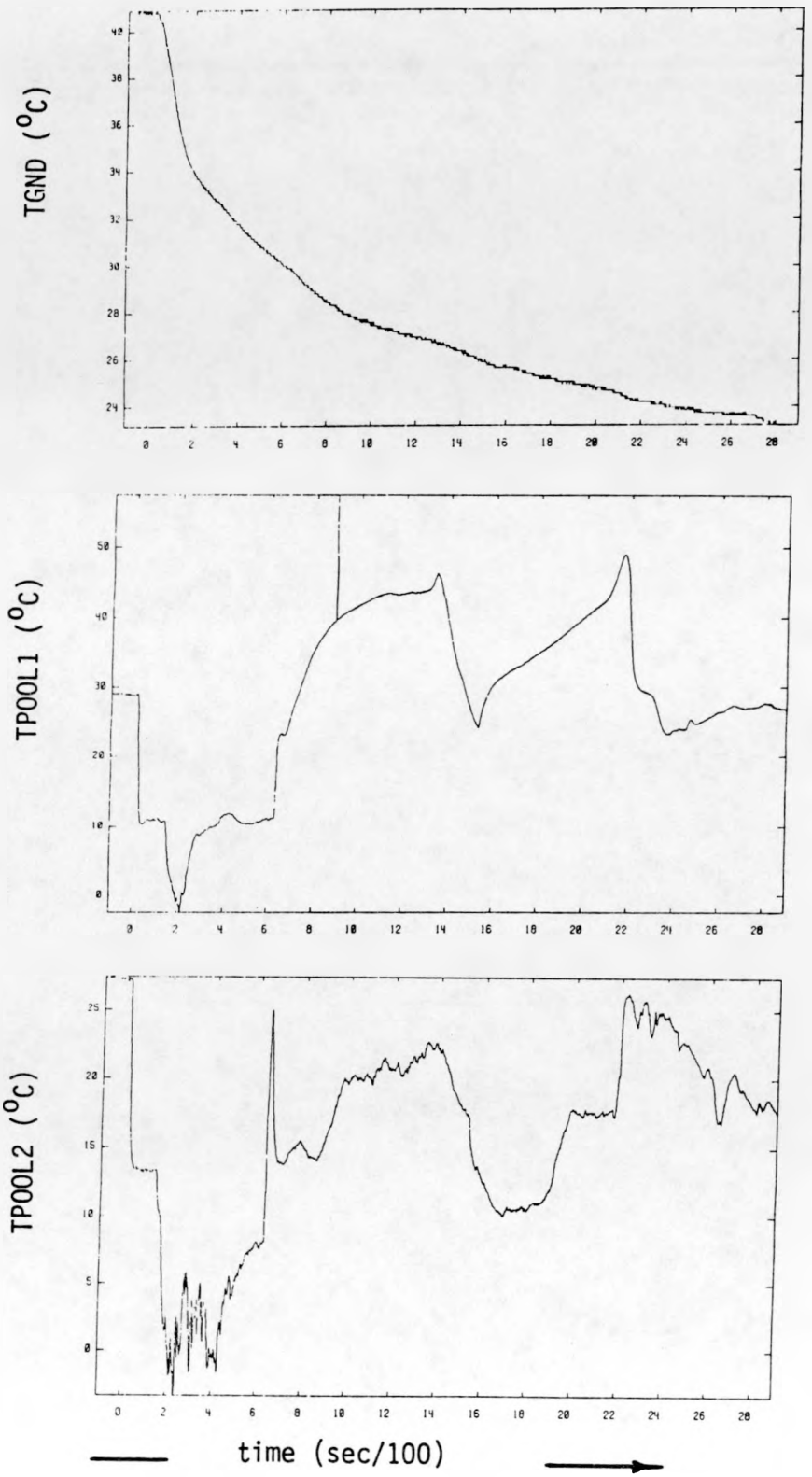

FIG. 43. EAG5 Temperature Profile Data

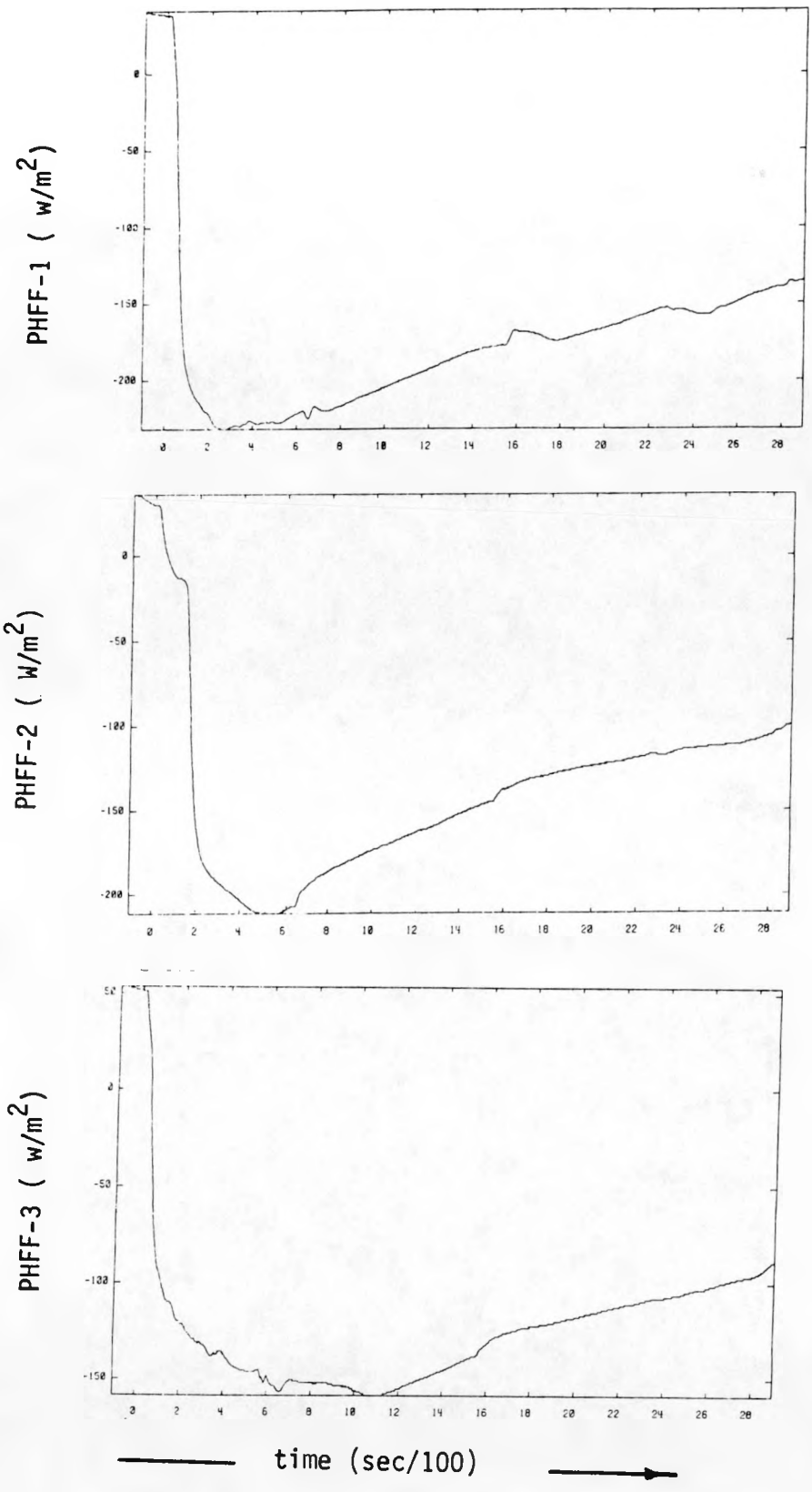

FIG. 44. EAG5 Spill Area Heat Flow Data

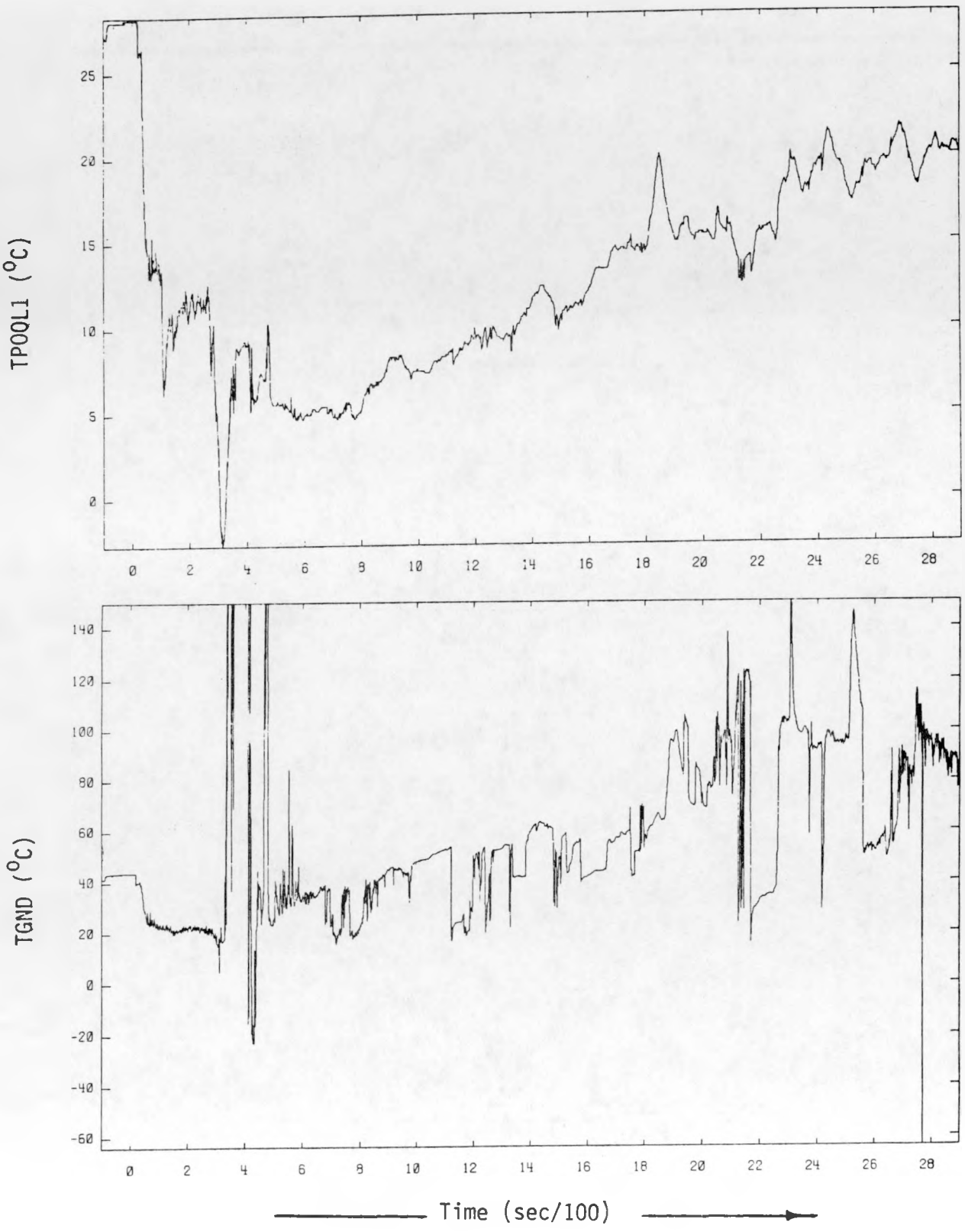

FIG. 45. EAG6 TEMPERATURE PROFILE DATA

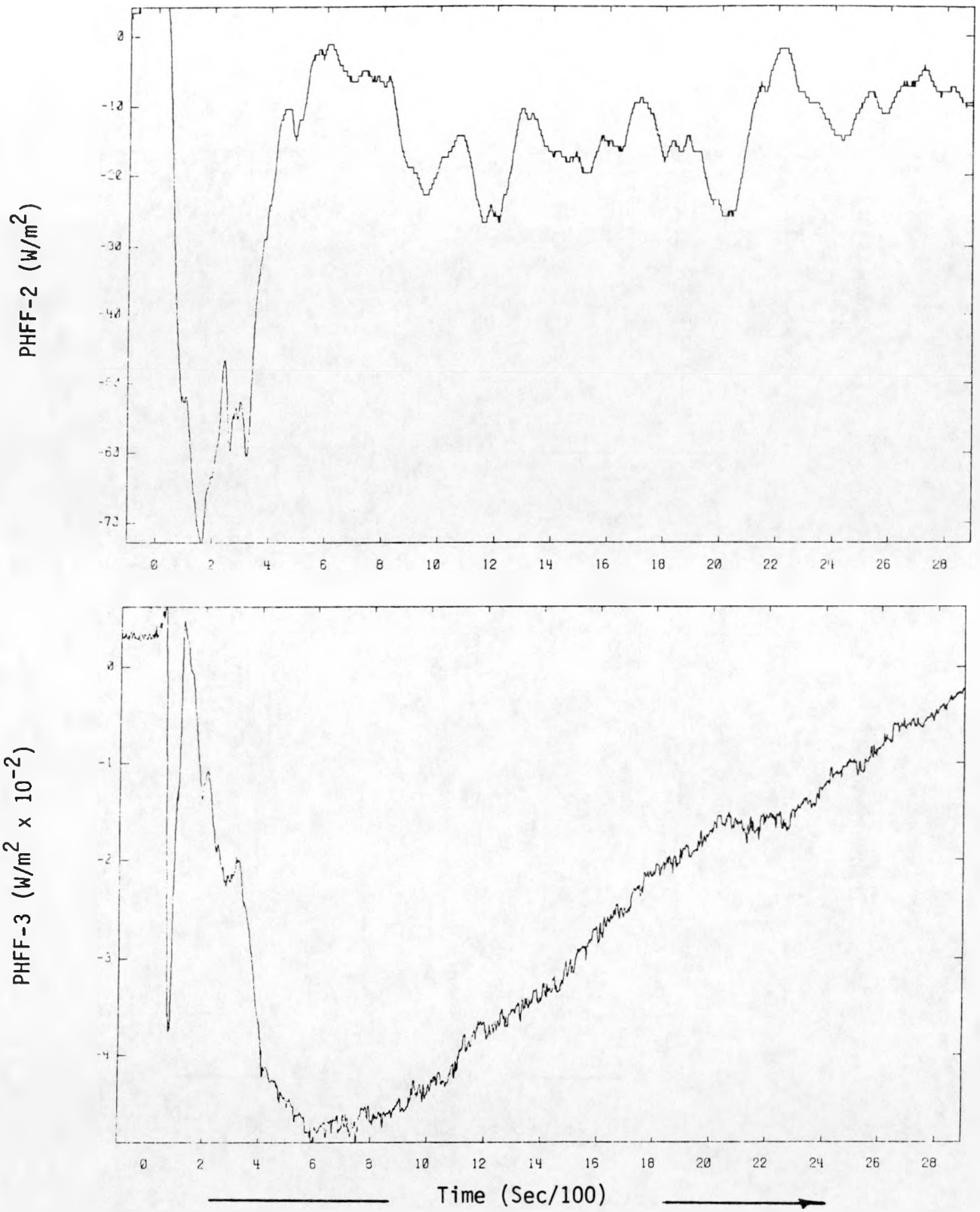

FIG. 46. EAG6 SPILL AREA HEAT FLOW DATA.

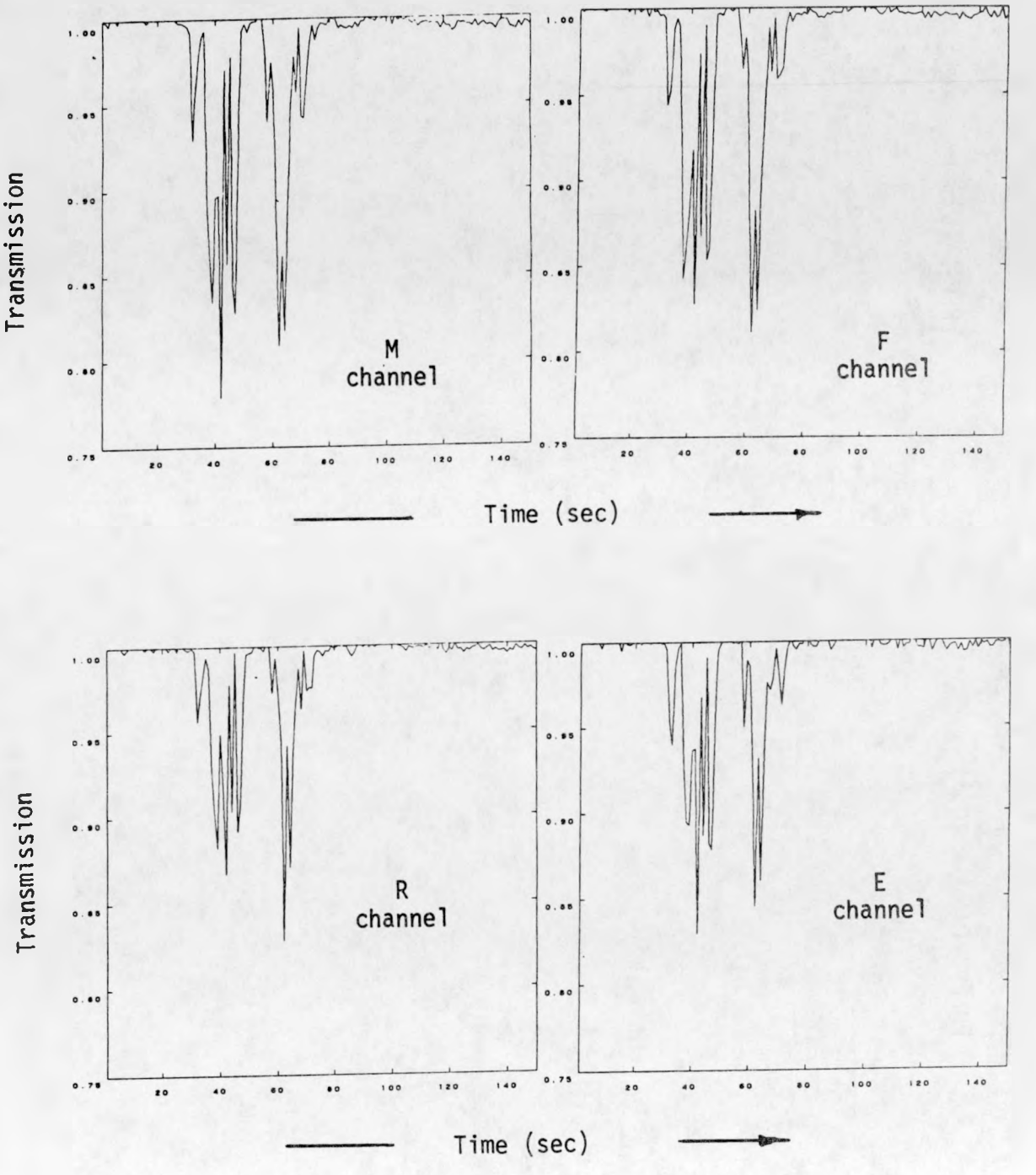

FIG. 47. IR GAS SENSOR CHANNEL TRANSMISSION DATA.

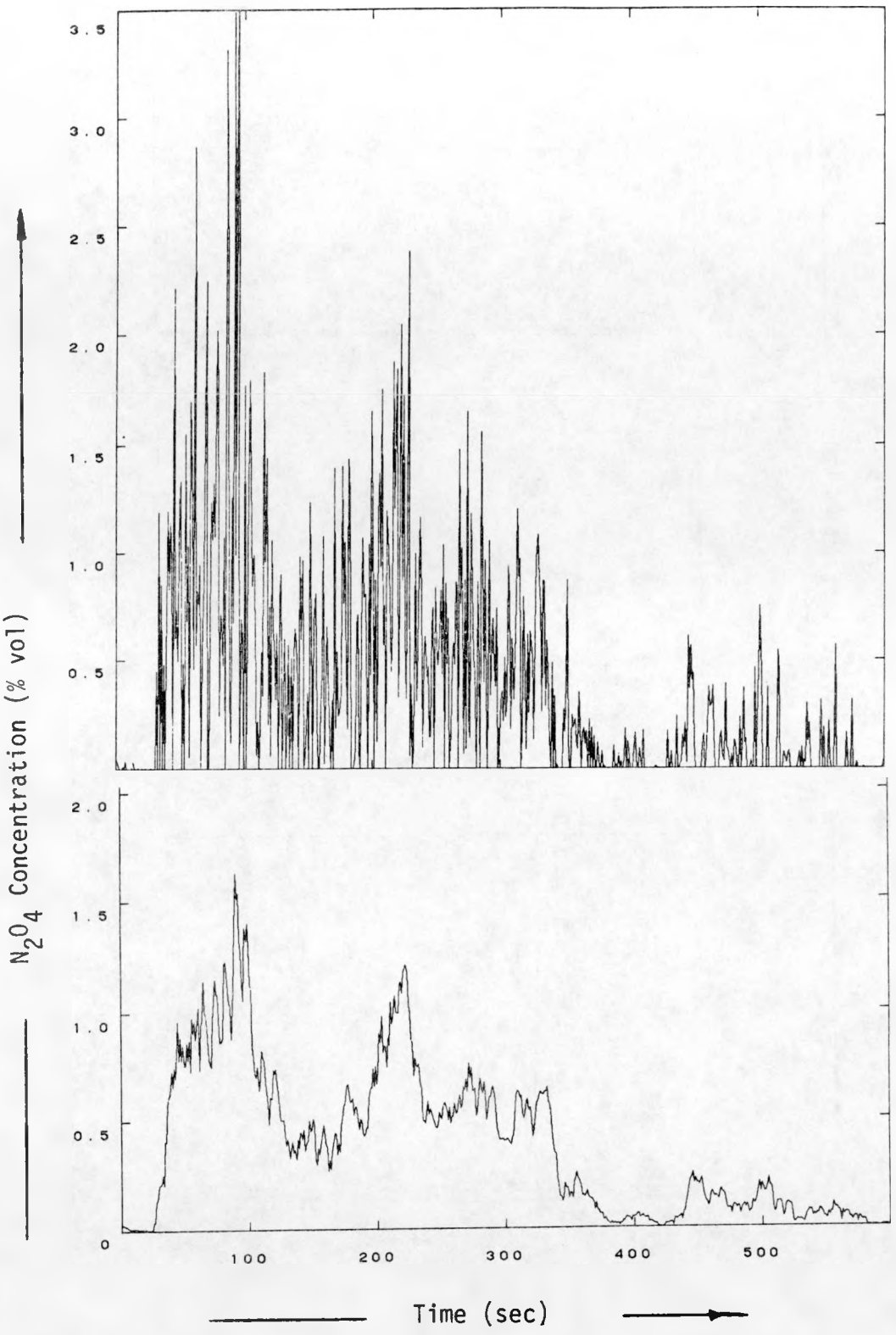

FIG. 48. EFFECT OF 11 POINT SLIDING AVERAGE on N_2O_4 DATA.

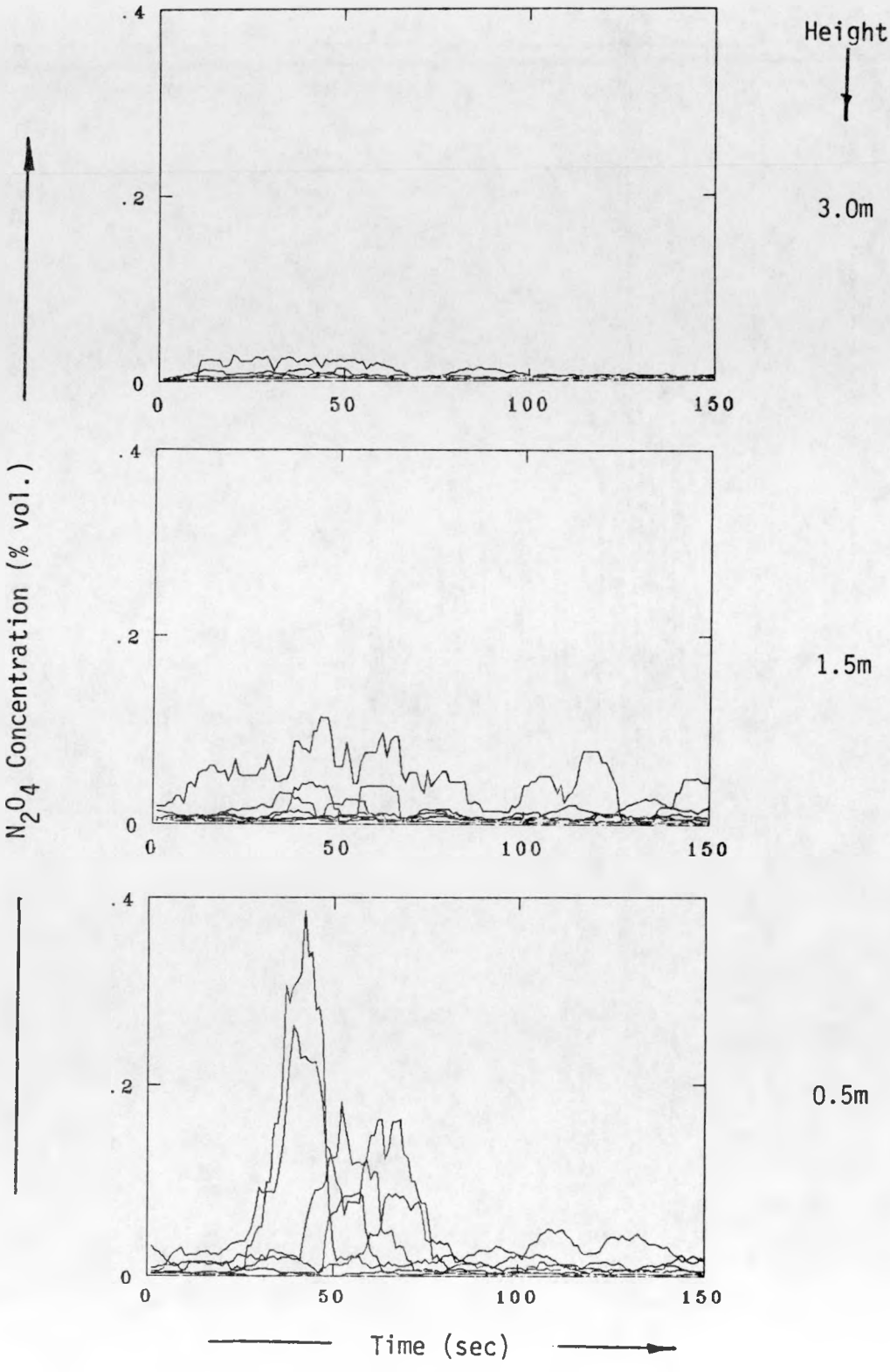

FIG. 49. EAG1 N_2O_4 VAPOR CONCENTRATION DATA @ 25m.

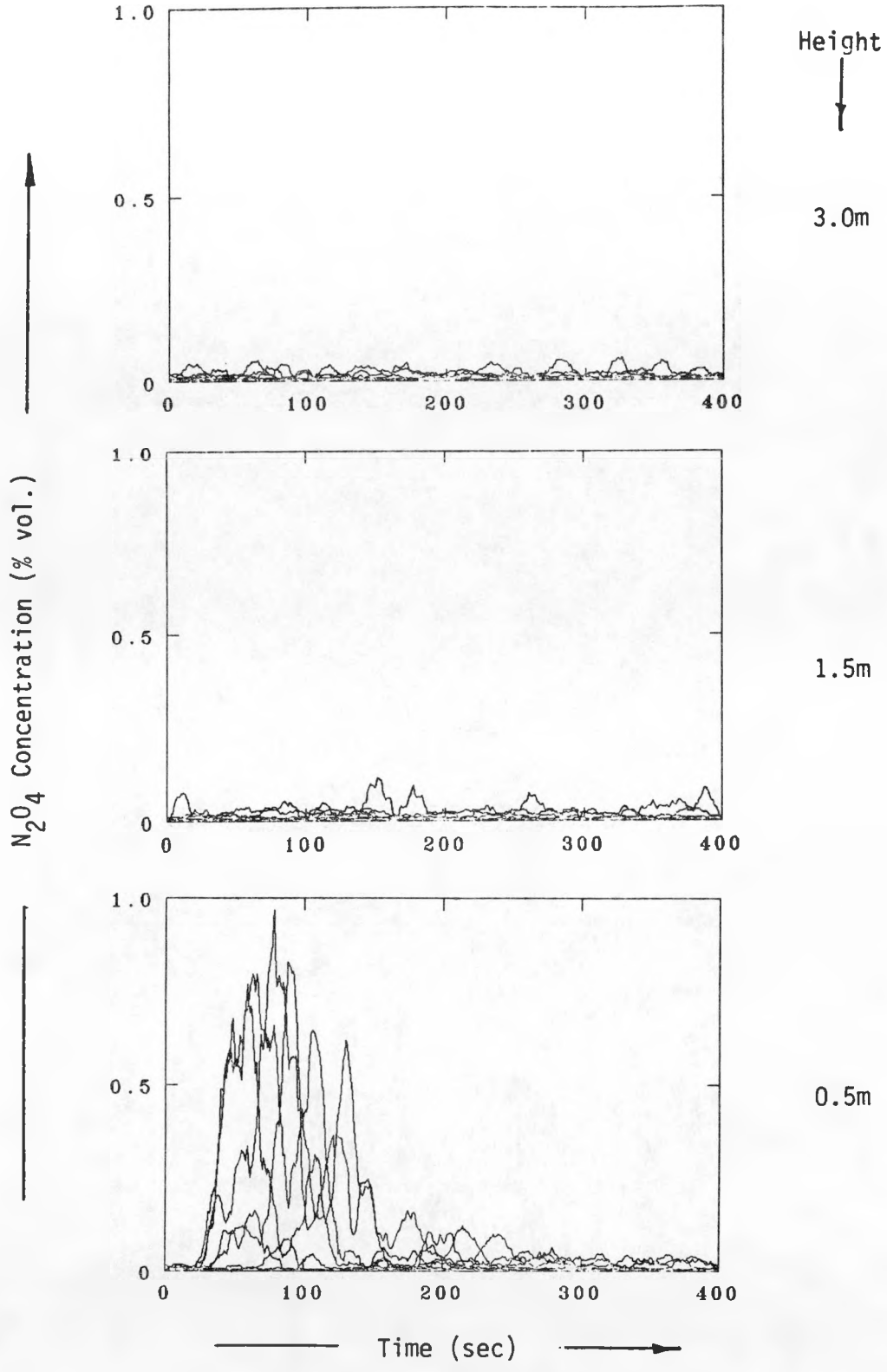

FIG. 50. EAG2 N_2O_4 VAPOR CONCENTRATION DATA @ 25m.

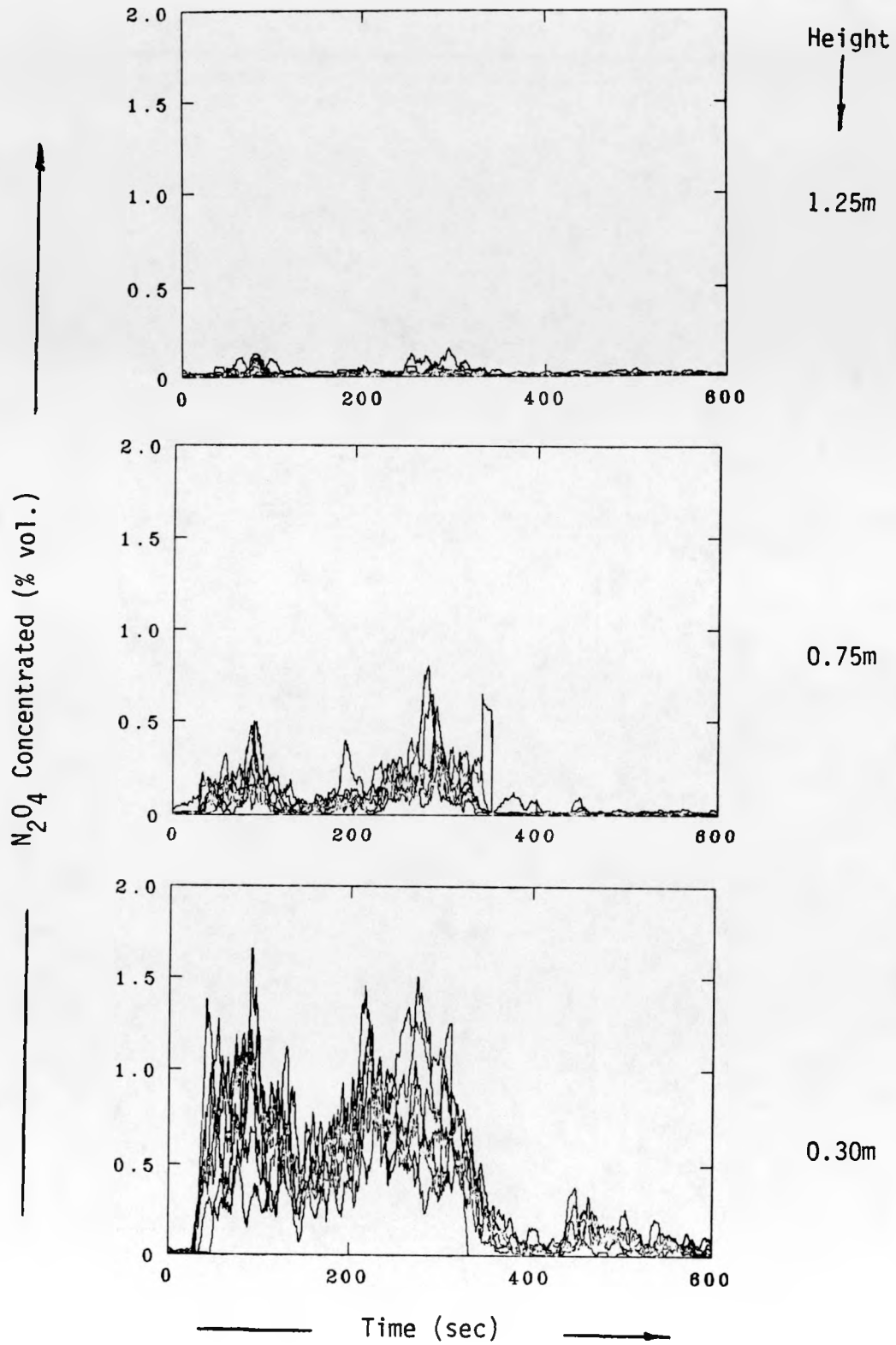

FIG. 51. EAG3 N_2O_4 VAPOR CONCENTRATION DATA @ 25m.

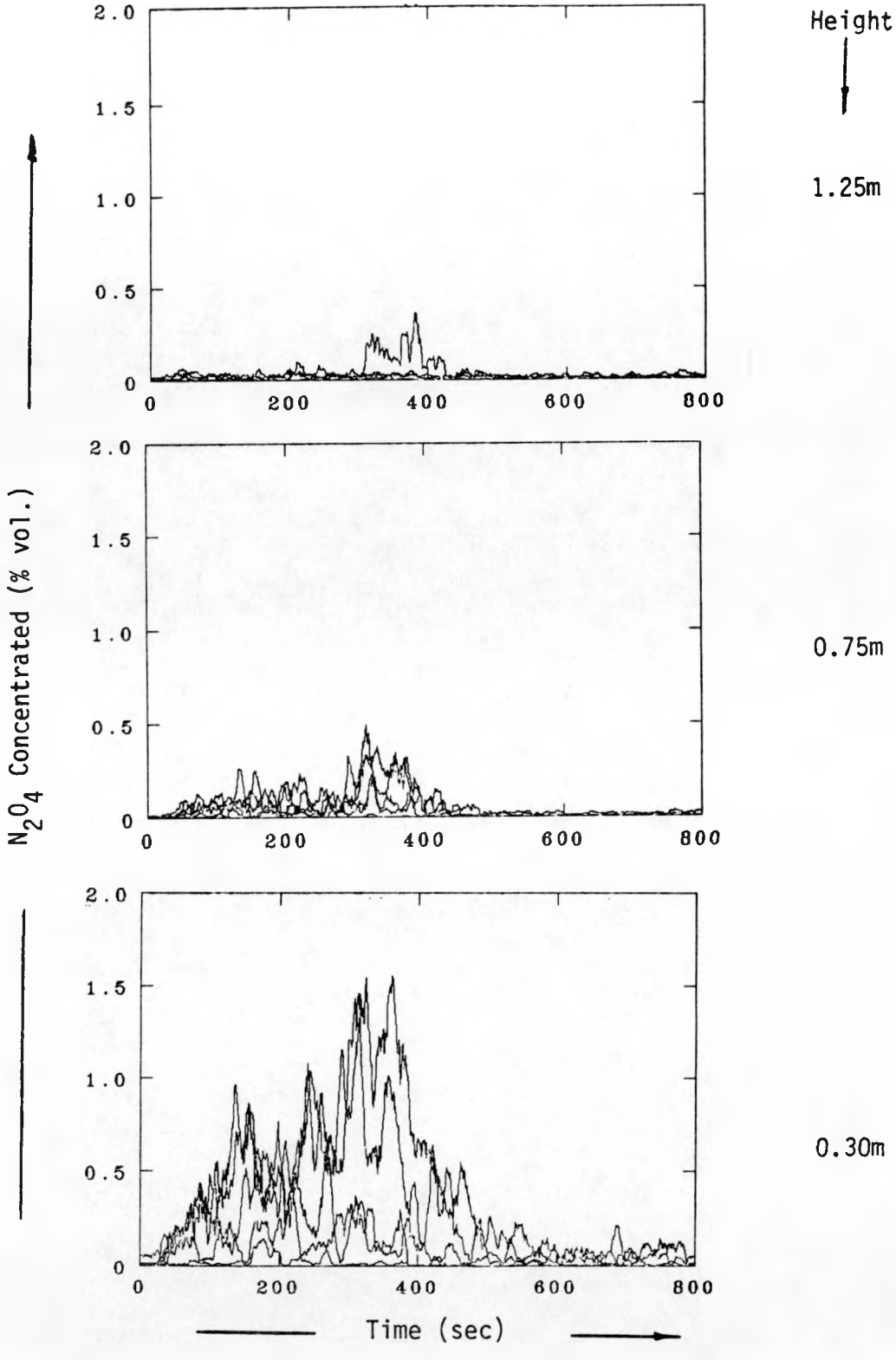

FIG. 52. EAG6 N_2O_4 VAPOR CONCENTRATION DATA @ 25m.

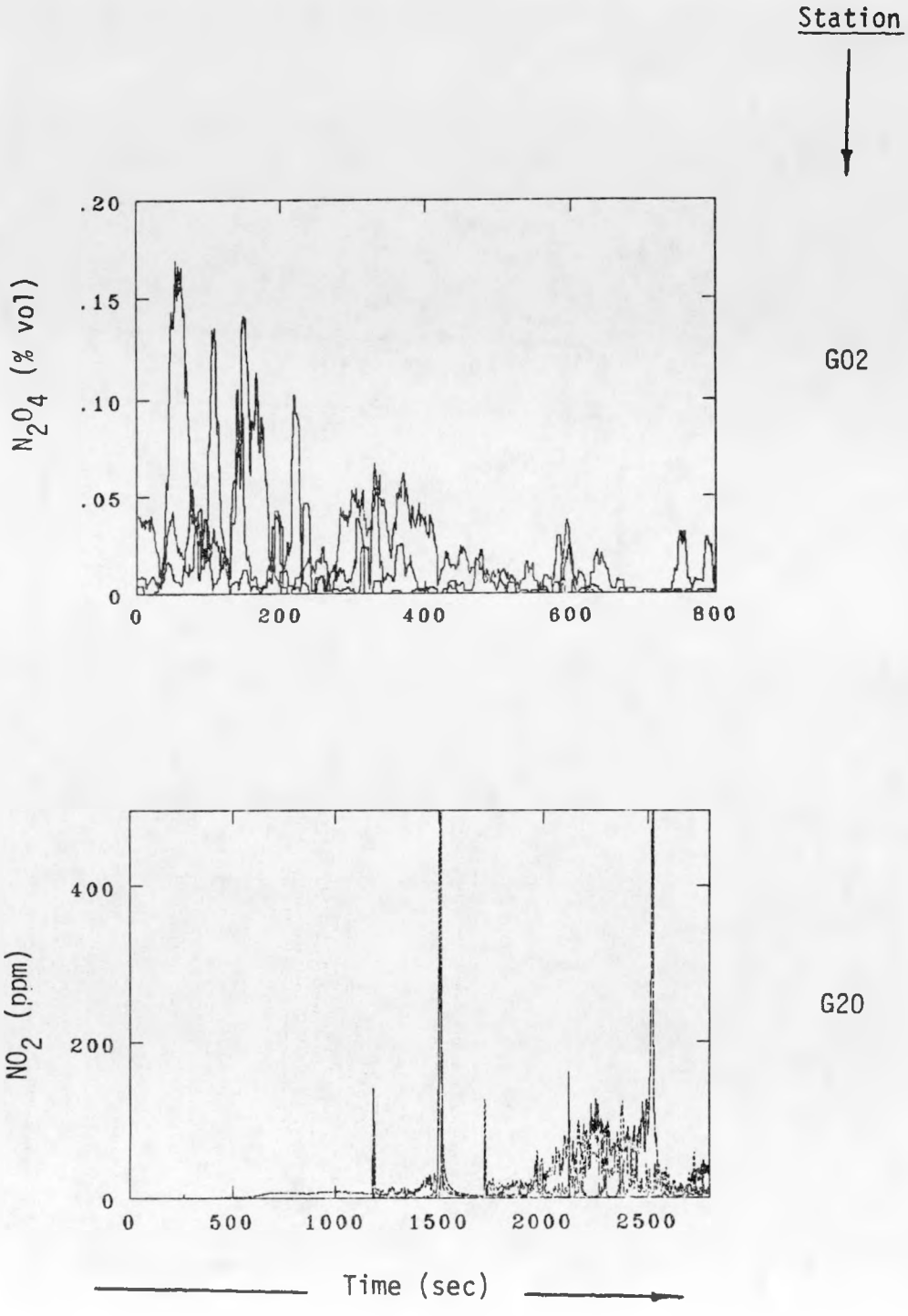

FIG. 53. EAG4 PFVSS SOURCE STRENGTH DATA.

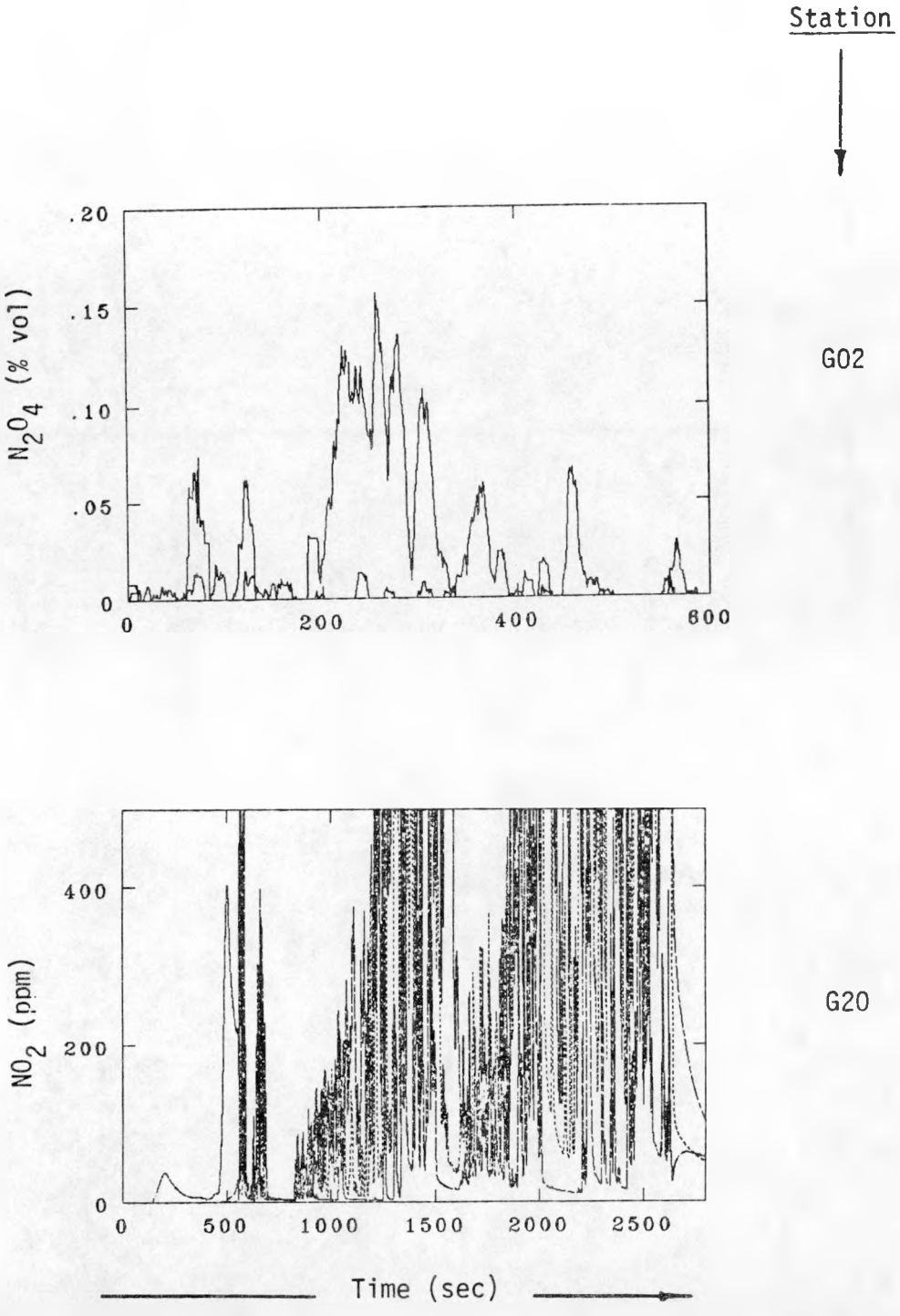

FIG. 54. EAG5 PFVSS SOURCE STRENGTH DATA.

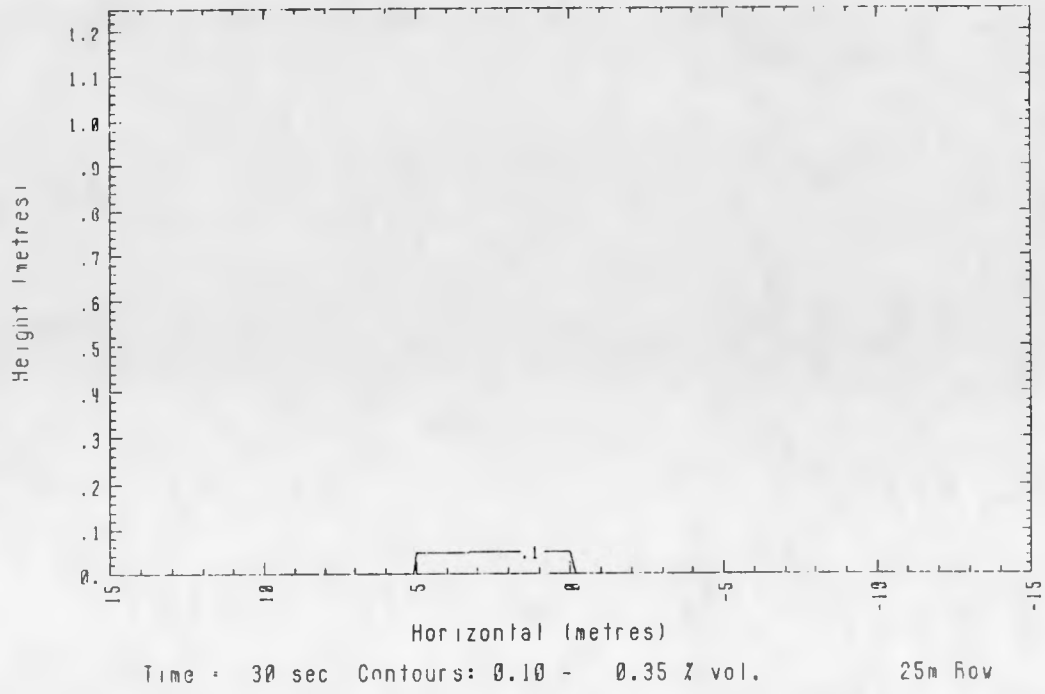

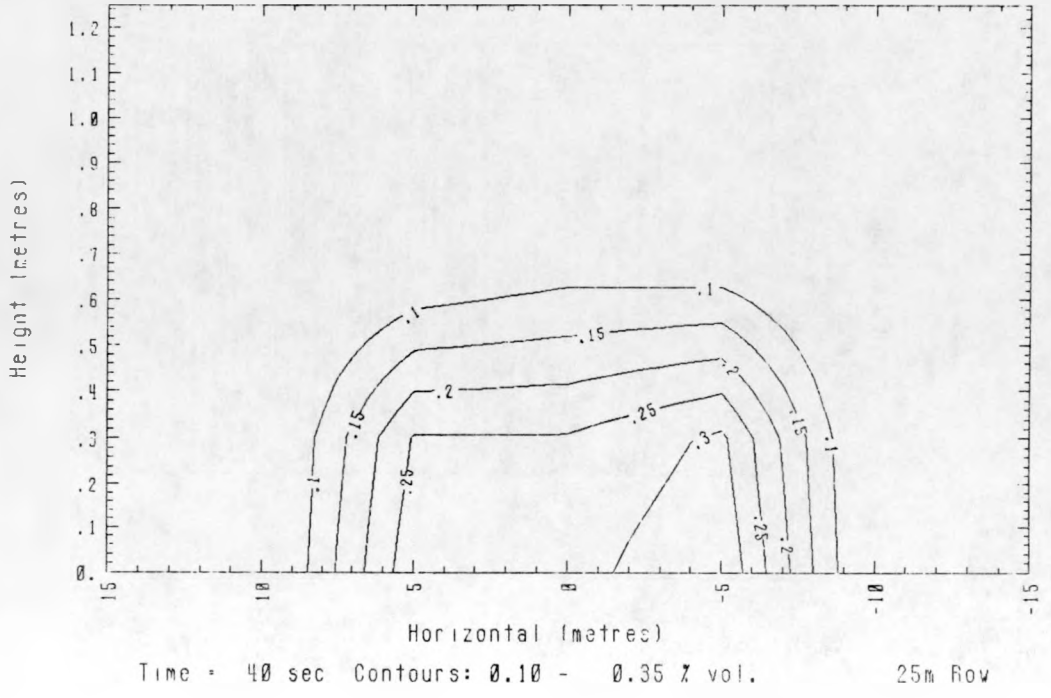

EAG. 55. EAG1 CROSSWIND CONCENTRATION CONTOURS @ 25m.

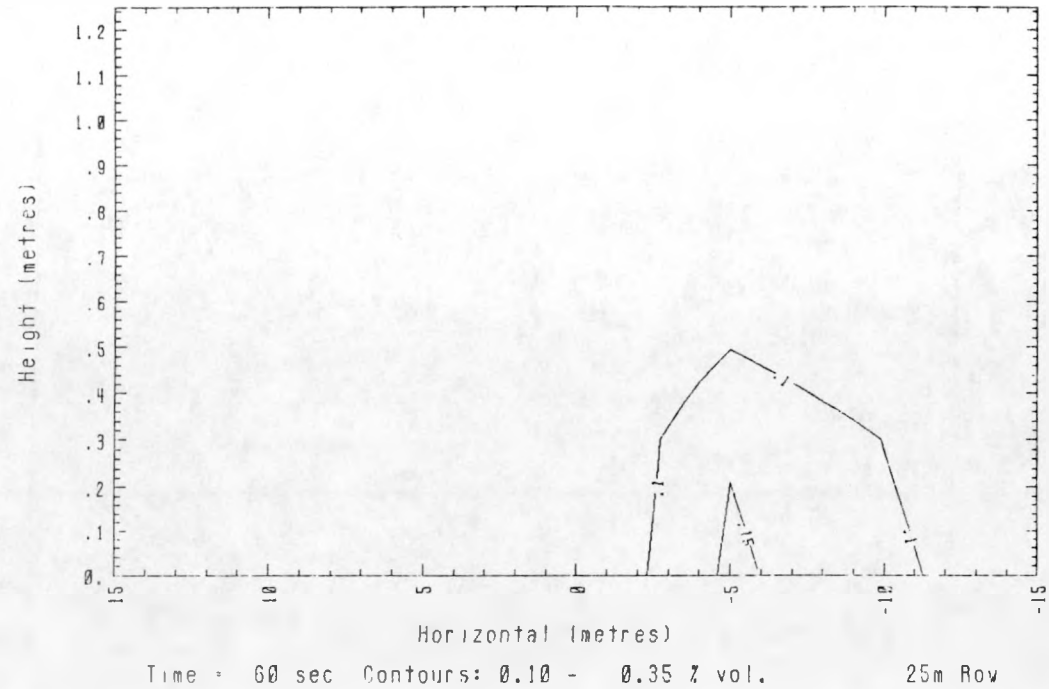

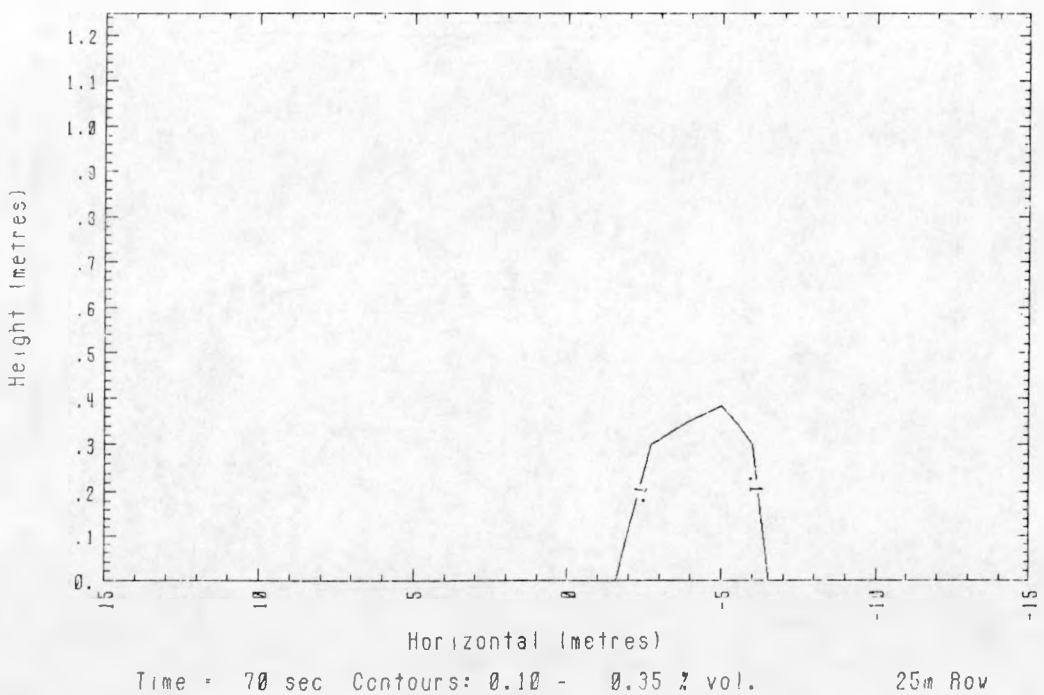

FIG. 55. EAG1 CROSSWIND CONCENTRATION CONTOURS @ 25m.
(continued)

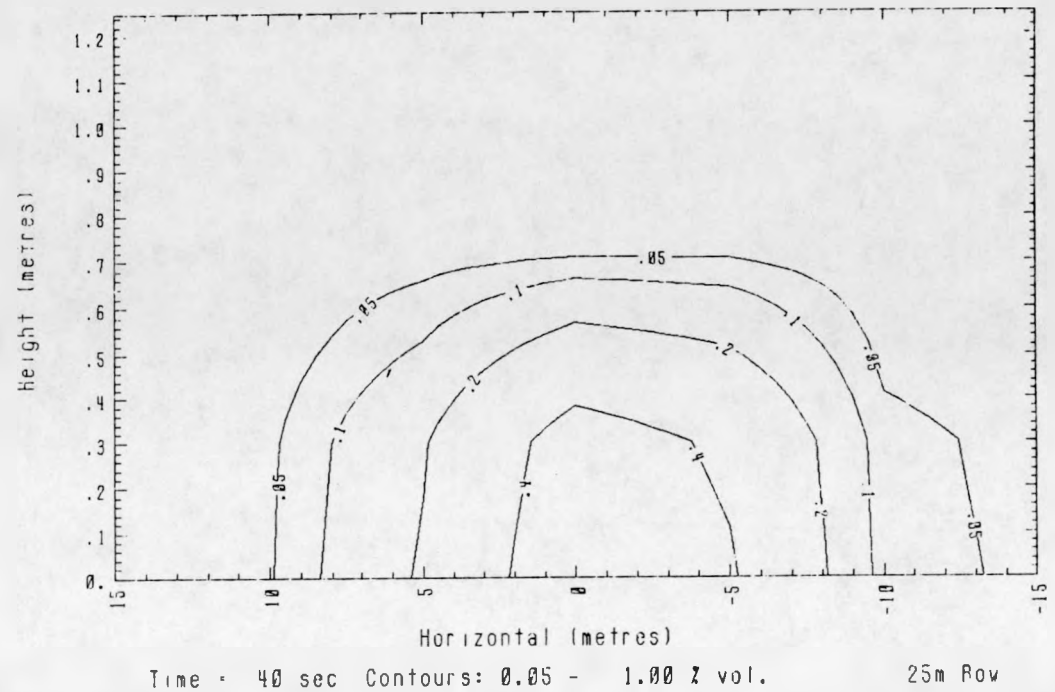

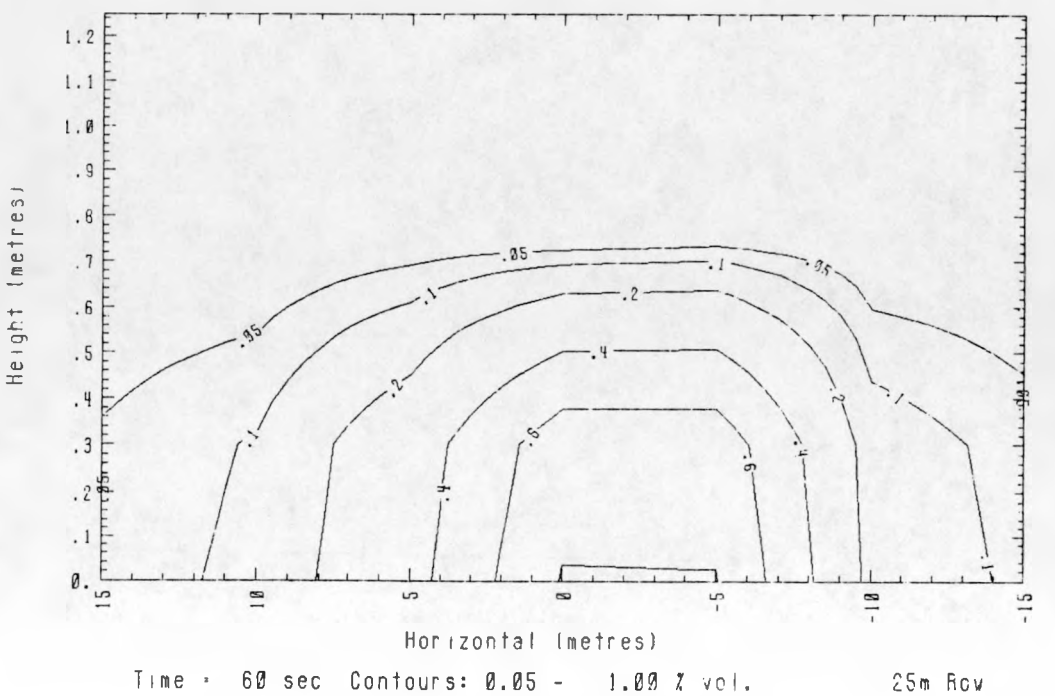

FIG. 56. EAG2 CROSSWIND CONCENTRATION CONTOURS @ 25m.

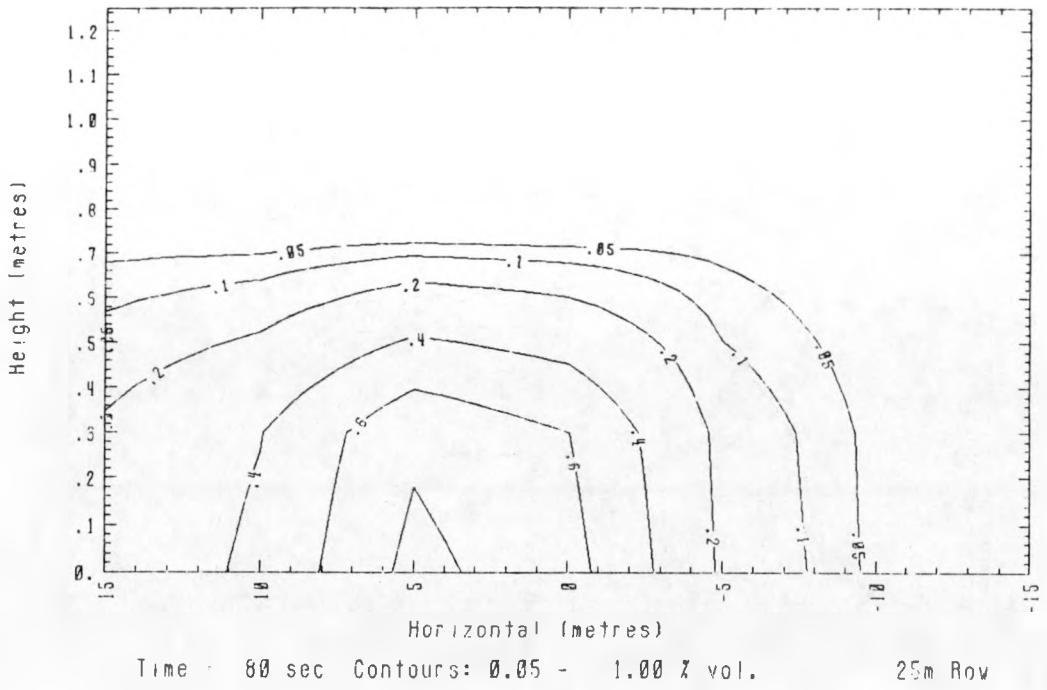

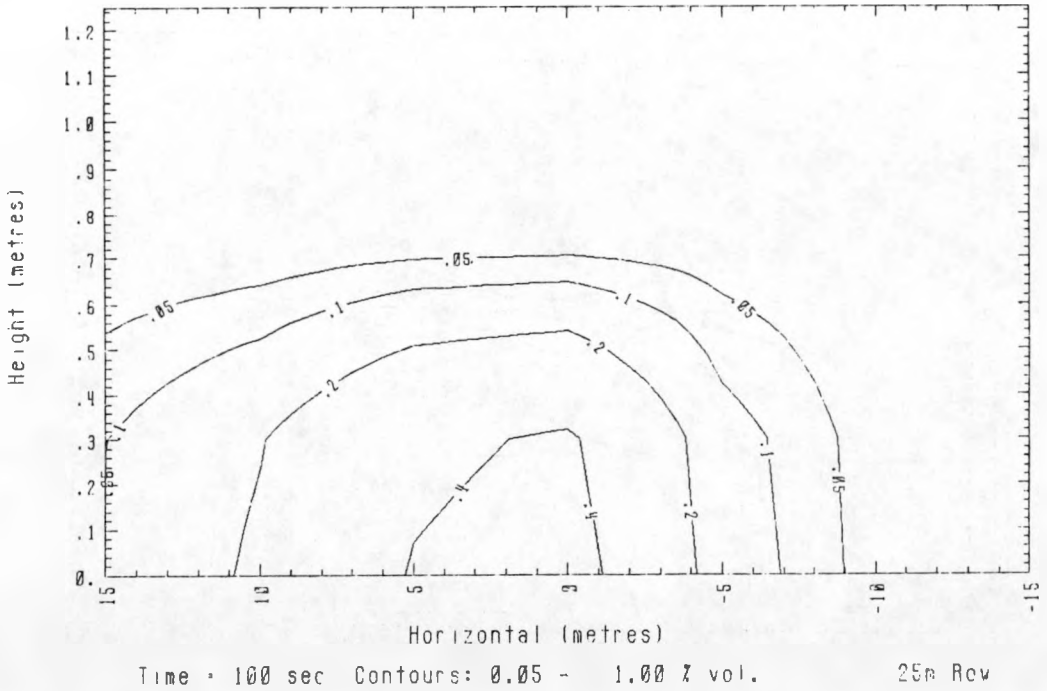

FIG. 56. EAG2 CROSSWIND CONCENTRATION CONTOURS @ 25m.
(continued)

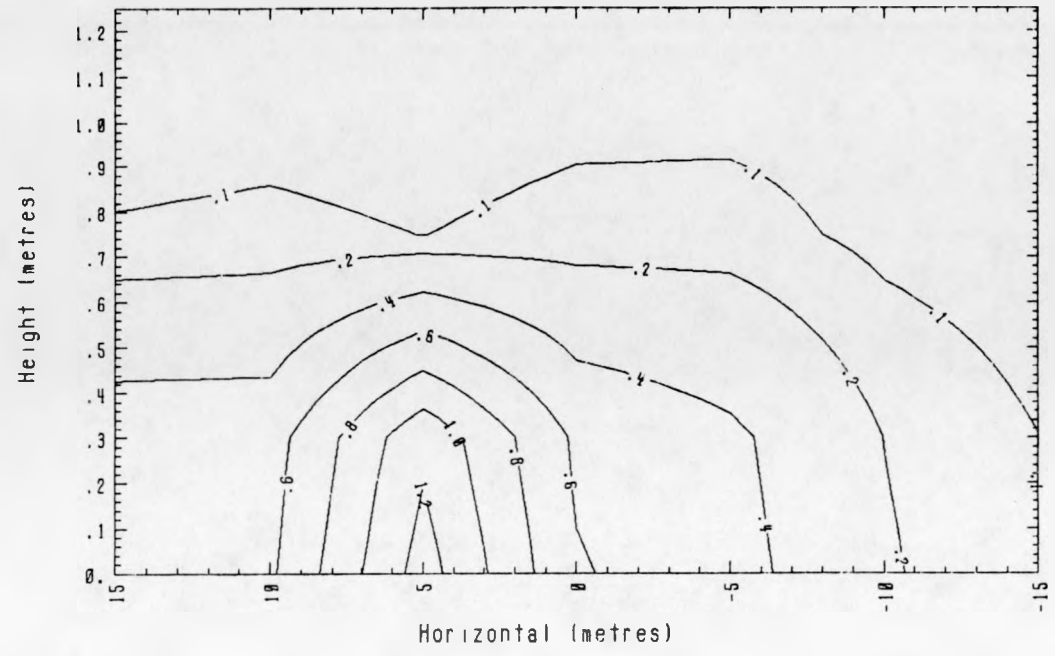

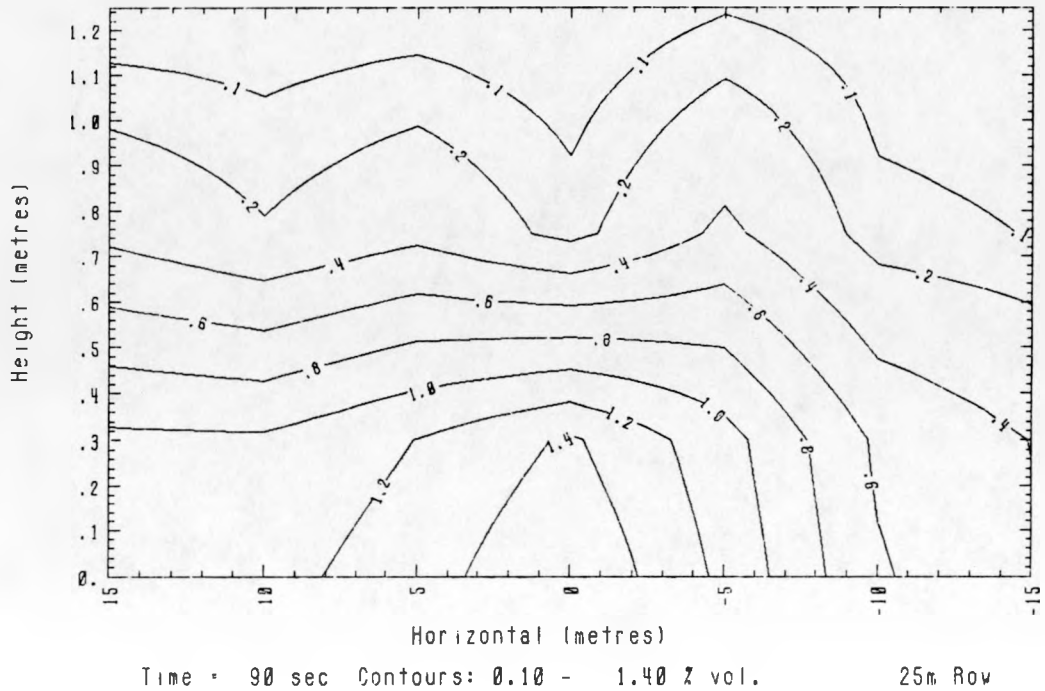

FIG. 57. EAG3 CROSSWIND CONCENTRATION CONTOURS @ 25m.

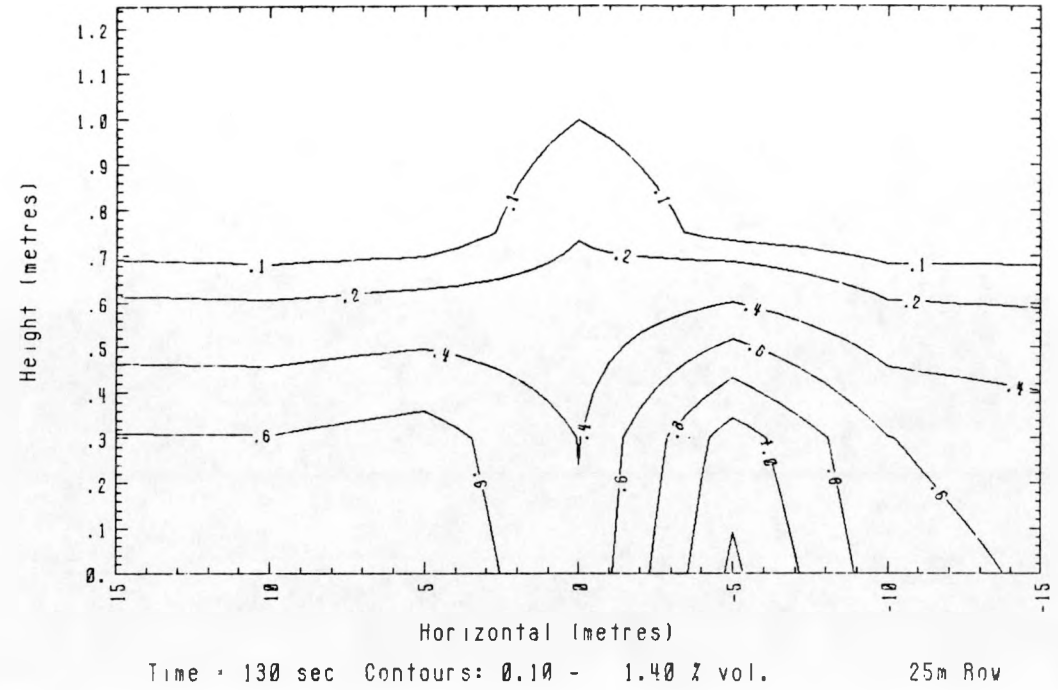

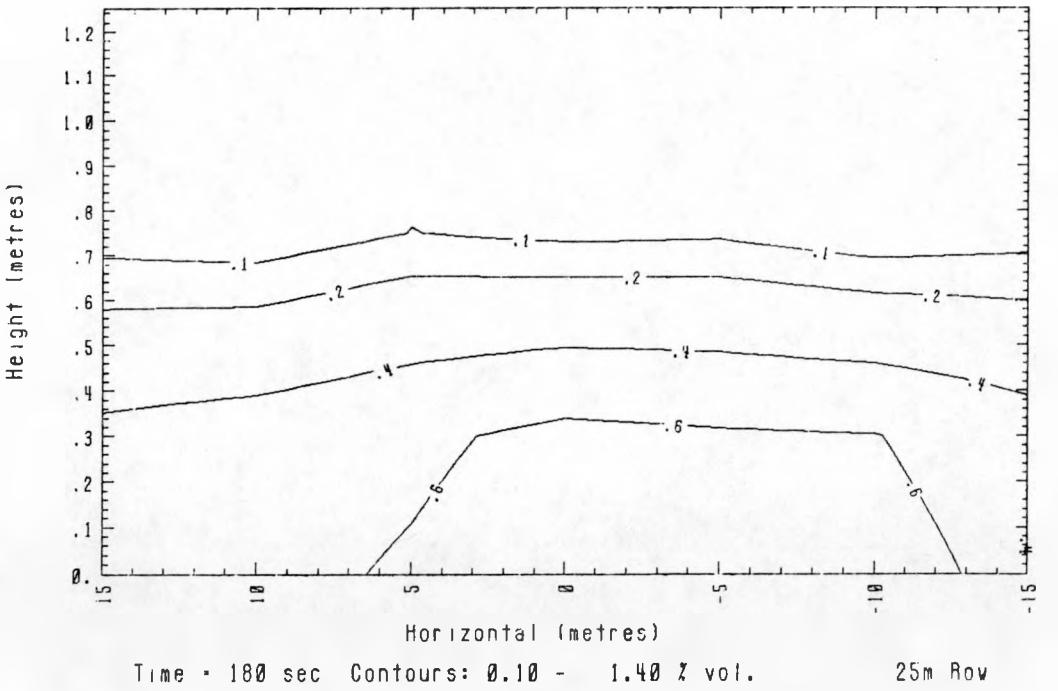

FIG. 57. EAG3 CROSSWIND CONCENTRATION CONTOURS @ 25m.
(continued)

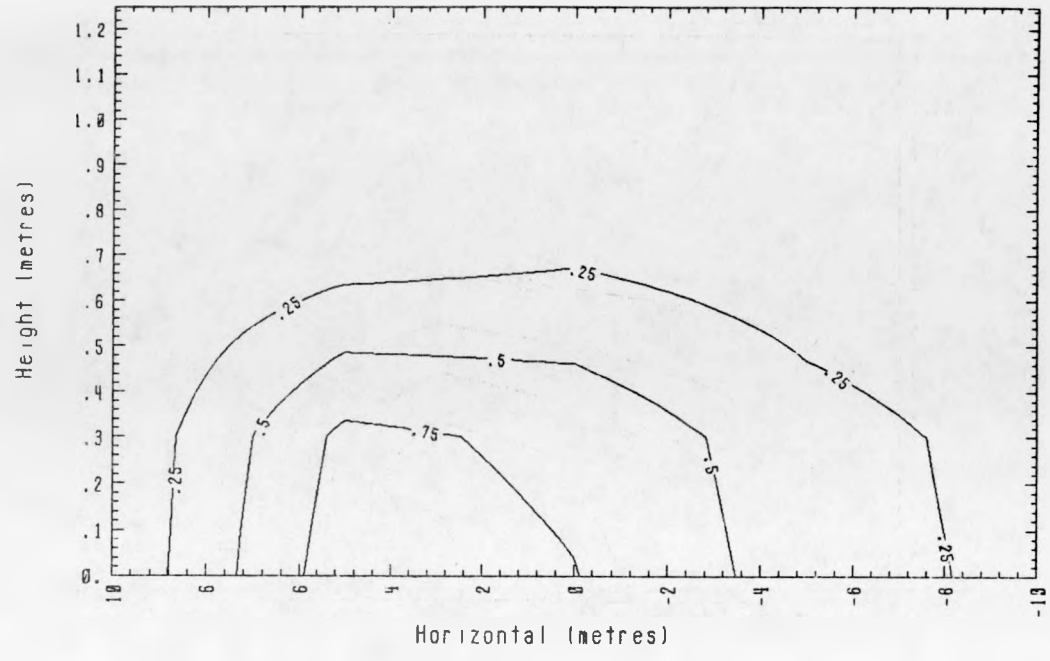

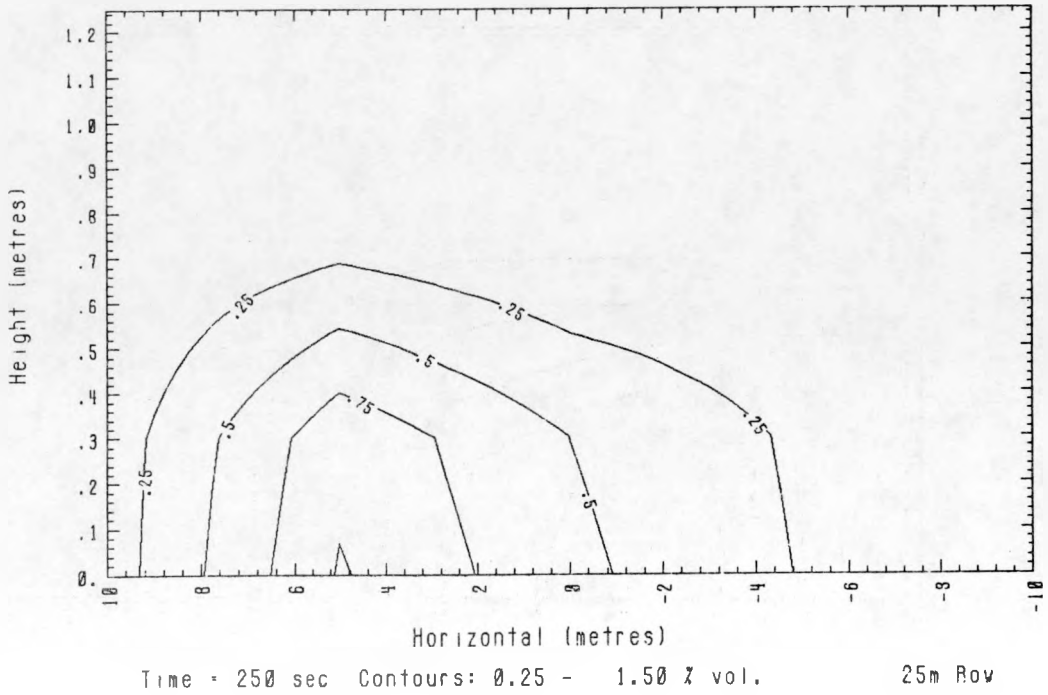

FIG. 58. EAG6 CROSSWIND CONCENTRATION CONTOURS @ 25m.

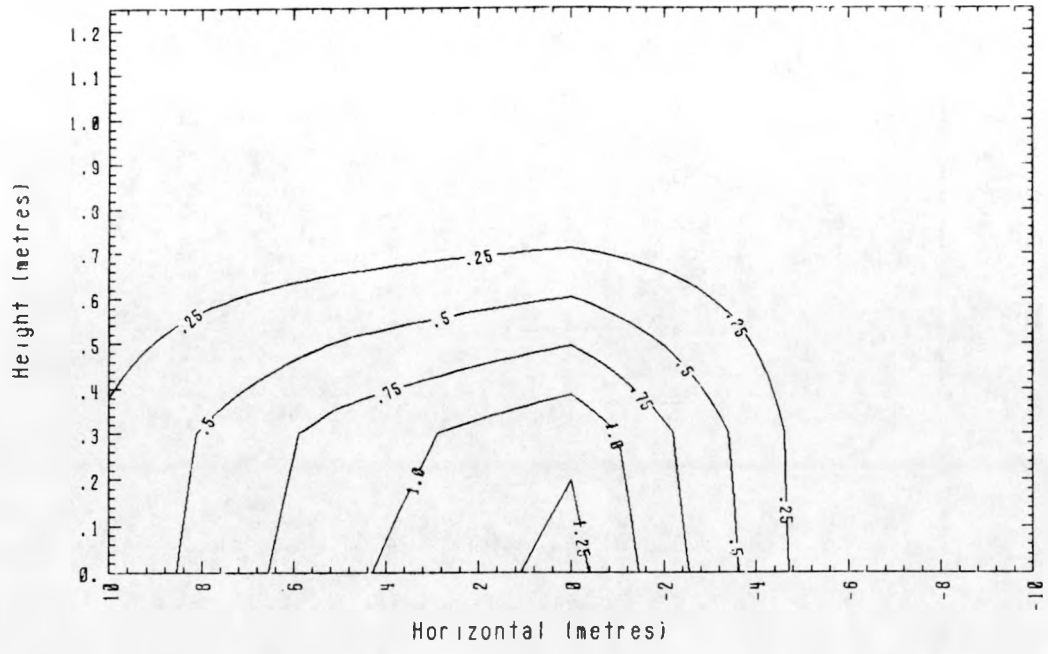

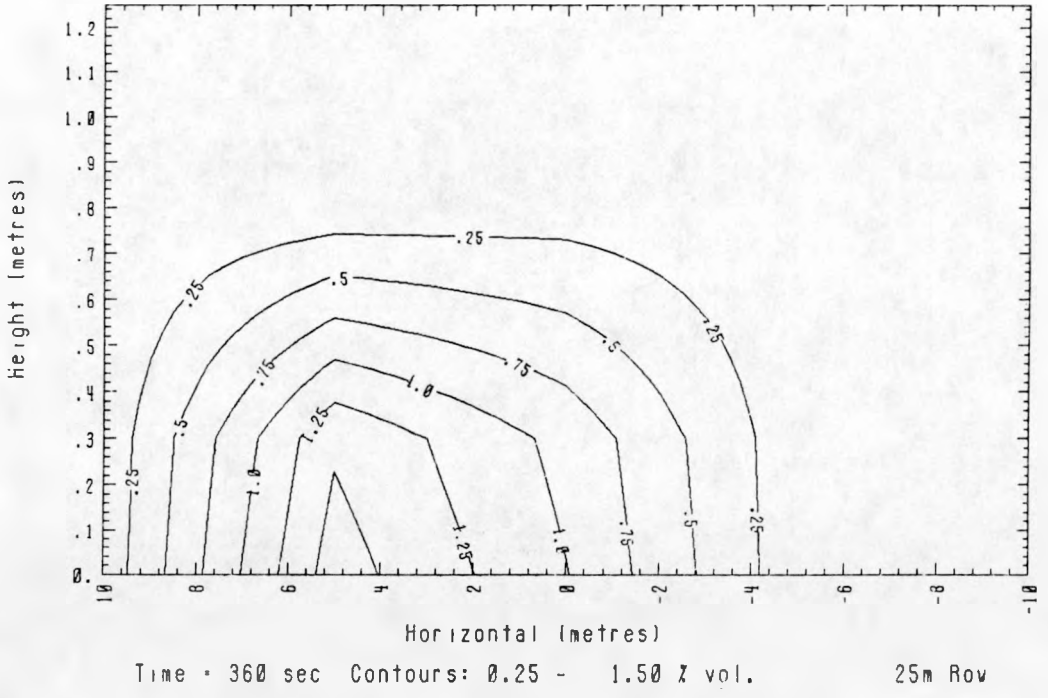

FIG. 58. EAG6 CROSSWIND CONCENTRATION CONTOURS @ 25m. (continued)

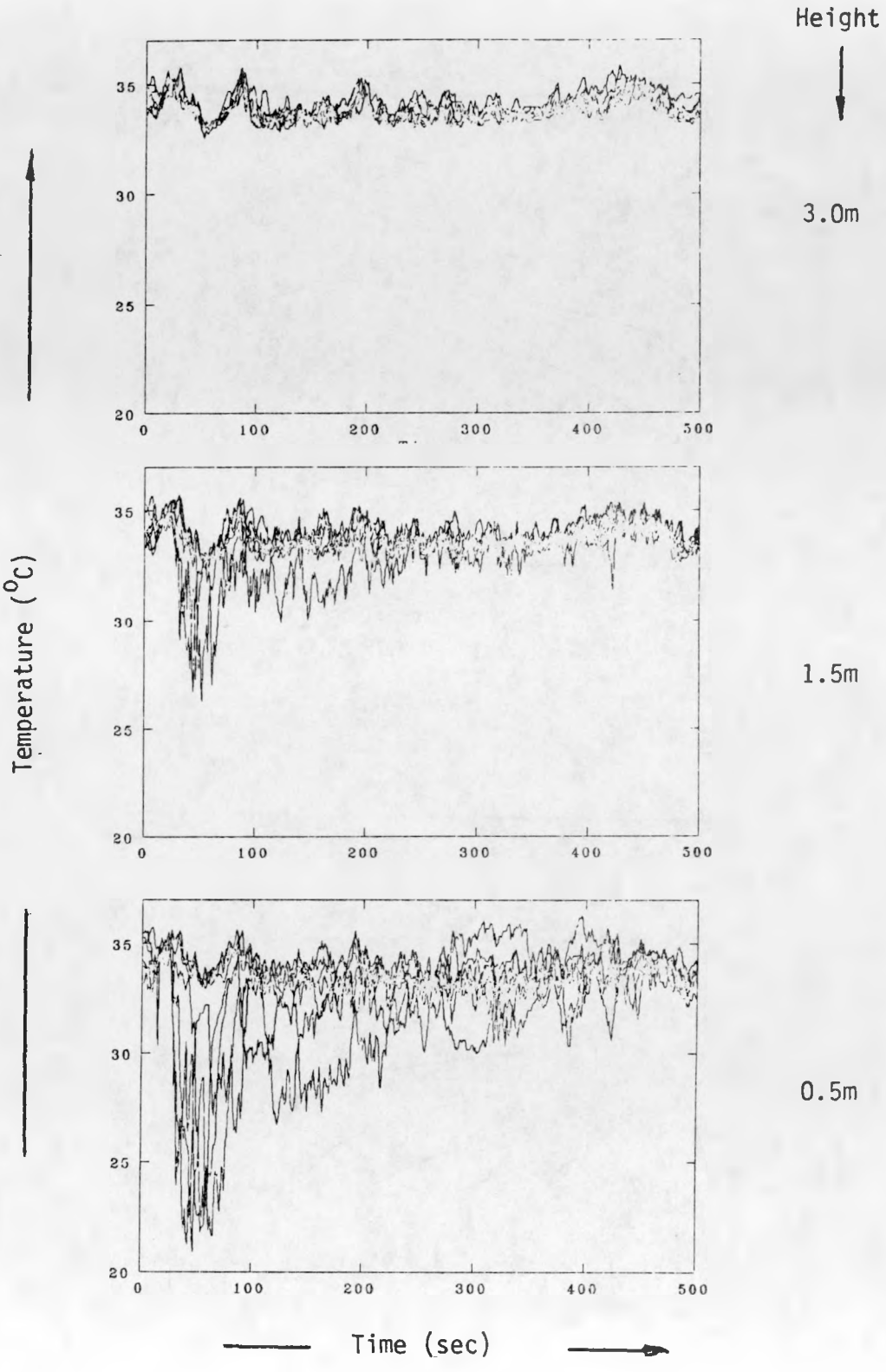

FIG. 59. EAG1 VAPOR CLOUD TEMPERATURE DATA @ 25m.

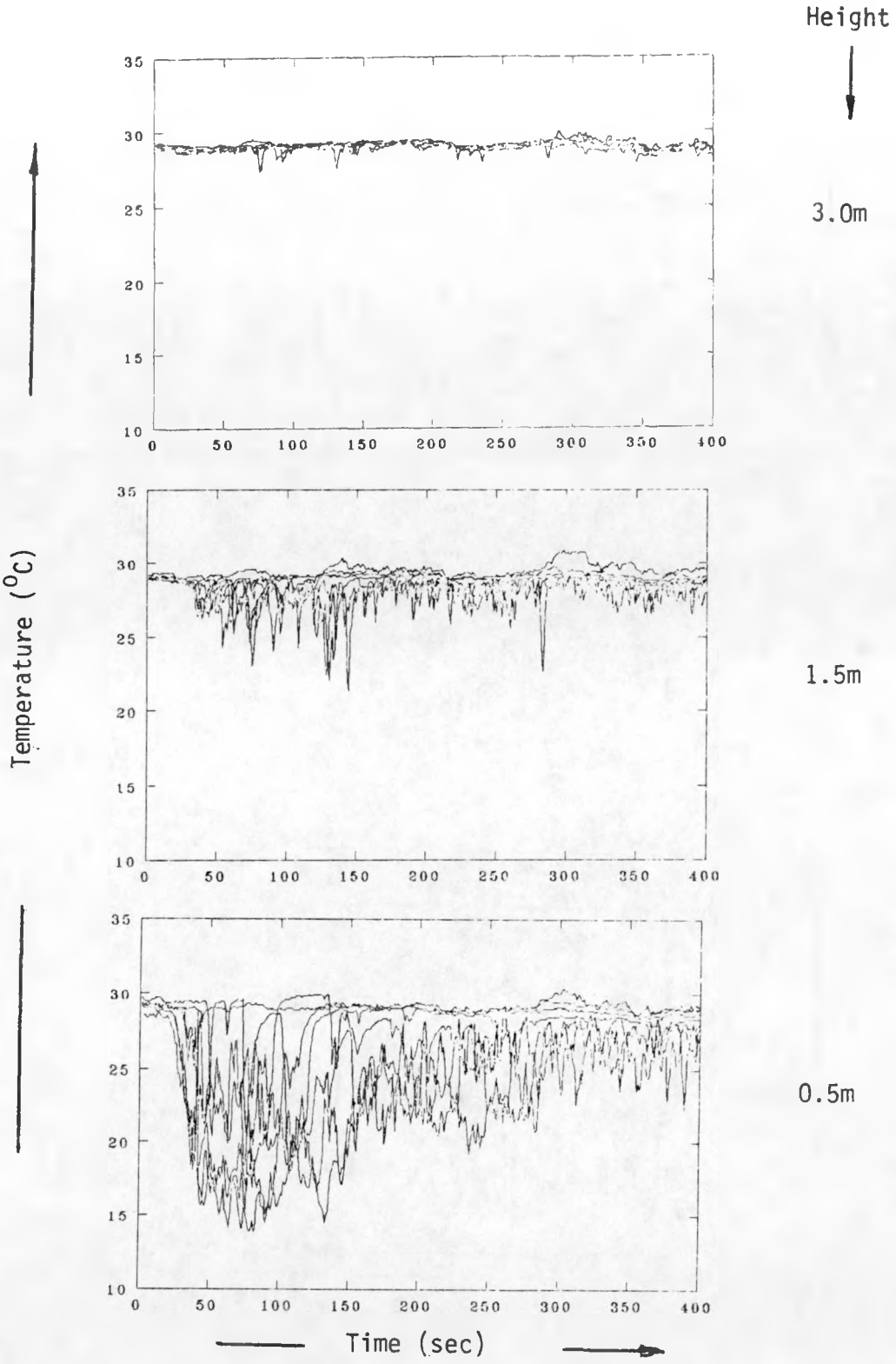

FIG. 60. EAG2 VAPOR CLOUD TEMPERATURE DATA @ 25m.

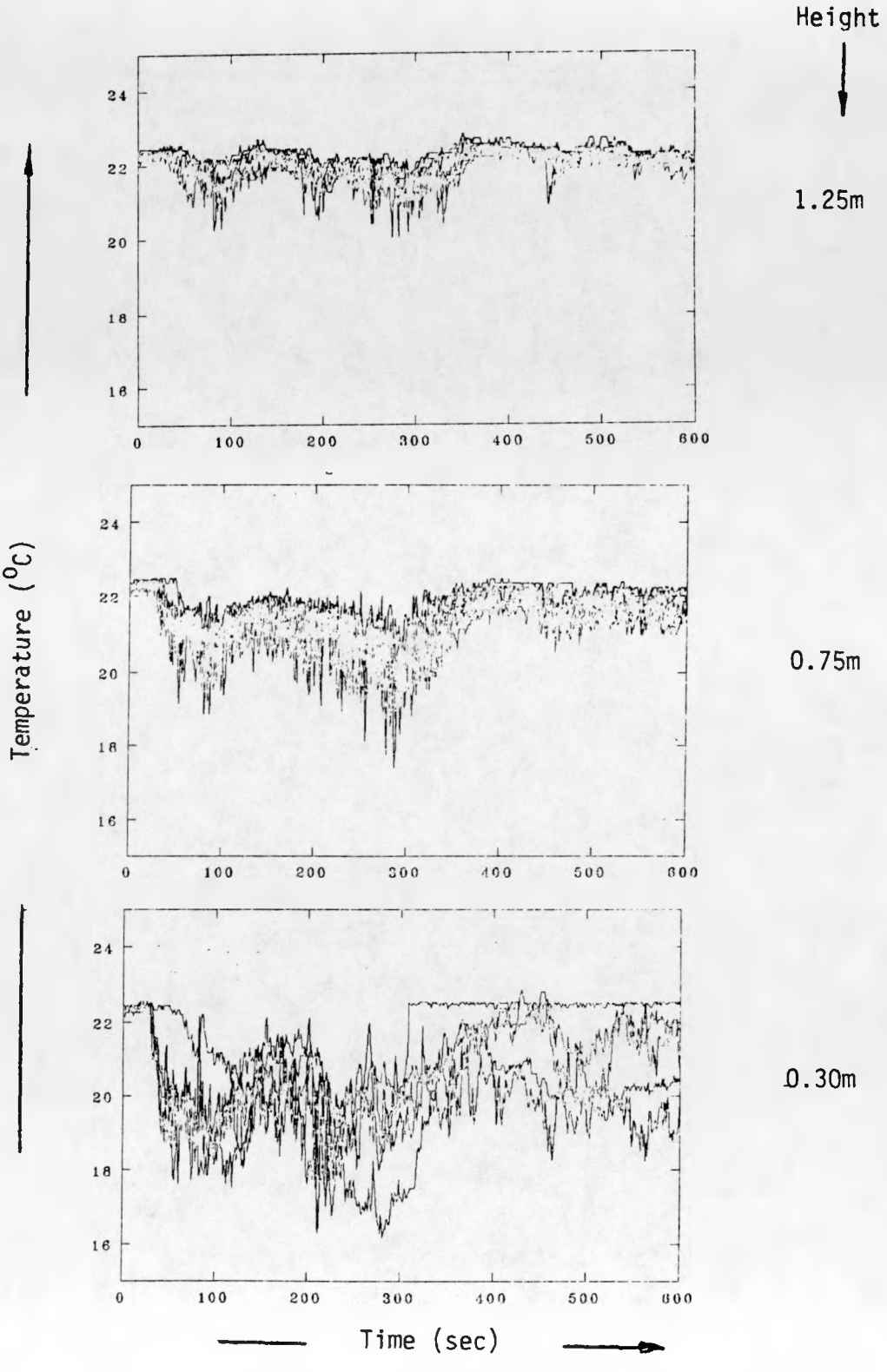

FIG. 61. EAG3 VAPOR CLOUD TEMPERATURE DATA @ 25m

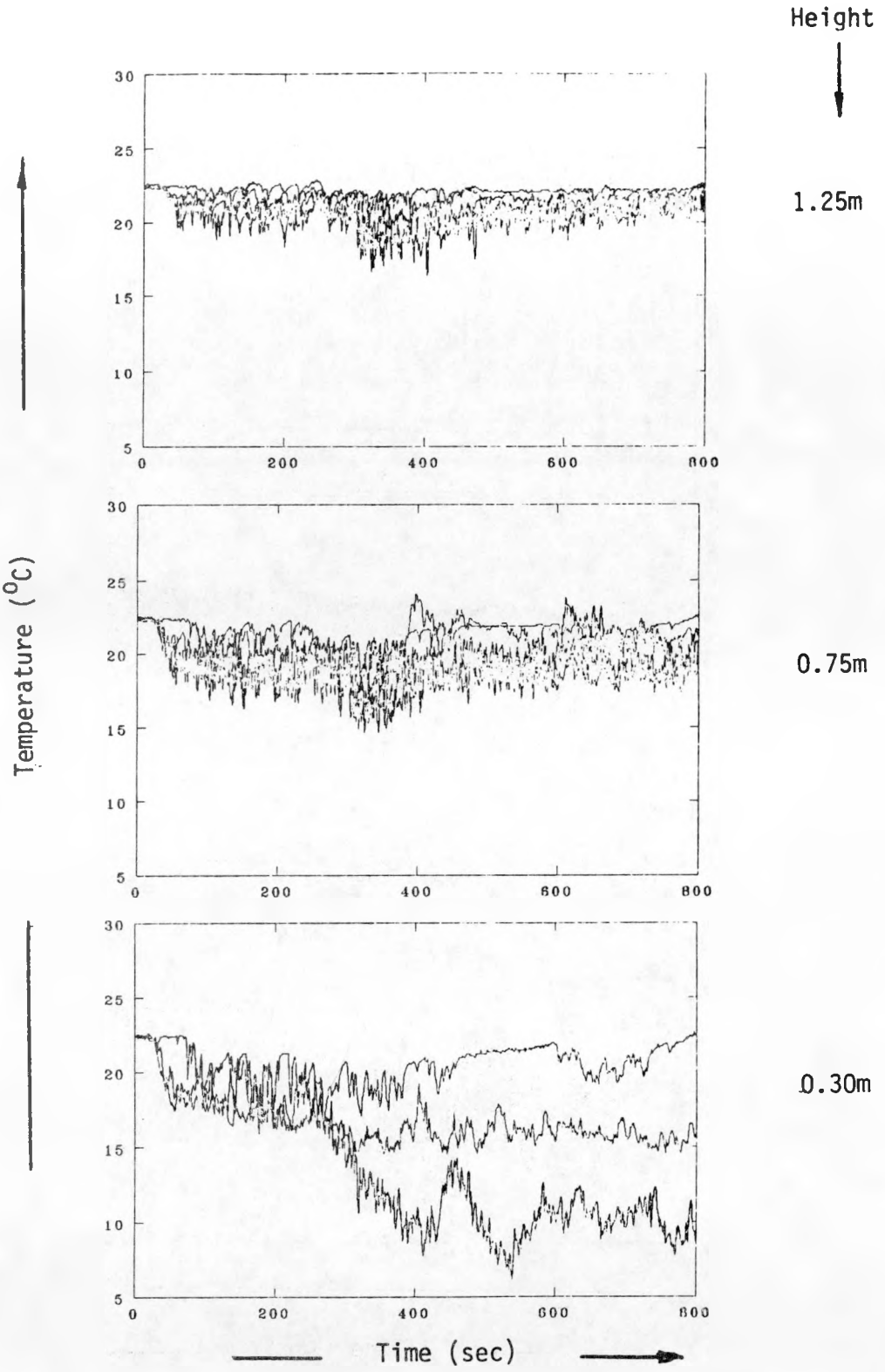

FIG. 62. EAG6 VAPOR CLOUD TEMPERATURE DATA @ 25m

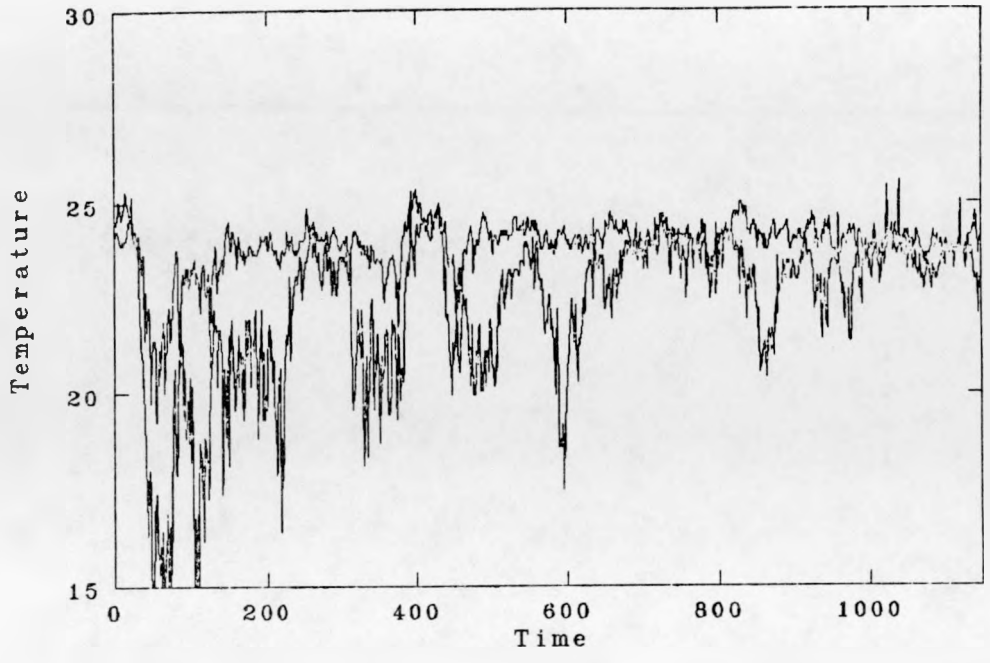

FIG. 63. EAG4 VAPOR TEMPERATURE @ 15m.

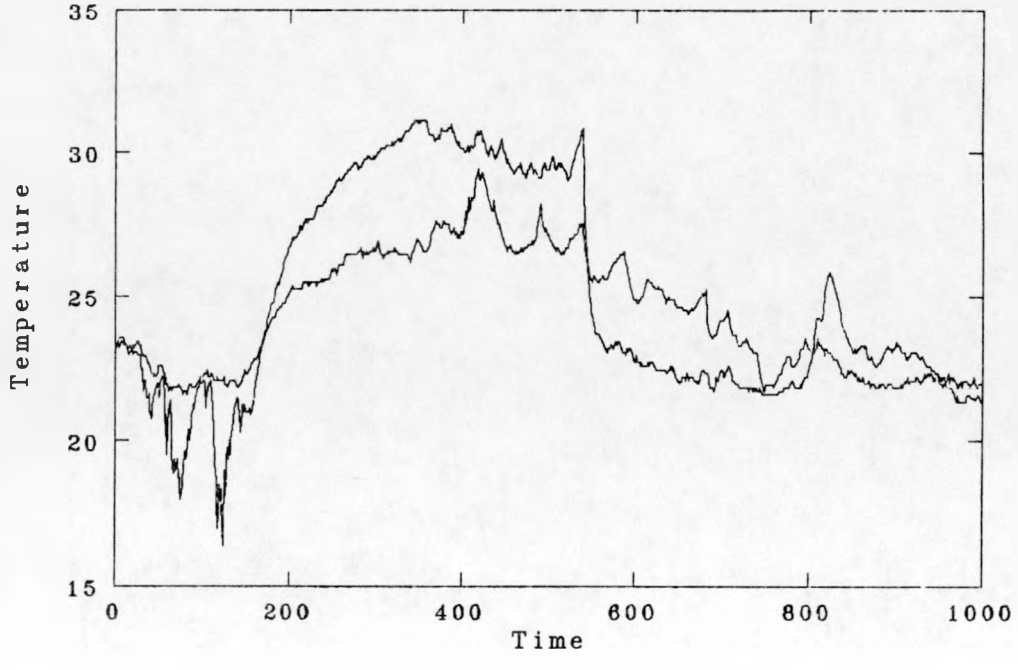

FIG. 64. EAG5 VAPOR TEMPERATURE @ 15m.

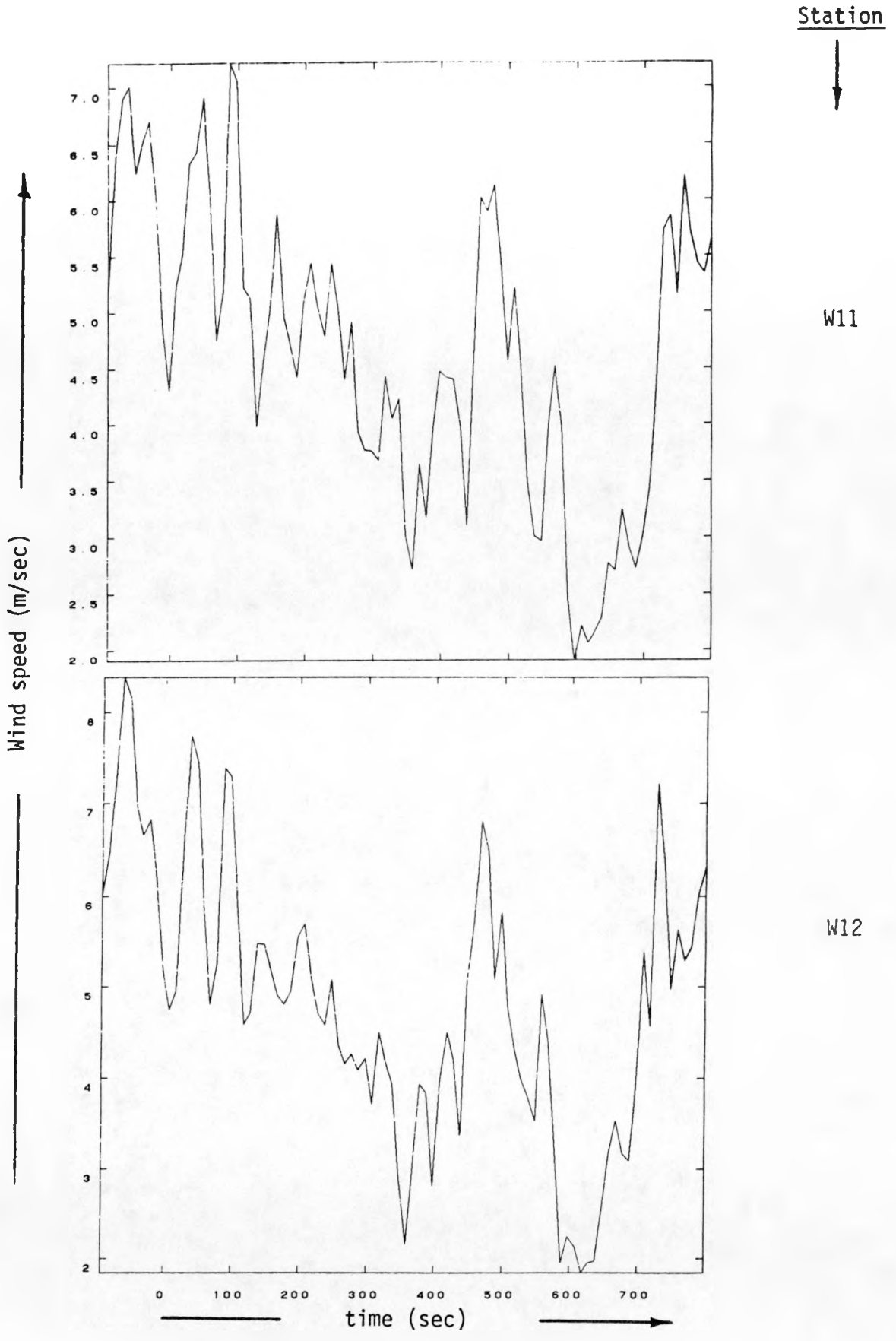

FIG. 65. EAG1 WIND SPEED DATA @ 25 m

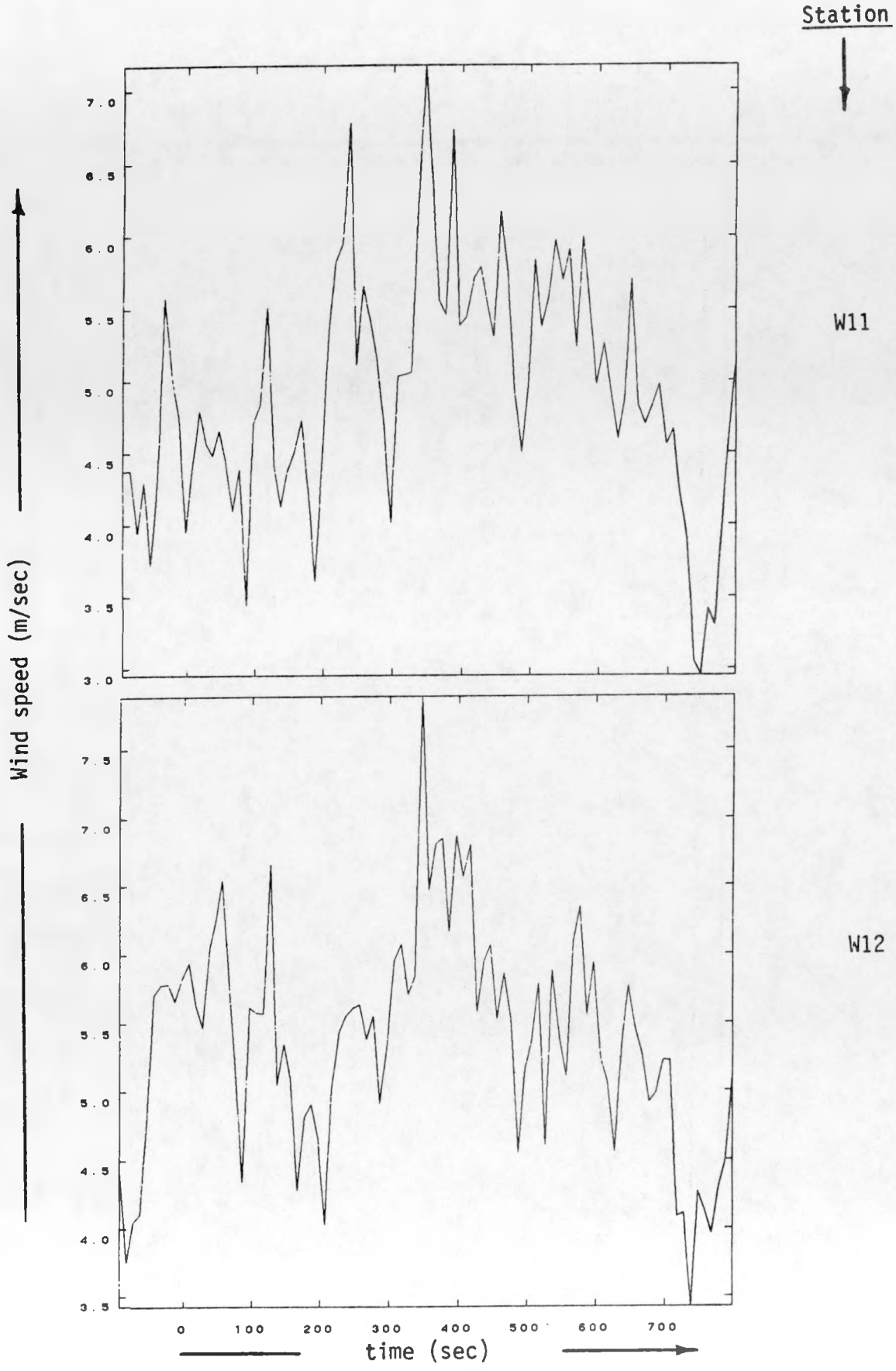

FIG. 66. EAG2 WIND SPEED DATA @ 25 m

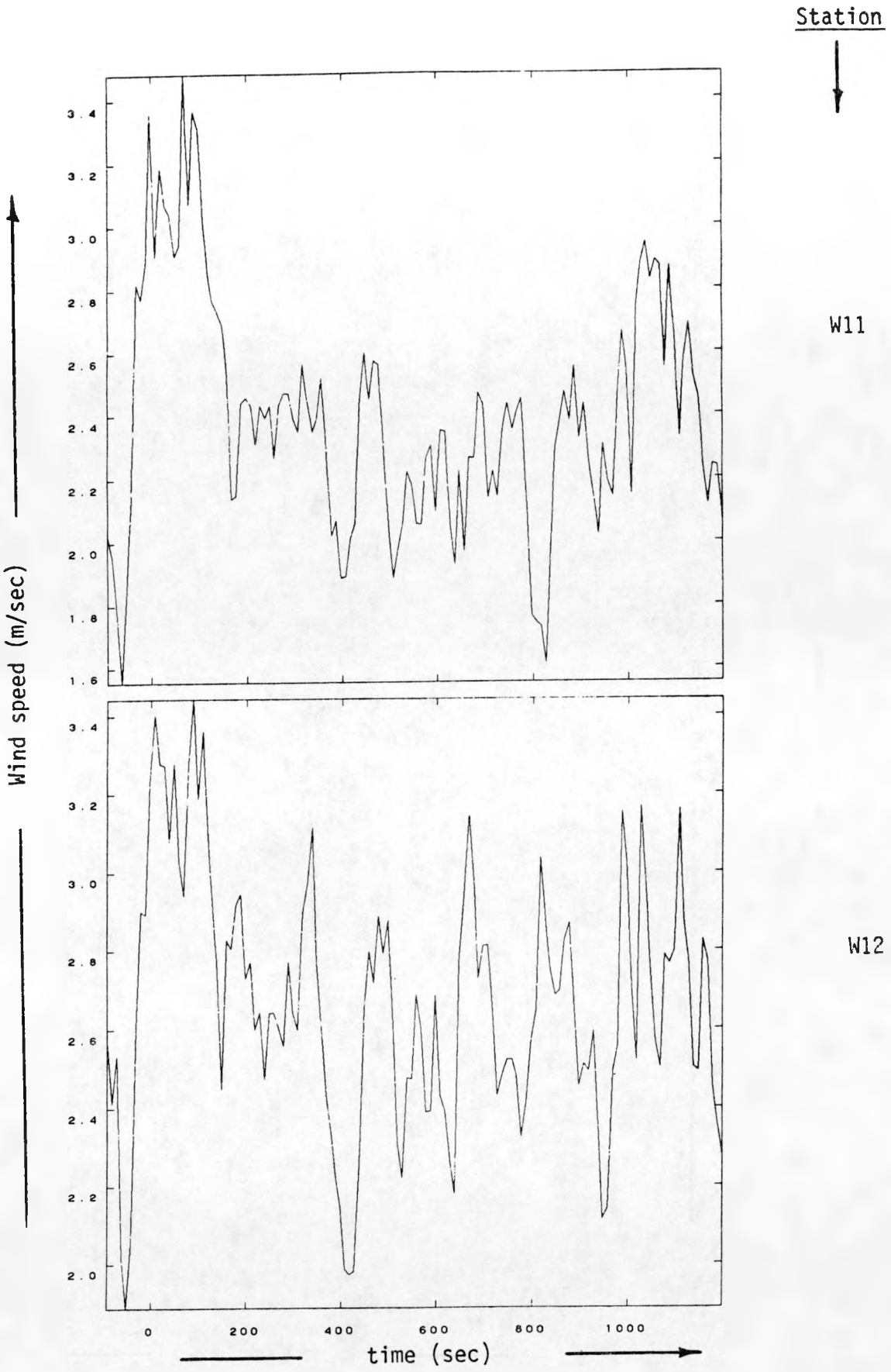

FIG. 67. EAG3 WIND SPEED DATA @ 25 m

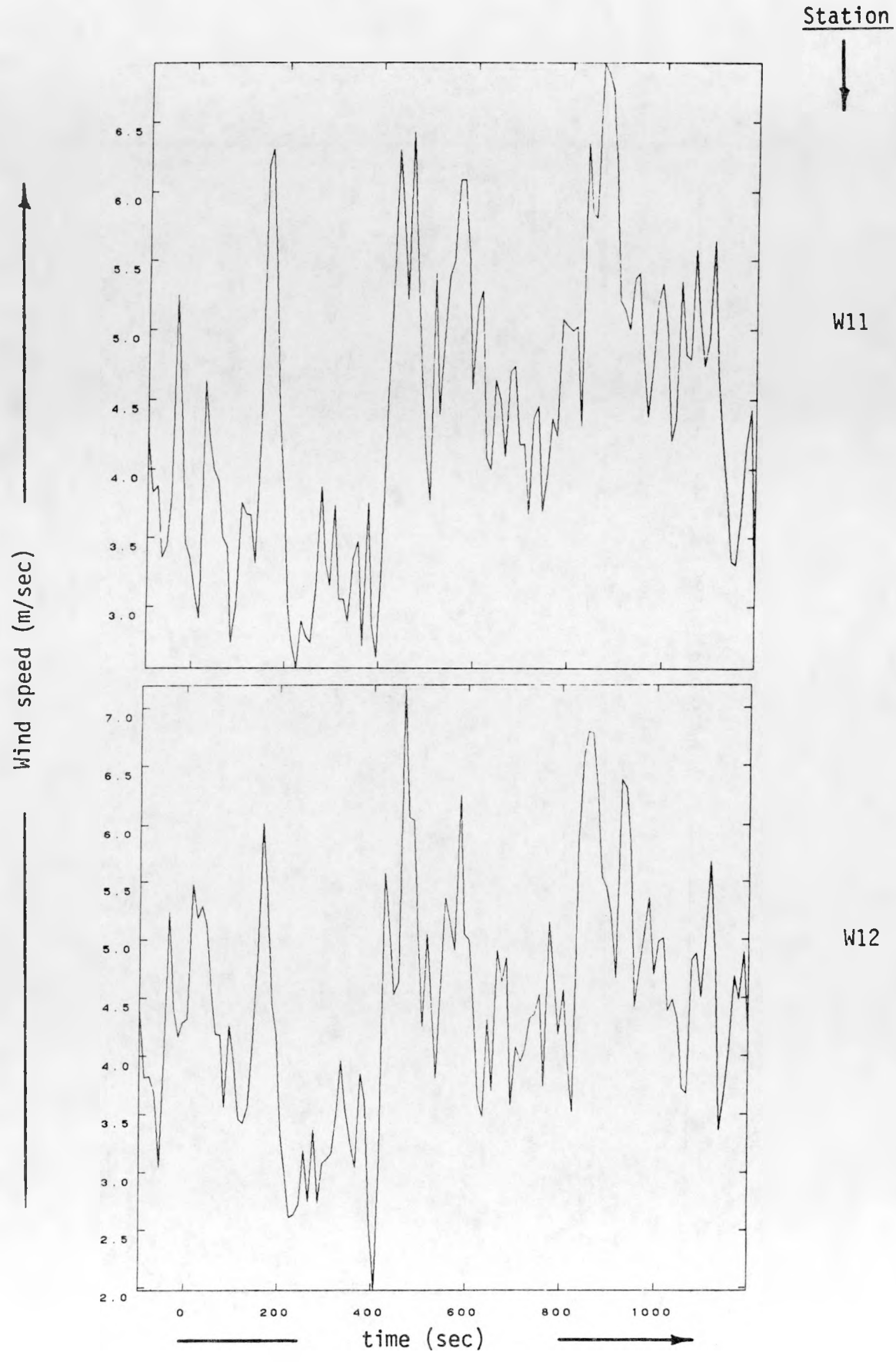

FIG. 68. EAG4 WIND SPEED DATA @ 25 m

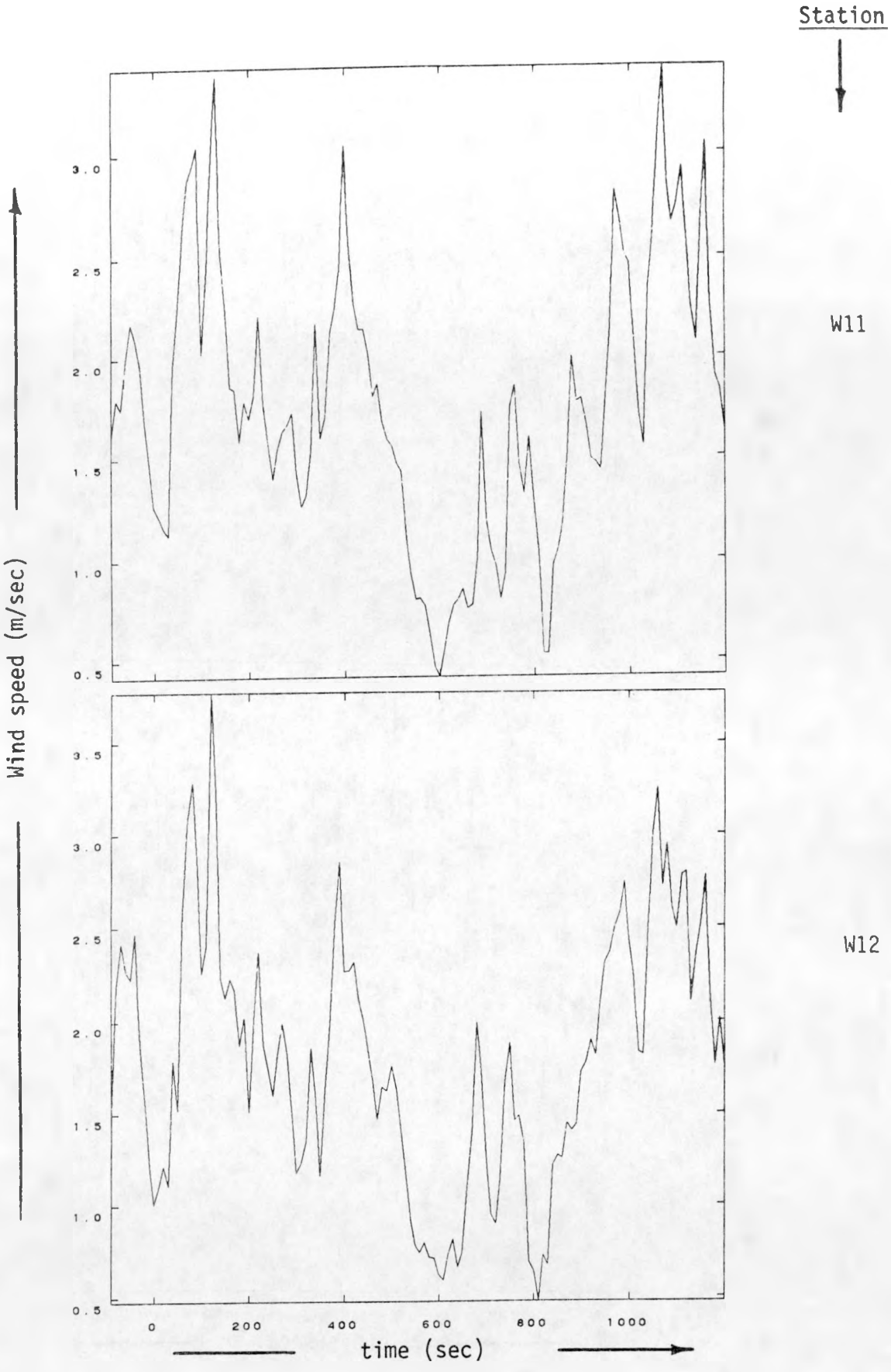

FIG. 69. EAG5 WIND SPEED DATA @ 25 m

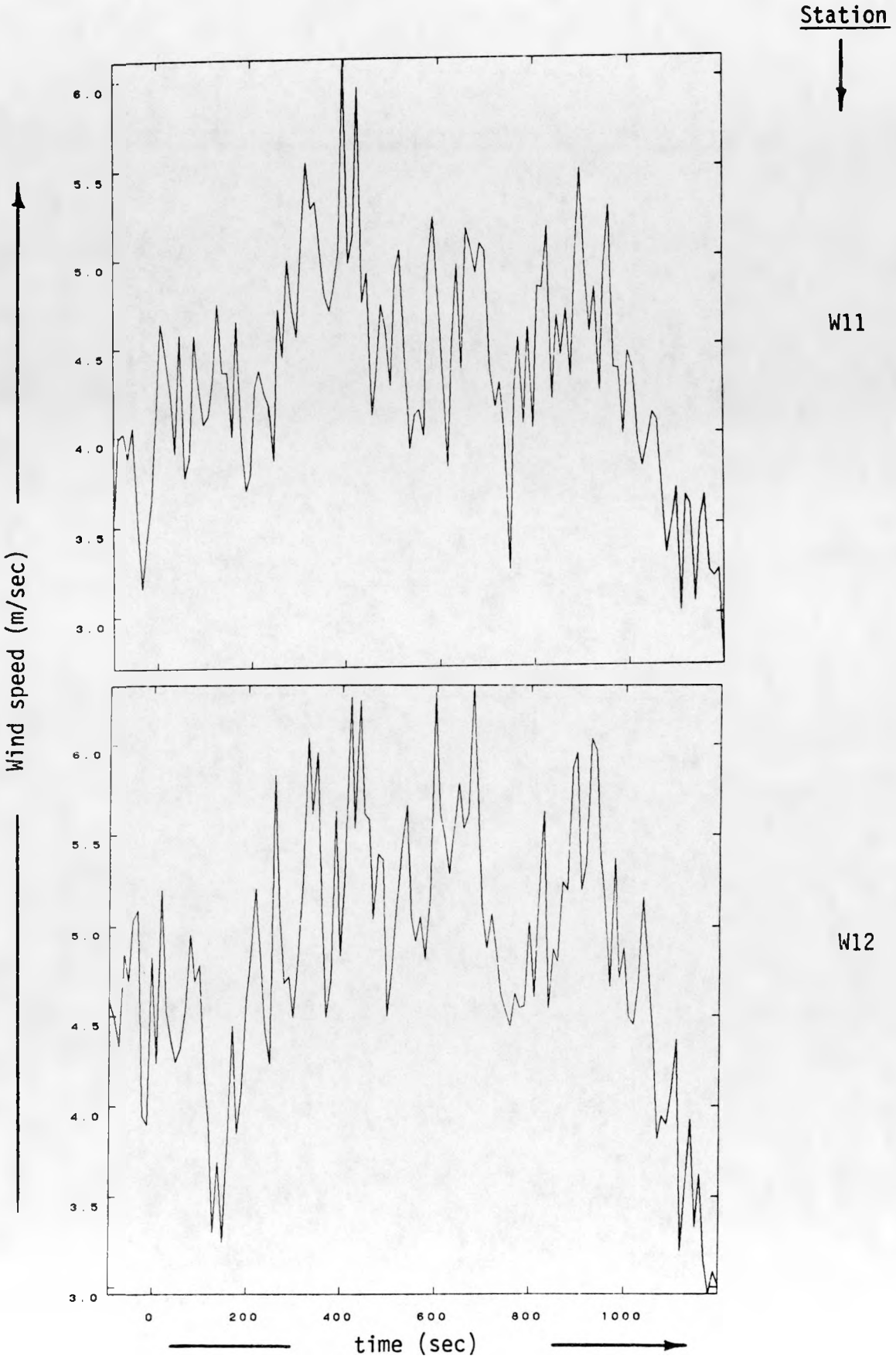

FIG. 70. EAG6 WIND SPEED DATA @ 25 m

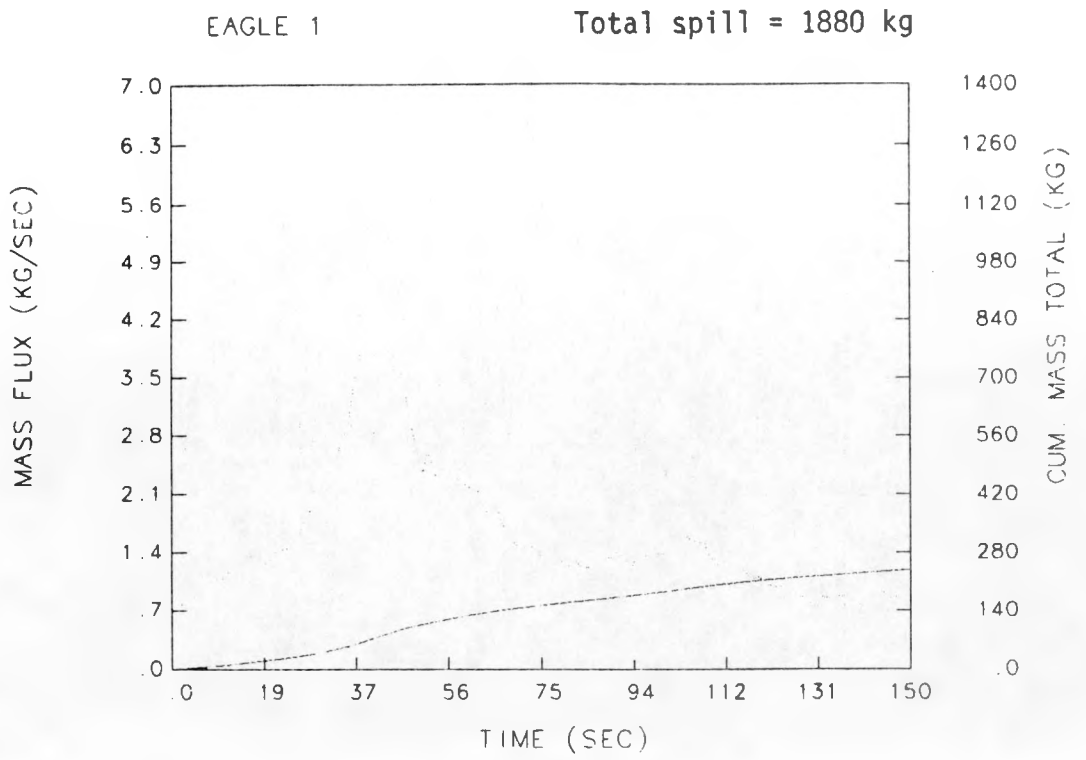

FIG. 71. EAG1 Vapor Flux Results

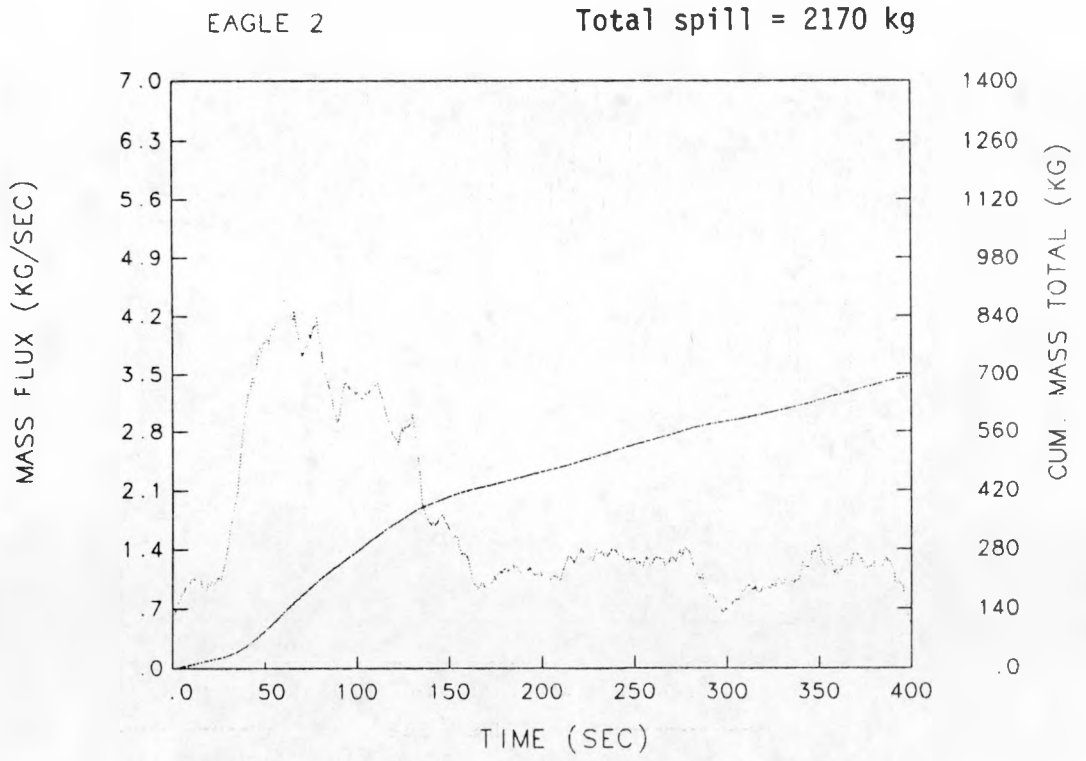

FIG. 72. EAG2 Vapor Flux Results

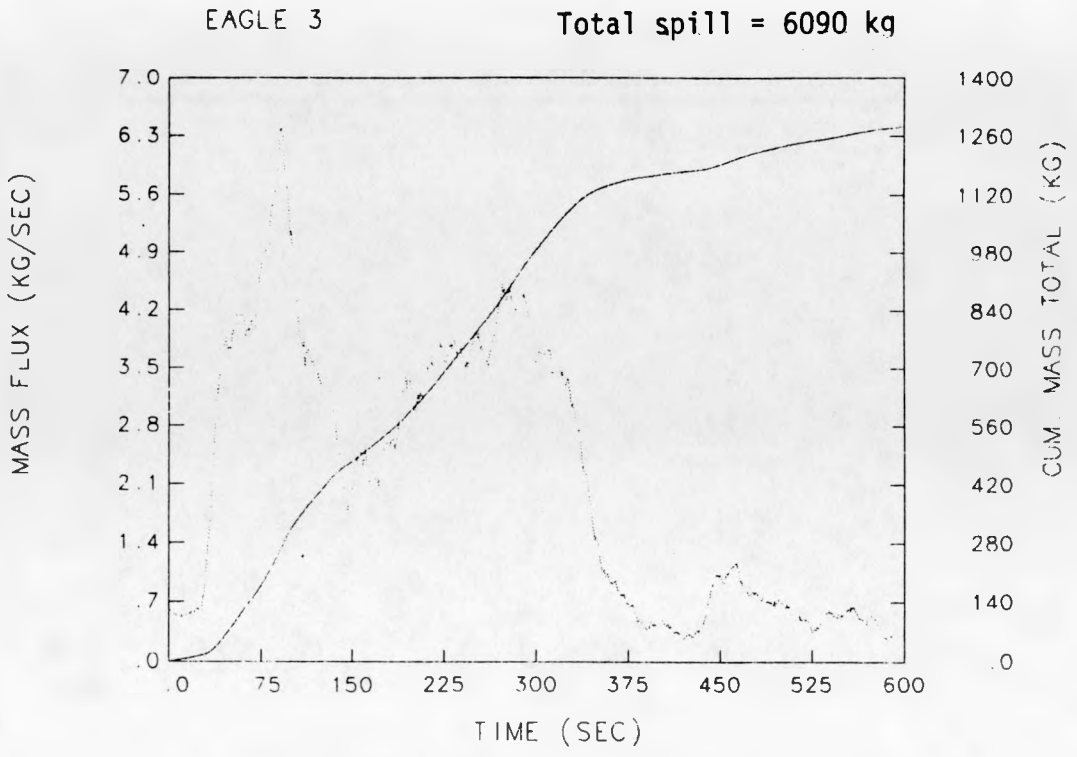

FIG. 73. EAG3 Vapor Flux Results

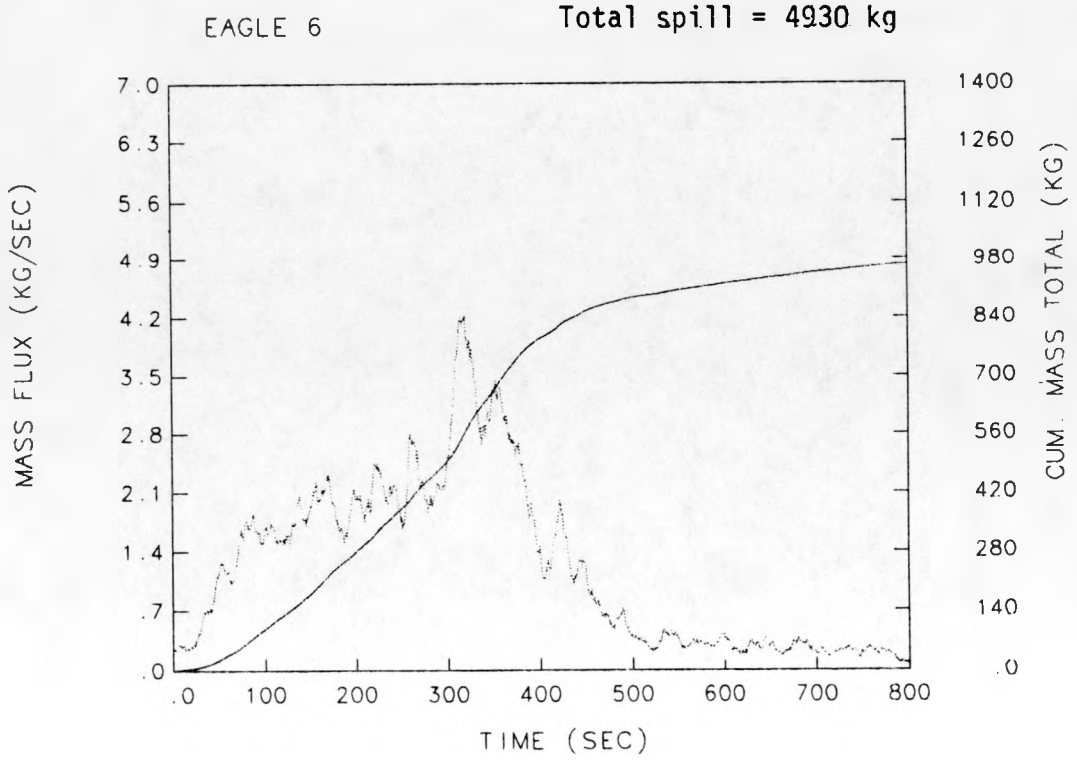

FIG. 74. EAG6 Vapor Flux Results

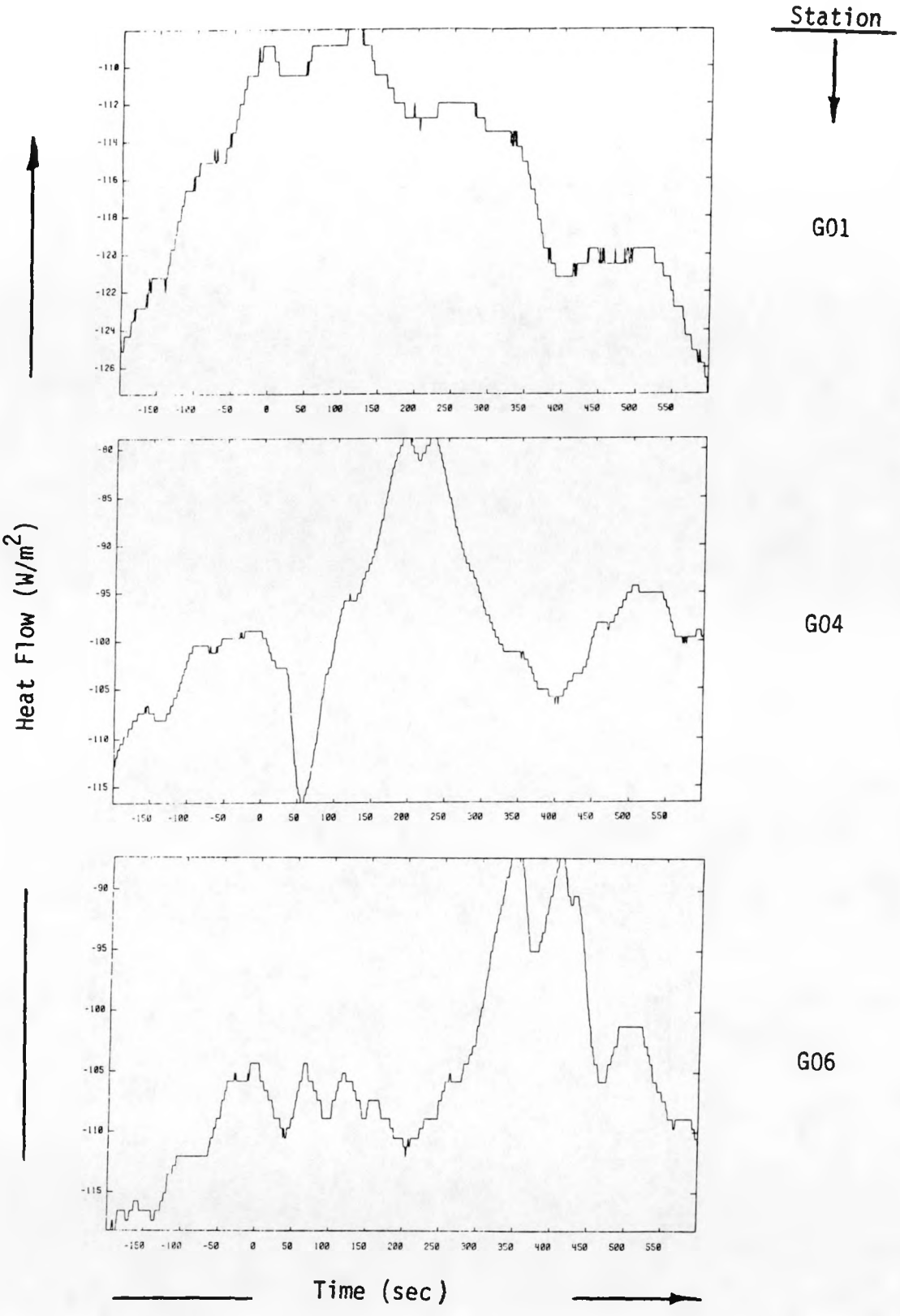

FIG. 75. EAG1 VAPOR CLOUD HEAT FLOW DATA @ 25m.

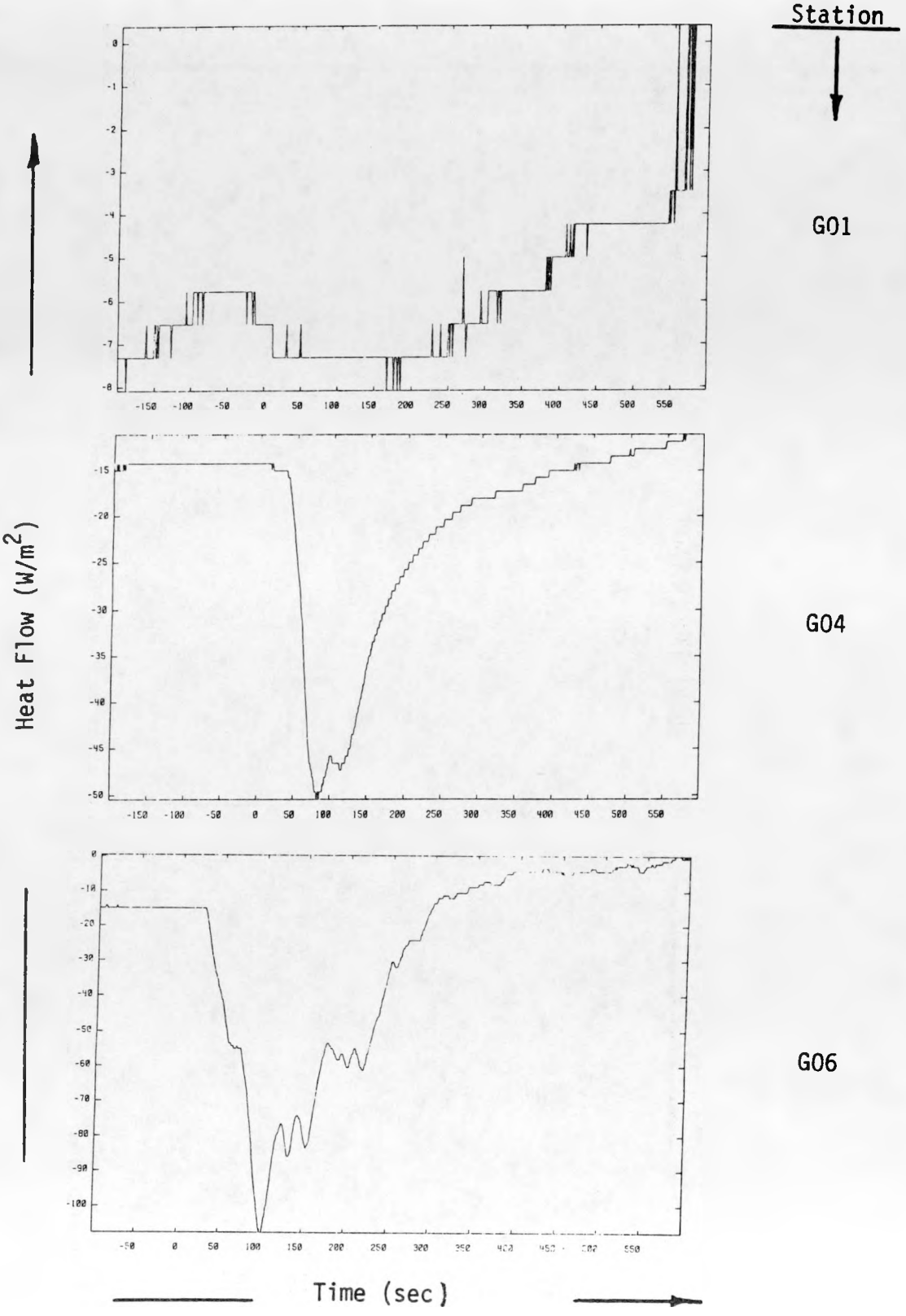

FIG. 76. EAG2 VAPOR CLOUD HEAT FLOW DATA @ 25m.

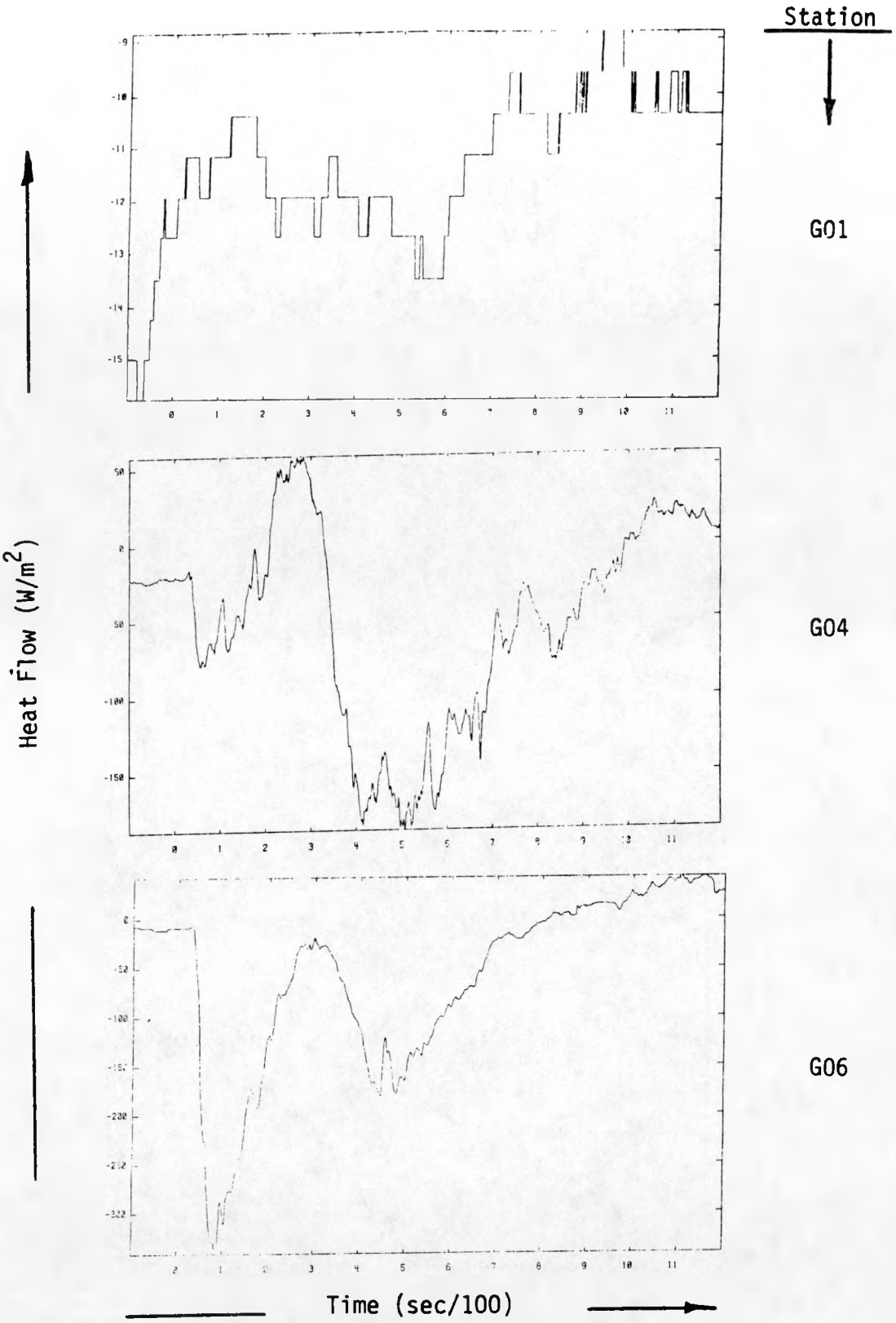

FIG. 77. EAG3 VAPOR CLOUD HEAT FLOW DATA @ 25m.

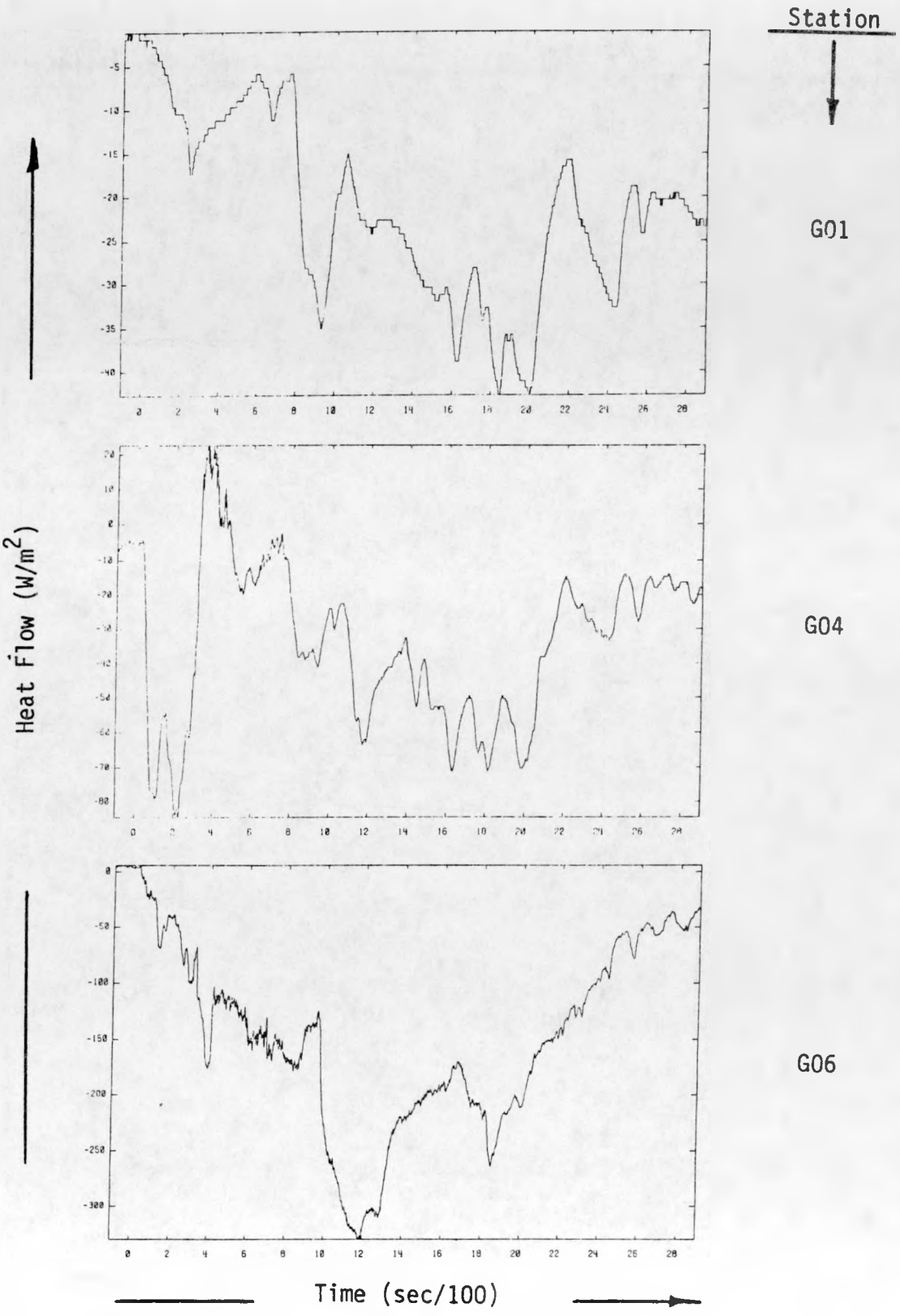

FIG. 78. EAG6 VAPOR CLOUD HEAT FLOW DATA @ 25m.

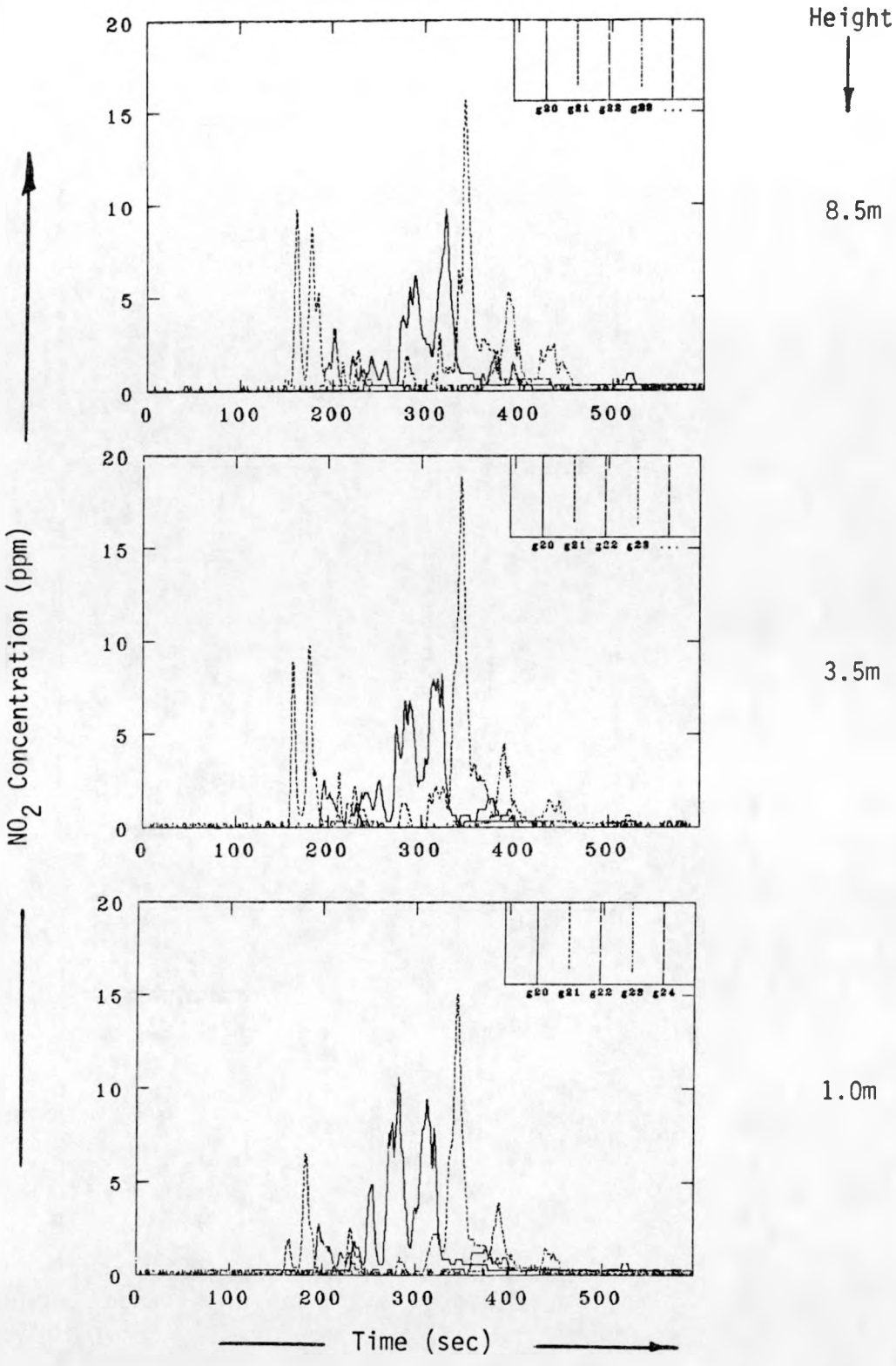

FIG. 79. EAG1 NO_2 CONCENTRATION DATA @ 785.

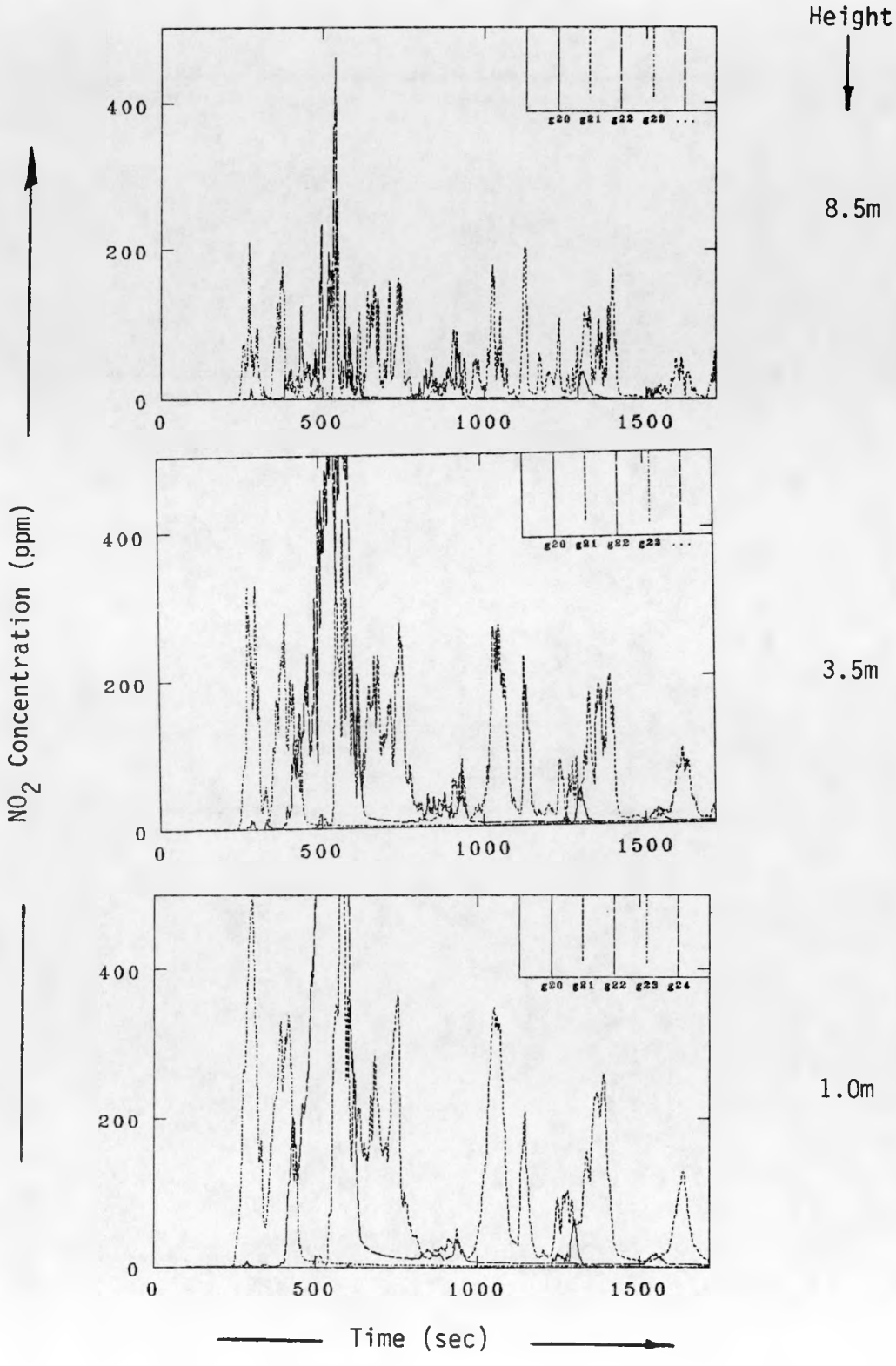

FIG. 80. EAG3 NO_2 CONCENTRATION DATA @ 785.

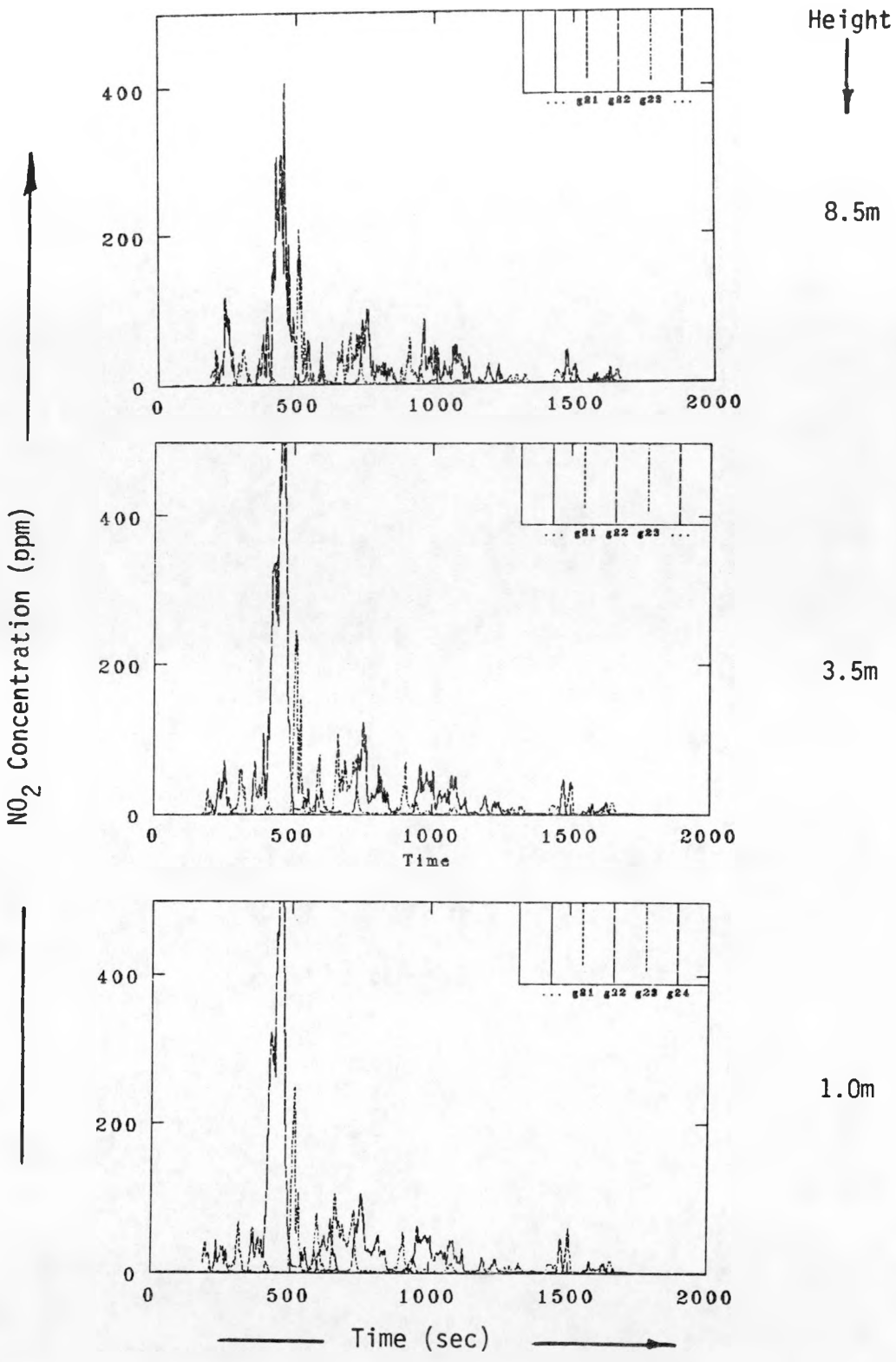

FIG. 81. EAG6 NO_2 CONCENTRATION DATA @ 785.

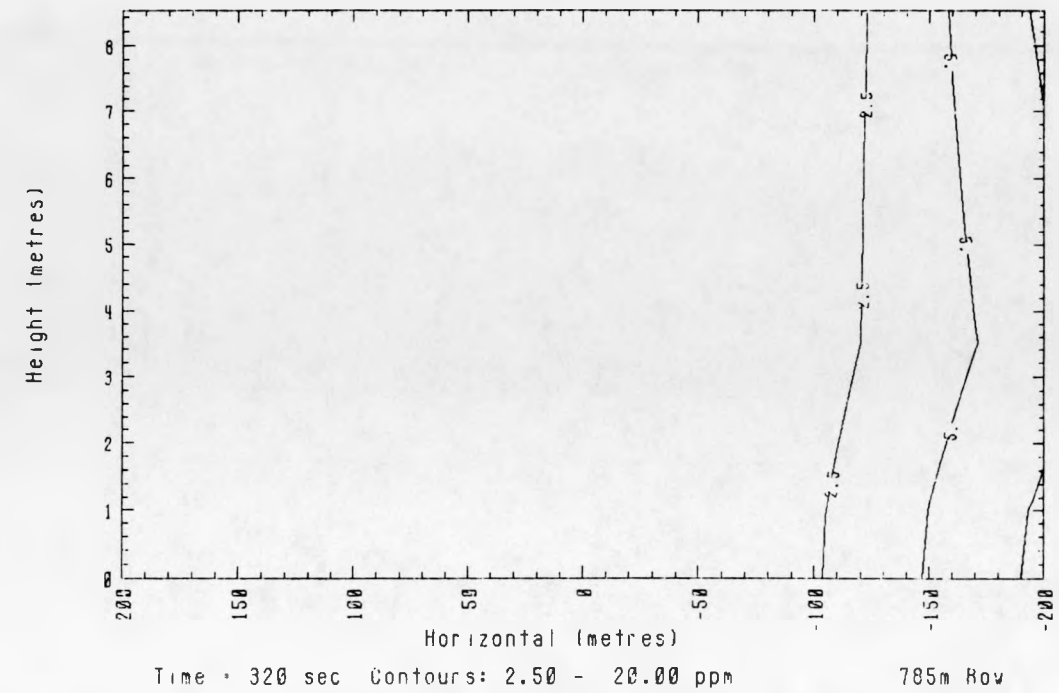

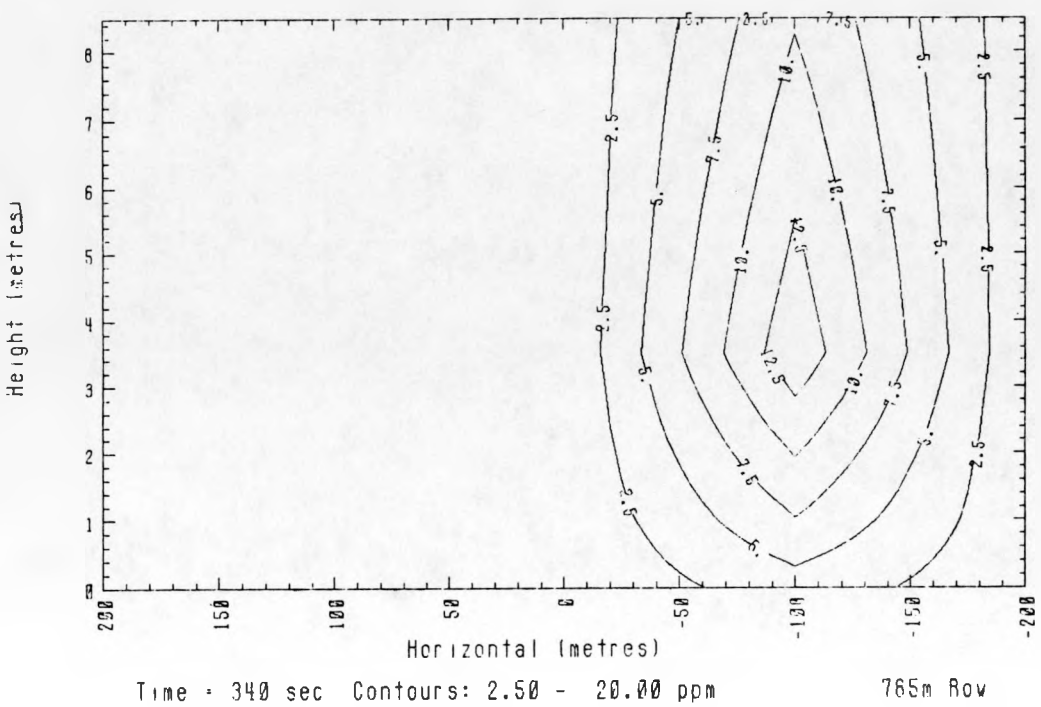

FIG. 82. EAG1 CROSSWIND CONCENTRATION CONTOURS @ 785m

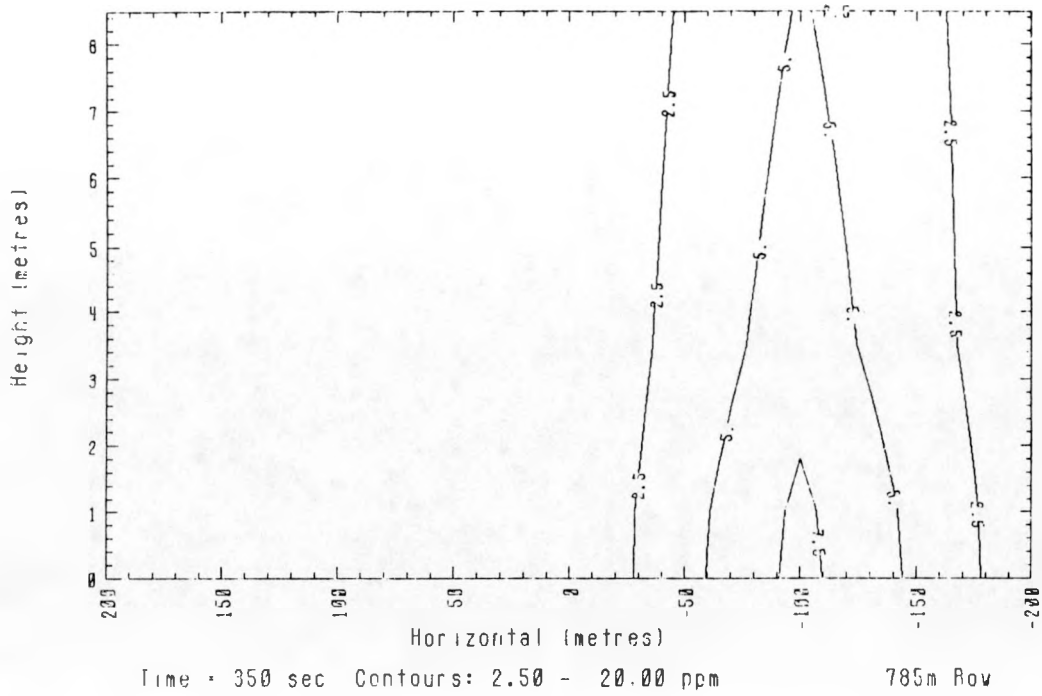

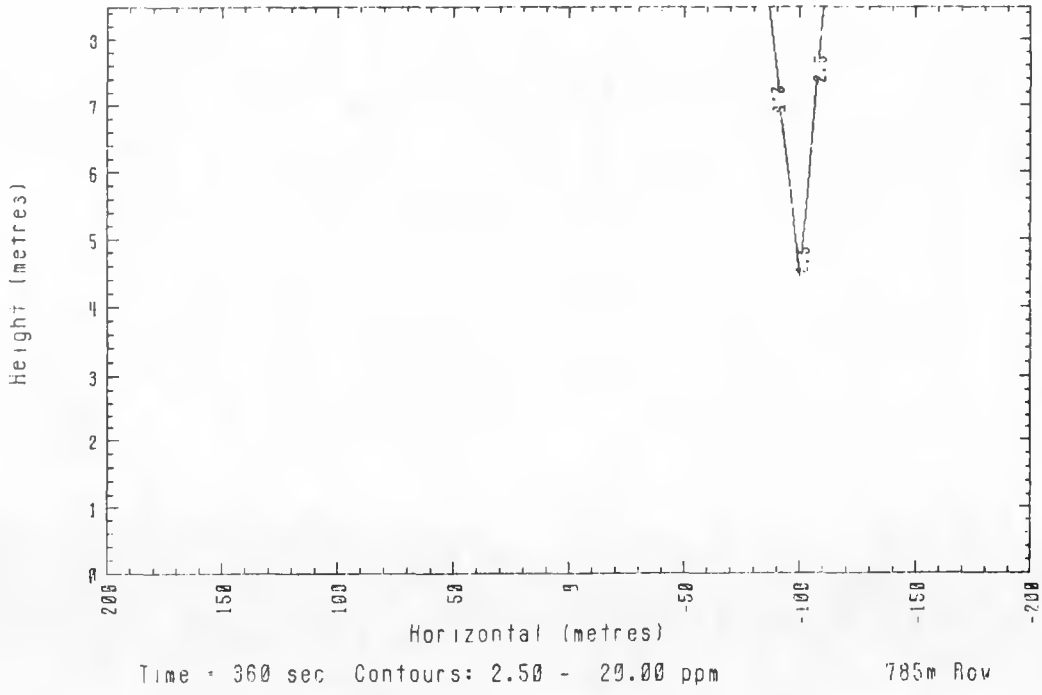

FIG. 82. EAG1 CROSSWIND CONCENTRATION CONTOURS @ 785m (continued)

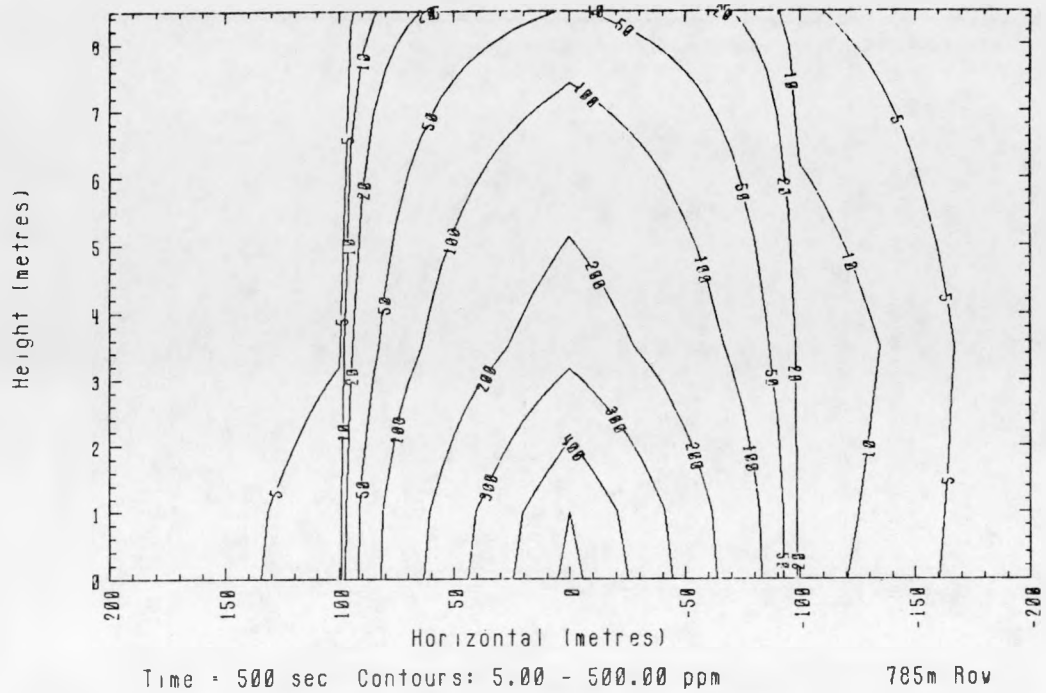

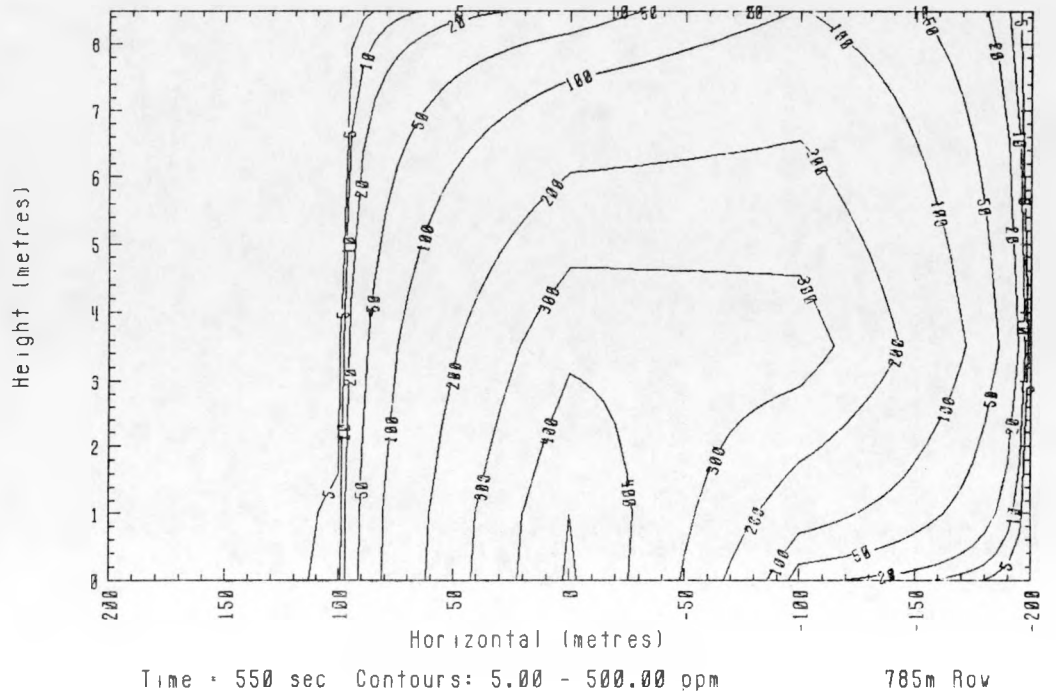

FIG. 83. EAG3 CROSSWIND CONCENTRATION CONTOURS @ 785m

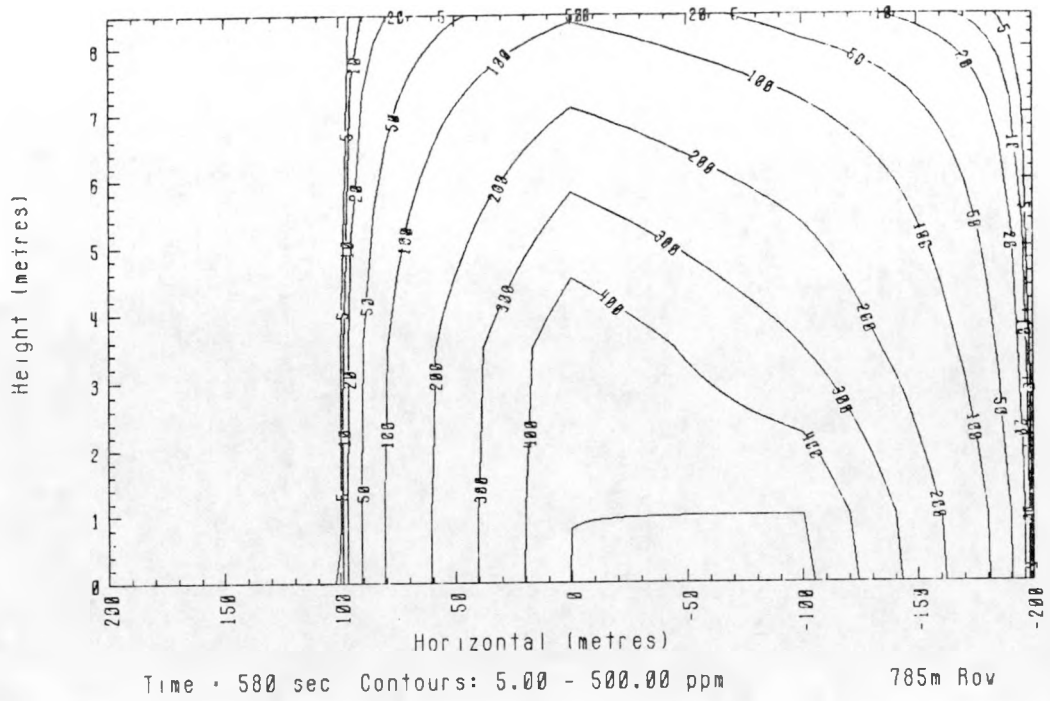

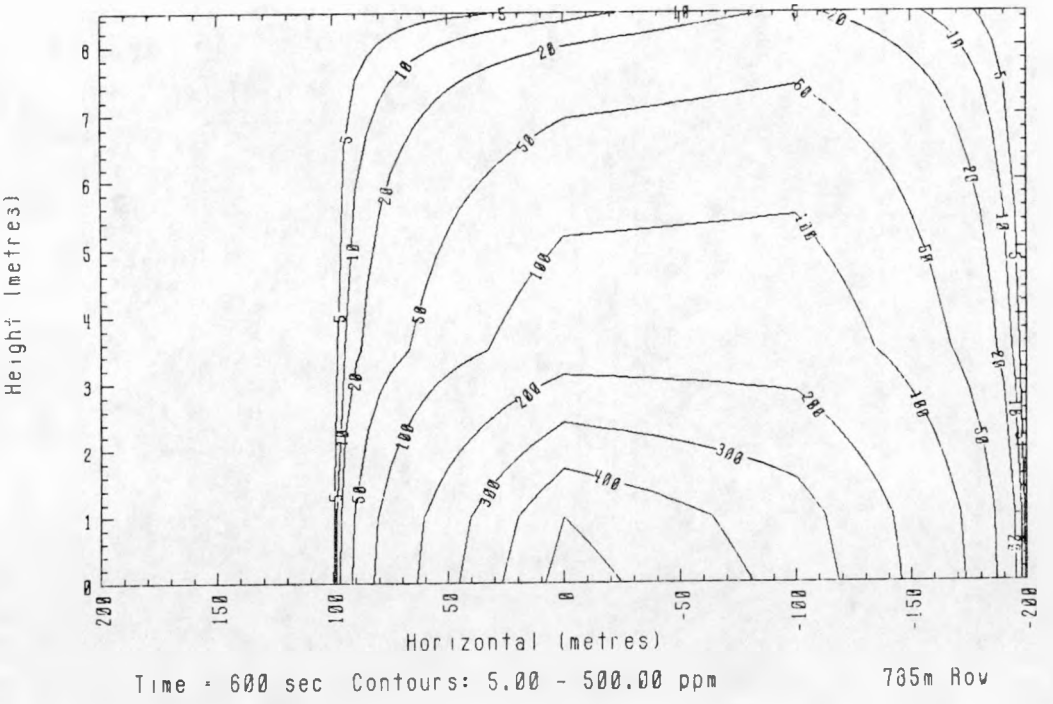

FIG. 83. EAG3 CROSSWIND CONCENTRATION CONTOURS @ 785m (continued)

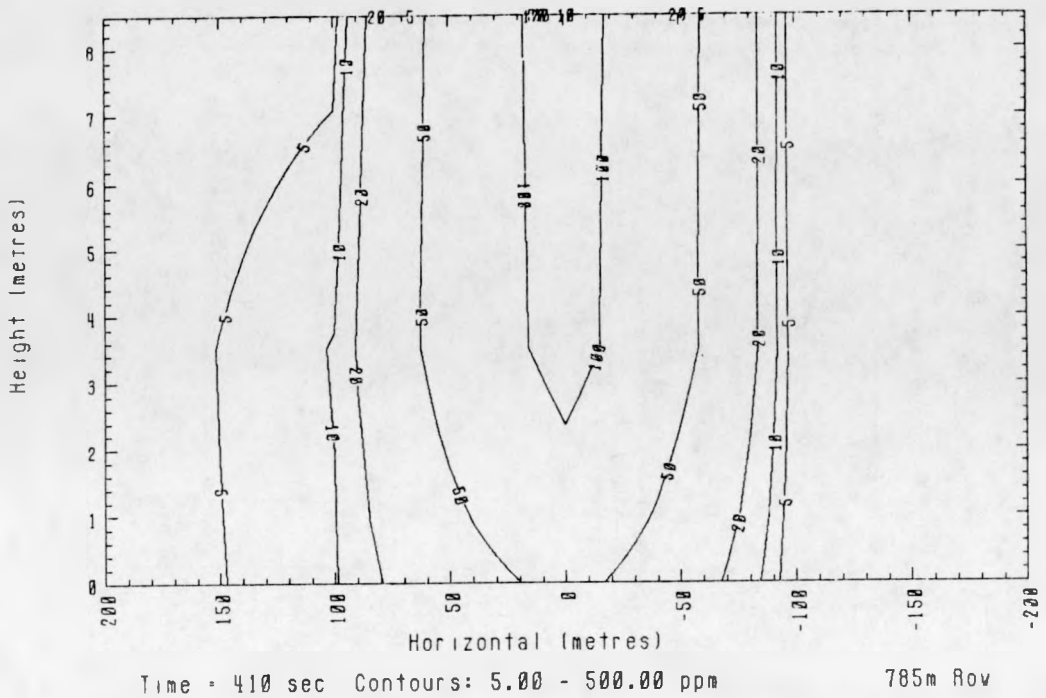

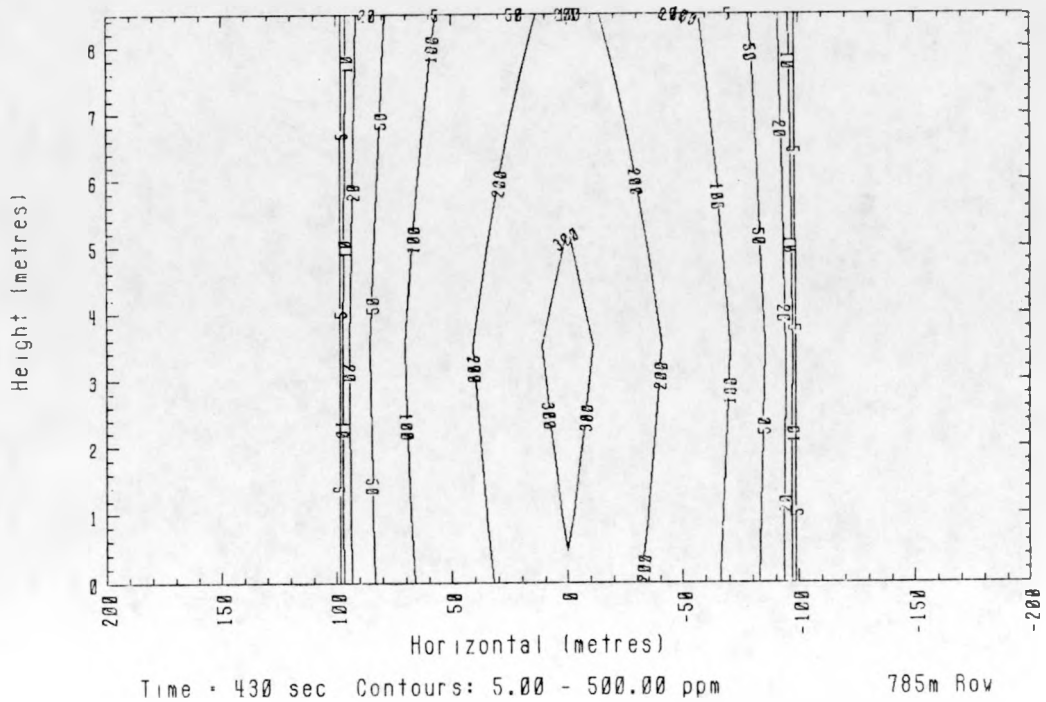

FIG. 84. EAG6 CROSSWIND CONCENTRATION CONTOURS @ 785m

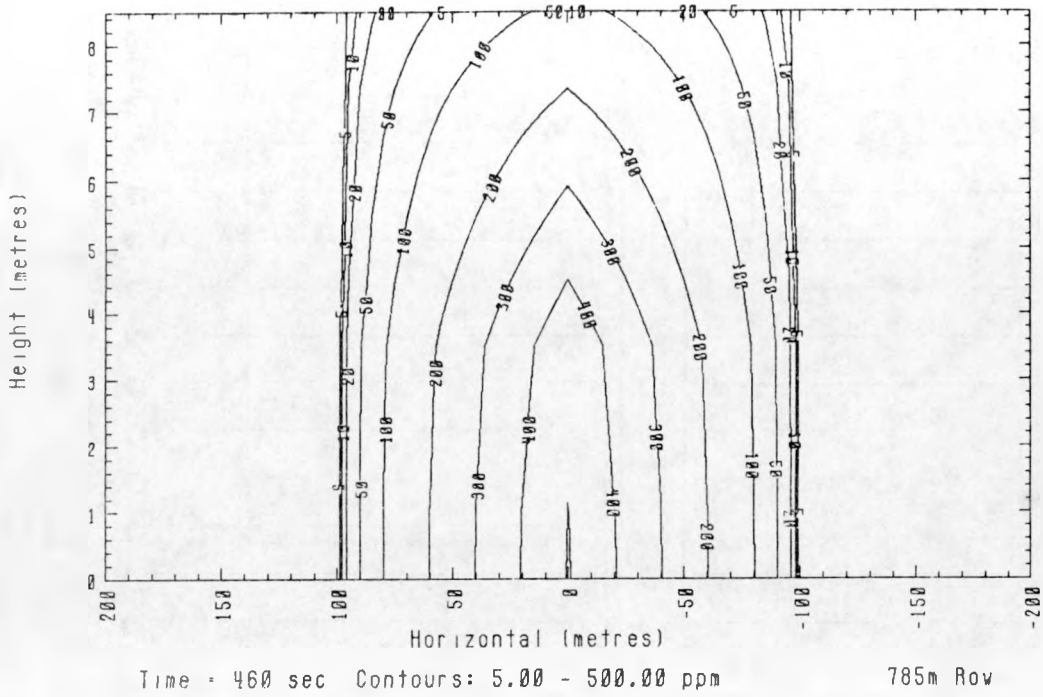

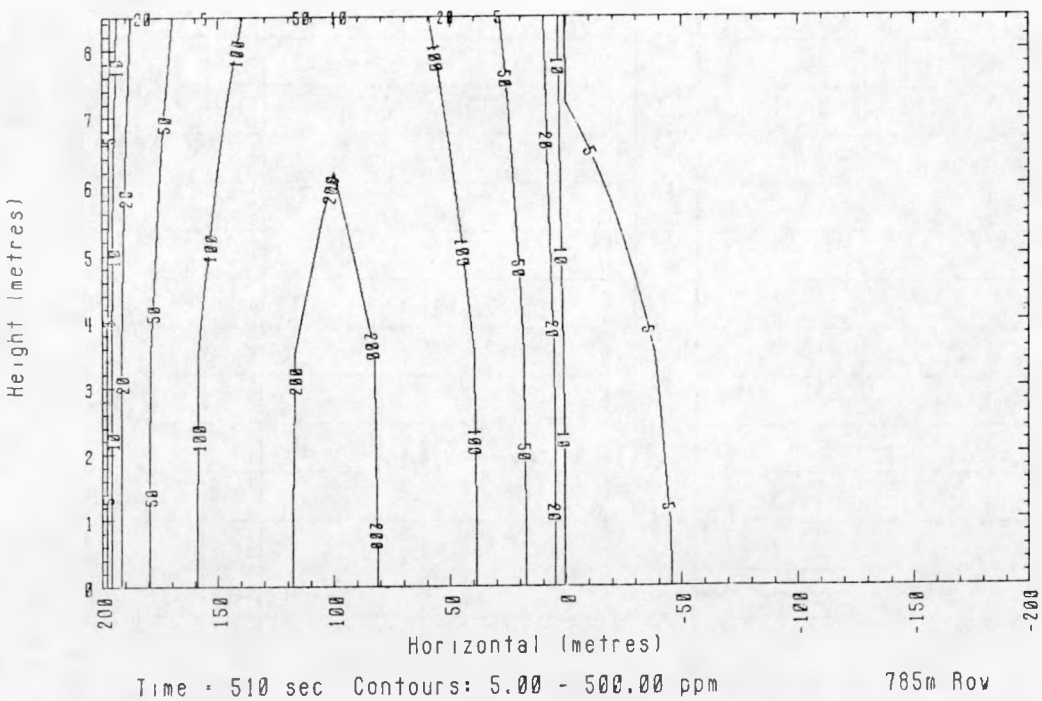

FIG. 84. EAG6 CROSSWIND CONCENTRATION CONTOURS @ 785m (continued)

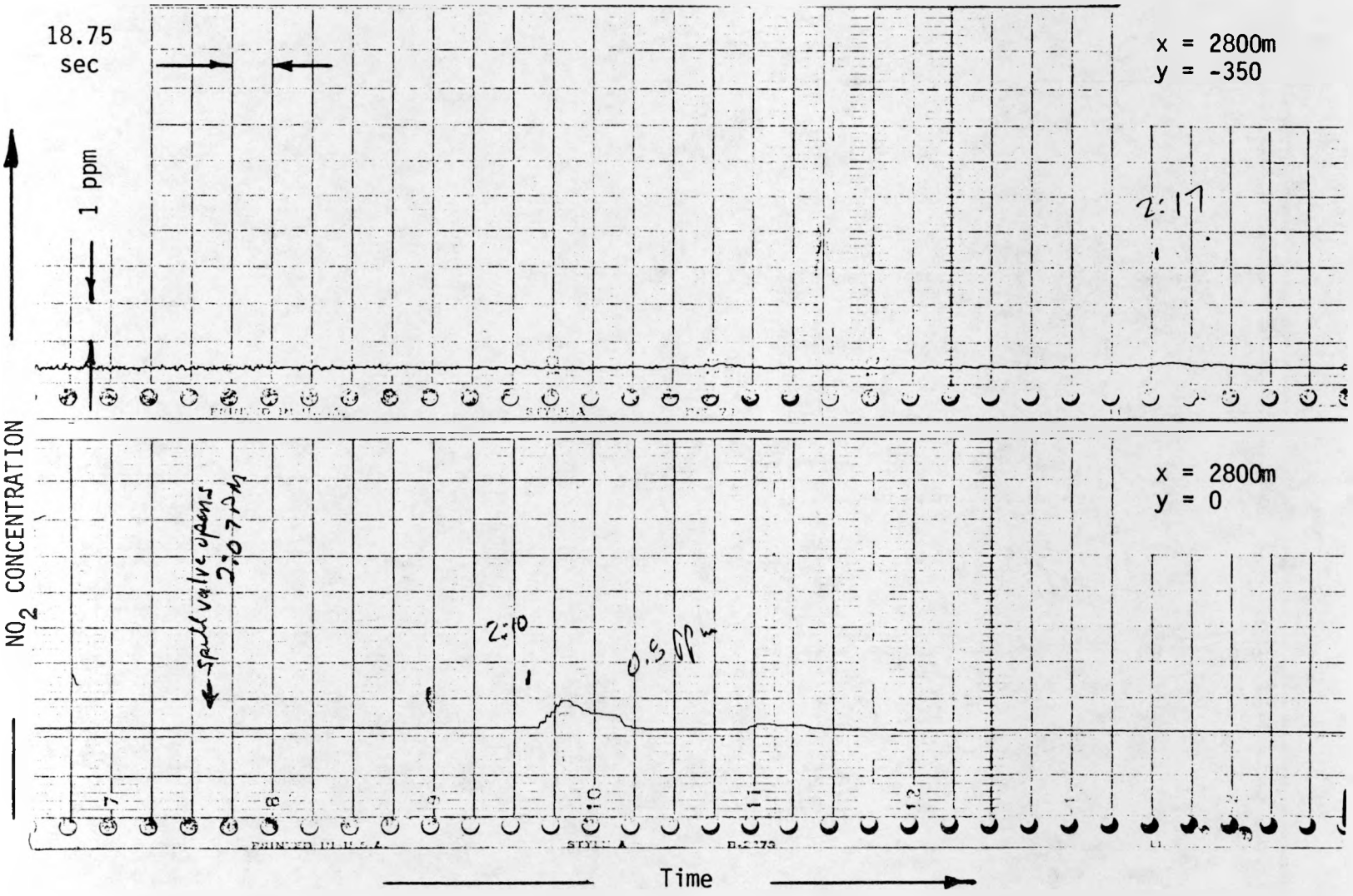

FIG. 85. EAG1 PORTABLE NO_2 SENSOR DATA.

GPO-785-002-68520

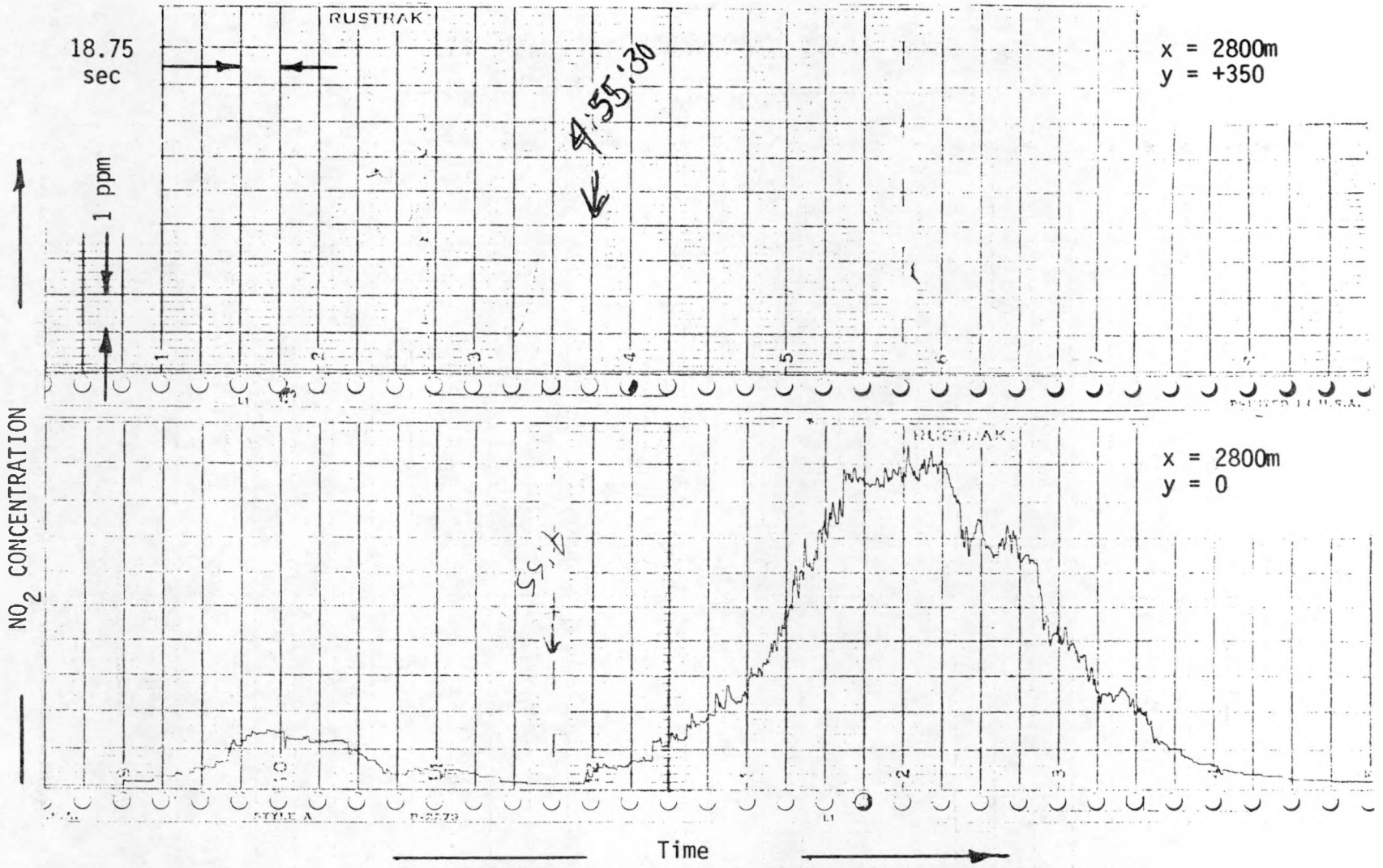

FIG. 86. EAG3 PORTABLE NO_2 SENSOR DATA.